ON THE DYNAMICS OF SYSTEMS WITH VASTLY DIFFERENT FREQUENCIES

A Dissertation

Presented to the Faculty of the Graduate School

of Cornell University

in Partial Fulfillment of the Requirements for the Degree of

Doctor of Philosophy

by

Hiba Sheheitli

January 2012

ON THE DYNAMICS OF SYSTEMS WITH VASTLY DIFFERENT FREQUENCIES

Hiba Sheheitli, Ph.D.

Cornell University 2012

The method of direct partition of motion (DPM) has been widely used to study the dynamics of non-autonomous oscillatory systems subject to external high frequency excitation. In this work, we explore the non-trivial dynamics that arise in autonomous systems with vastly different frequencies, in which the fast excitation is intrinsic to the system and possibly influenced by the slow dynamics. Using three model problems, we illustrate how DPM could be useful for the analysis of such systems and when combined with WKB can serve to capture the strong modulation of a fast oscillator due to coupling to a much slower one -a phenomenon that is not readily handled using standard perturbation methods. First, we study a system of three coupled limit cycle oscillators, which when uncoupled, have the frequencies $\omega_1 = O(1)$, $\omega_2 = O(1/\varepsilon)$ and $\omega_3 = O(1/\varepsilon^2)$, respectively, where $\varepsilon << 1$. Approximate expressions for the limit cycles of oscillators 1 and 2 are found in terms of Jacobi elliptic functions. For coupling strengths exceeding critical bifurcation values, the limit cycle of oscillator 1 or 2 is found to disappear. In the second problem, we consider a simple pendulum coupled to a horizontal mass-spring system of a much higher frequency. In contrast to the first problem, the coupling here allows the slow oscillator to affect the leading order dynamics of the fast oscillator. This calls for a rescaling of fast time, inspired by the WKB method, to be employed in conjunction with DPM. We obtain a critical energy value at which a pitchfork bifurcation of periodic

orbits is found to occur, giving rise to non-local periodic and quasi-periodic orbits in which the pendulum oscillates about an angle between zero and $\pi/2$ from the downwards position. Finally, the developed method is utilized to explain the non-trivial dynamics arising in a model of a thin elastica presented by Cusumano and Moon in 1995. We observe that for the corresponding experimental system, the ratio of the two natural frequencies of the system was ≈ 44 which can be considered to be of $O(1/\varepsilon)$ where $\varepsilon << 1$. Hence, the system is best viewed as one with vastly different frequencies. The method leads to an approximate expression for the non-local modes of the type observed in the experiments as well as the bifurcation energy value at which these modes are born. The formal approximate solutions obtained for these problems are validated by comparison with numerical integration.

BIOGRAPHICAL SKETCH

Born in 1986 in her home country Lebanon, Hiba was allowed in 1990 by her pre-school to finish the 2-year kindergarten curriculum in one year. Though she has no memory of this story, her parents see it as a first indicator of her academic excellence and will proudly retell it to strangers every once in a while. In 2003, she graduated from high school with a strong interest in math, physics and chemistry so she decided to study Mechanical Engineering at the American University of Beirut (AUB), as a major that would integrate all of them. Her philosophical fascination with consciousness led her to repeated encounters with the subject of Neuroscience and motivated her to pursue a minor degree in Biology. She then realized that really it's living systems that integrate all of science... and traditional engineering investigations were suddenly no longer fulfilling for her. To figure out an alternative, she took a year after graduation to explore interdisciplinary fields and apply to graduate schools. Meanwhile, to keep her sanity and connection to the world, she put her engineering skills to use at the AUB Aerosol lab. She had taken a course in Nonlinear Dynamics in her senior year and was pushed into the basin of attraction of the field by the elegance, power and breadth of applicability of its approach. This was the primary reason that moved her to join the Field of Theoretical & Applied Mechanics at Cornell University in August 2008. During her years at Cornell, among the many things she learned about was how to understand dynamical systems, how nonlinear time can be, how happy people can get just because it's suddenly sunny, and the Fredholm Alternative. She was privileged to get to know great professors during her studies and hopes one day she will live up to their example and be a great researcher, teacher and mentor.

To my family who has given me all that I am,

To Sara who was there all throughout,

To Jihad who inspired me to go down this road.

ACKNOWLEDGEMENTS

I would like to thank the Cornell University Graduate School for offering me the McMullen Fellowship to start my PhD studies in 2008. I also thank the Department of Theoretical & Applied Mechanics, the Department of Mechanical & Aerospace Engineering and the Department of Mathematics for supporting me through teaching assistantships for the rest of my studies at Cornell. I would like to express my gratitude and respect for my research committee members, Prof. Richard Rand, Prof. Steven Strogatz, and Prof. Timothy Healey, for all that they have taught me, and for the time that was required from them to be on my research committee. It is an honor and pleasure to have gotten to know them. To my advisor, Prof. Richard Rand, you have given me the freedom to steer my research endeavors but were always there with valuable insight and resources when I needed it. I am deeply grateful to you for the great balance between guidance and autonomy that you have provided me with. Thank you for being a wonderful mentor.

TABLE OF CONTENTS

LIST OF FIGURES

CHAPTER 1

INTRODUCTION

The effects of high frequency excitation on nonlinear mechanical systems have been extensively studied and reviewed in recent years [4, 15, 30, 31]. These effects include apparent changes in system properties such as the number of equilibrium points, stability of equilibrium points, natural frequencies, stiffness, and bifurcation paths [31]. The most famous non-trivial effect of fast excitation is the stabilization of the pendulum in the upright position when its point of support is subjected to an imperceptible but very fast vertical oscillation. Often these problems can be analyzed using standard perturbation methods such as the method of multiple timescales or the method or averaging [31]. However, *the method of direct partition of motion* (DPM), developed by Blekhman [4], serves to facilitate the study of this class of problems. Unlike the averaging method or the method of multiple timescales, DPM offers no systematic way to obtain higher order terms in an asymptotic expansion of the solution, and instead is limited to the leading order dynamics of the system. In return for this limitation, one gains efficiency in terms of the required mathematical manipulations. Particularly, DPM is most useful when the main interest is in the leading order slow motion of the system that is subject to the fast excitation. More recently, Belhaq and his associates have used DPM to study the effect of high frequency excitation on systems possessing self-excited motions [2, 5, 12, 25]. It was shown that the fast excitation could lead to the disappearance of the stable limit cycle. [5].

A common feature of all the aforementioned works is that the fast excitation is due to an external source, that is, all the systems considered are non-

autonomous, and the amplitude and frequency of the fast forcer are constant and known. In this thesis we show that similar non-trivial effects can occur if the fast excitation is internal to the system, instead of coming from an external source. An example of such a case would be a nonlinear oscillator coupled to a much faster oscillator. Systems of coupled nonlinear oscillators with widely separated frequencies have been investigated in the literature [20, 21, 33]. Particularly, in [20], a system of two coupled oscillators with widely spaced frequencies is studied to elucidate how "modal interactions can channel energy from a low amplitude, high frequency excitation into low frequency, high amplitude vibrations". Their investigation was motivated by previous experiments in which a cantilever beam is clamped to a shaker at one end so that a simple harmonic planar excitation is applied transverse to the axis of the beam. It was found that when the beam is excited near the natural frequency of its third or any higher mode, a large first-mode response occurs and it is accompanied by modulation of the amplitudes and phases of the high frequency modes [20]. As it is often the case for such systems with vastly different frequencies, the method of averaging was used to study the dynamics of the proposed model [20]. We find that DPM can also serve to study such systems, without having to transform the equations into standard form. We also propose that DPM, when applied in conjunction with the WKB method, can be useful in analyzing systems where the amplitude and frequency of the fast oscillator are strongly modulated by the slow oscillator, an effect which is observed in experiments [23] but can not be captured by other standard perturbation techniques that assume this modulation to be of $O(\varepsilon)$, where $\varepsilon << 1$. While the WKB method is often used to find the solution to an equation of a fast oscillator with a frequency that is explicitly a function of slow time, here, we extend its use to the situation where the

frequency of the fast oscillator is implicitly a function of slow time through the dependence on the amplitude of the slow oscillator that it is coupled to. The purpose of this thesis is to illustrate these latter ideas through three examples of systems with vastly different frequencies, for which DPM was found to be instrumental in understanding the non-trivial solutions that arise.

In section 1.1, we state the basic assumptions of DPM and illustrate the implementation of the method by applying it to the classical example of a pendulum with a rapidly oscillating point of suspension. Then in section 1.2, we consider a simple two degree of freedom system with vastly different frequencies. Unlike in previous problems studied in the literature [20, 21, 33], the slow oscillator is allowed to significantly influence the dynamics of the fast oscillator, an effect which the method of first order averaging fails to capture. This motivates the use of a rescaling of fast time inspired by the WKB method, along with DPM, and serves to outline the method that is later used in chapters 3 and 4.

In chapter 2, we use the assumptions of DPM to study a system of three coupled limit cycle oscillators, which when uncoupled, have the frequencies $\omega_1 = O(1)$, $\omega_2 = O(1/\varepsilon)$ and $\omega_3 = O(1/\varepsilon^2)$, respectively, where $\varepsilon << 1$. It is shown that the limit cycles of oscillators 1 and 2, to leading order, take the form of a Jacobi elliptic function whose amplitude and frequency are modulated as the strength of coupling is varied. For coupling strengths exceeding critical bifurcation values, the limit cycle of oscillator 1 or 2 is found to disappear.

In chapter 3, we investigate the dynamics of a simple pendulum coupled to a horizontal mass-spring system having a natural frequency that is an order of

magnitude larger than that of the linear oscillations of the pendulum. In contrast to the first problem, the coupling here allows the slow oscillator to affect the leading order dynamics of the fast oscillator. This calls for a rescaling of fast time, inspired by the WKB method, to be employed in conjunction with DPM. A pitchfork bifurcation of periodic orbits is found to occur for energy values larger than a critical value. The bifurcation gives rise to non-local periodic and quasi-periodic orbits in which the pendulum oscillates about an angle between zero and $\pi/2$ from the downwards position. The bifurcating periodic orbits are nonlinear normal modes of the coupled system and correspond to fixed points of a Poincare map. An approximate expression for the value of the new fixed points of the map is obtained.

Finally, in chapter 4, the method developed in chapter 3 is utilized to shed light on the non-trivial dynamics arising in a model of a thin elastica presented by Cusumano and Moon in 1995. We observe that for the corresponding experimental system, the ratio of the two natural frequencies of the system was ≈ 44 which can be considered to be of $O(1/\varepsilon)$ where $\varepsilon << 1$. Hence, the system is best viewed as one with vastly different frequencies. Previous analytical studies of the model were done using standard perturbation methods which required the assumption that the strength of the nonlinear coupling is of $O(\varepsilon)$ when in fact the value of the parameter reported in [11] is rather of $O(1)$. By combining DPM with the WKB rescaling of time, we can study the model while allowing the strength of nonlinear coupling to be of $O(1)$. Using this procedure, we obtain an approximate expression for the solutions corresponding to non-local modes of the type observed in the experiments. In addition, we show that these non-local modes will exist for energy values larger than a critical energy value

that is expressed in terms of the parameters. This analysis leads to a new understanding of the dynamics, that is, we see that these non-local nonlinear modes are due to the presence of strong nonlinear inertial coupling between the slow first bending mode and the much faster first torsional mode.

1.1 The method of direct partition of motion

Formalized by Blekhman and generalized to a wide range of physical systems [4], the main idea behind DPM can be dated back to Kapitza's approach to the problem of the stability of a pendulum with an oscillating point of suspension [17, 30]. The same heuristic approach is also often presented in the physics literature [18]. The method is based on three main assumptions [30] that can be summarized as follows:

- the motion of the system under fast excitation can be partitioned into a purely slow component and an overlaid fast component.
- any function of fast time is periodic with a zero average over a period of fast time.
- any purely slow function is invariant under averaging over fast time.

We will elaborate on the details of the method by applying it to the classical problem of a pendulum with a point of suspension that is oscillating horizontally with a small amplitude and high frequency. The analysis of this problem is present in the literature of non-trivial effects of fast excitation [13, 15, 30], still we include it here as a simple example serving to illustrate the method.

1.1.1 A pendulum with a rapidly oscillating suspension point

We consider a simple pendulum whose point of suspension is constrained to move horizontally with a displacement $a\cos\Omega t$ such that $a = O(\varepsilon)$ and $\Omega = O(1/\varepsilon)$, where $\varepsilon << 1$. Ignoring dissipation, the equation governing the motion of the pendulum can be written as:

$$\frac{d^2\theta}{dt^2} + \sin\theta - (A\Omega\cos\Omega t)\cos\theta = 0 \quad \text{where } A = a\Omega = O(1) \tag{1.1}$$

where θ is measured from the vertically down position. First, we numerically integrate the equation with $\Omega = 20$ ($\varepsilon = 0.05$), for different typical values of the parameter A and initial amplitudes with $\dot{\theta}(0) = 0$. We can see in Fig.1.1(a) that for a small enough value of A, the motion of the pendulum is a slow oscillation about the origin with a small overlaid fast oscillation. As A is increased, Fig.1.1(b) shows how the slow oscillation of the pendulum is now about an angle other than the downwards position, and for a particular initial amplitude it seems to be merely of $O(\varepsilon)$ (Fig.1.1(c)). For the same value of A that allows these non-local motions, large oscillations about the origin are still possible, as shown in Fig.1.1(d). How can we understand the occurrence of these non-local oscillations as A is increased and how does the type of solution depend on the initial conditions? We will use DPM to try to answer these questions. We will then apply to the same problem the standard method of averaging for the sake of comparison.

The first step in DPM is to partition the motion into a purely slow component and an overlaid fast one, as follows:

$$\theta = \theta_0(\eta) + \varepsilon\theta_1(\eta,\tau) \quad \text{where } \eta = t \ , \ \tau = \Omega t = \frac{1}{\varepsilon}t \tag{1.2}$$

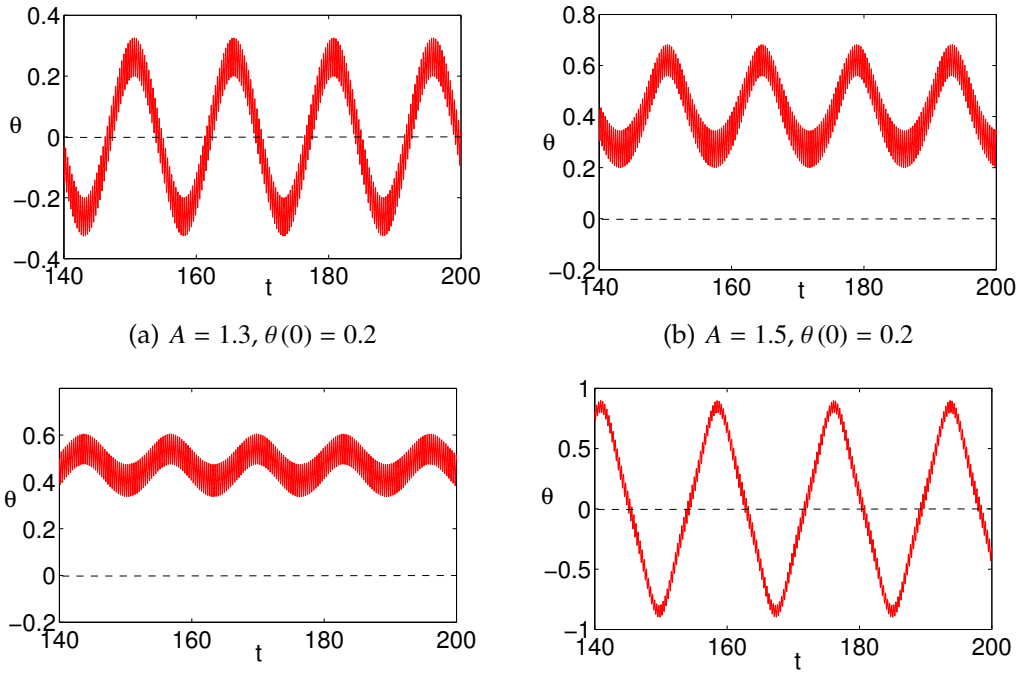

(a) $A = 1.3, \theta(0) = 0.2$ (b) $A = 1.5, \theta(0) = 0.2$

(c) $A = 1.5, \theta(0) = 0.48$ (d) $A = 1.5, \theta(0) = 0.8$

Figure 1.1: θ vs. time

We note here that this step, in general, is not equivalent to expanding θ into an asymptotic series; the method in its most general form allows the overlaid fast component $\theta_1(\eta, \tau)$ to be of $O(1)$ or larger. This would be in the case where the order of magnitude of the fast term in the equation of motion is larger than in the case of the problem we are considering [4].

Substituting the assumed expression for θ, Eq.(1.2), into Eq.(1.1), we get:

$$\frac{d^2\theta_0}{d\eta^2} + \frac{1}{\varepsilon}\frac{\partial^2\theta_1}{\partial\tau^2} + 2\frac{\partial^2\theta_1}{\partial\eta\partial\tau} + \varepsilon\frac{\partial^2\theta_1}{\partial\eta^2} + \sin\theta_0 + \varepsilon\theta_1\cos\theta_0 \tag{1.3}$$

$$-A\frac{1}{\varepsilon}\cos\tau\cos\theta_0 + A\theta_1\cos\tau\sin\theta_0 = 0$$

where we have used the approximations:

$$\sin(\theta_0 + \varepsilon\theta_1) \approx \sin\theta_0 + \varepsilon\theta_1\cos\theta_0 \quad , \quad \cos(\theta_0 + \varepsilon\theta_1) \approx \cos\theta_0 - \varepsilon\theta_1\sin\theta_0$$

The next step of DPM is to average Eq.(1.3) over a period of fast time τ, assuming that any function of fast time is periodic with a zero average, while any purely slow function is invariant under this operation of averaging. The averaged equation becomes:

$$\frac{d^2\theta_0}{d\eta^2} + \sin\theta_0 + A\left\langle\theta_1\cos\tau\right\rangle_\tau \sin\theta_0 + O(\varepsilon) = 0 \tag{1.4}$$

$$\text{where}\quad \langle\bullet\rangle_\tau = \frac{1}{2\pi}\int_0^{2\pi} \bullet\, d\tau$$

The third step of DPM is to subtract the averaged equation from the full equation given by Eq.(1.3), resulting in an equation governing the fast component of motion:

$$\frac{1}{\varepsilon}\left(\frac{\partial^2\theta_1}{\partial\tau^2} - A\cos\tau\cos\theta_0\right) + O(1) = 0$$

Since θ_0 is a function of slow time only, the above equation can be integrated twice with respect to fast time, τ, to obtain an expression for the fast component of motion:

$$\theta_1 = -A\cos\tau\cos\theta_0 + c_1\tau + c_2$$

Enforcing the DPM assumption that functions of fast time are periodic with a zero average, we set the arbitrary constants c_1 and c_2 to zero. Then, the expression for θ_1 reduces to:

$$\theta_1 = -A\cos\tau\cos\theta_0 \tag{1.5}$$

We are now ready to evaluate the integral that appears in Eq.(1.4):

$$\left\langle\theta_1\cos\tau\right\rangle_\tau = \frac{1}{2\pi}\int_0^{2\pi}\left(-A\cos^2\tau\cos\theta_0\right)\, d\tau = -\frac{1}{2}A\cos\theta_0$$

Substituting this into Eq.(1.4), we arrive at what is often the aim of DPM: an equation governing the leading order slow dynamics in the system:

$$\frac{d^2\theta_0}{d\eta^2} + \sin\theta_0 - \frac{1}{2}A^2\cos\theta_0\sin\theta_0 = 0 \tag{1.6}$$

This autonomous equation appears similar to the original equation of motion, but with the external excitation term replaced by what is often called a "Vibrational Force" [4], which represents an averaged effect of the fast excitation on the slow dynamics.

Since the equation at hand is autonomous we can readily plot the phase portrait for a given value of the parameter A. We can see from Fig.1.2(b) that the origin

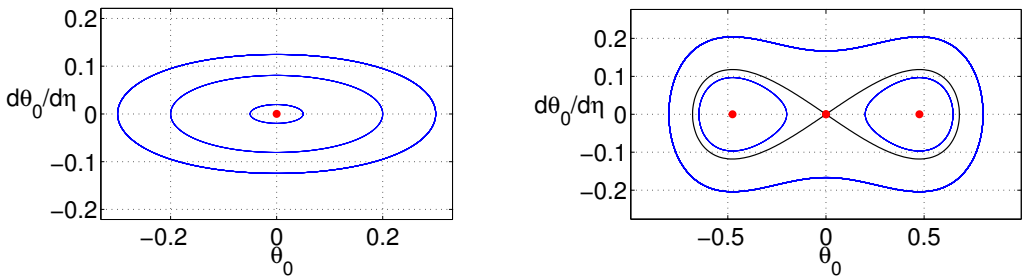

(a) $A = 1.3$ (b) $A = 1.5$

Figure 1.2: Phase portrait for the θ_0 equation

has gone unstable and instead, two new centers exist. This explains the different types of solution that we observed for $A = 1.5$. For the solution in Fig.1.1(b), $\theta_0(0) \approx \theta(0) = 0.2$, this would correspond to the small oscillation about one of the non-trivial centers in Fig.1.2(b). The solution for $\theta_0(0) \approx \theta(0) = 0.8$, shown in Fig.1.1(d), corresponds to the large oscillation outside the homoclinic orbit in Fig.1.2(b). The initial amplitude $\theta_0(0) \approx \theta(0) = 0.48$, for the solution in Fig.1.1(c), coincides with one of the non-trivial centers in Fig.1.2(b), so the slow component of motion is expected be a mere static deflection from the downright position. Instead of a static slow component of motion, we see in Fig.1.1(c) a slow oscillation of $O(\varepsilon)$, this is due to the fact that the equation governing θ_0 is only accurate up to $O(\varepsilon)$. Looking at the equilibrium points of the θ_0 equation, we find that the origin loses stability through a pitchfork bifurcation at $A = \sqrt{2} \approx 1.4$, after

which two non-trivial equilibrium points are born at $\theta_0 = \pm\cos^{-1}\left(\sqrt{2}/A\right)$.

In summary, DPM serves to reduce the dynamics of a slow oscillator, with high frequency excitation, to an autonomous equation that governs the leading order slow dynamics. The fast component of the response is found in terms of the excitation function and the slow component of motion. The analysis of the slow dynamics equation provides insight into the bifurcations that occur in the original system as parameters are varied, and allows one to predict the type of non-trivial solutions that might arise.

For the sake of comparison, we will now apply the standard method of first order averaging to this problem. For that purpose, we transform the equation of motion in Eq.(1.1) into fast time:

$$\frac{d^2\theta}{d\tau^2} + \varepsilon^2 \sin\theta - \varepsilon\,(A\cos\tau)\cos\theta = 0 \tag{1.7}$$

Then, we rewrite it as a system of two first order equations:

$$\frac{d\theta}{d\tau} = \varepsilon\phi \quad , \quad \frac{d\phi}{d\tau} = -\varepsilon\sin\theta + (A\cos\tau)\cos\theta \tag{1.8}$$

The method of averaging requires the system to be in standard form, in which all the derivatives are of $O(\varepsilon)$. To achieve that, we notice that the unperturbed system has the solution:

$$\theta = \text{constant} = \theta_0$$

$$\phi = A\sin\tau\cos\theta_0 + \phi_0$$

Allowing the constants appearing in this solution to vary with time, we obtain the following transformation of variables:

$$\theta = \theta_0(\tau) \quad , \quad \phi = A\sin\tau\cos\theta_0 + \phi_0(\tau)$$

We substitute this into Eqs.(1.8) in order to obtain the system of equations governing the new variables:

$$\frac{d\theta_0}{d\tau} = \varepsilon\left(A\sin\tau\cos\theta_0 + \phi_0\right)$$

$$\frac{d\phi_0}{d\tau} = -\varepsilon\sin\theta + (A\cos\tau)\cos\theta - \frac{d}{d\tau}\left(A\sin\tau\cos\theta_0\right) = -\varepsilon\sin\theta_0 + A\sin\tau\sin\theta_0\frac{d\theta_0}{d\tau}$$

$$\Rightarrow \frac{d\phi_0}{d\tau} = -\varepsilon\sin\theta_0 + \varepsilon A^2\sin^2\tau\sin\theta_0\cos\theta_0 + \varepsilon A\phi_0\sin\tau\sin\theta_0$$

Now, the right hand side of both equations is $O(\varepsilon)$, that is, the system is in standard form:

$$\frac{d\theta_0}{d\tau} = \varepsilon\left(A\sin\tau\cos\theta_0 + \phi_0\right)$$

$$\frac{d\phi_0}{d\tau} = \varepsilon\left(-\sin\theta_0 + A^2\sin^2\tau\sin\theta_0\cos\theta_0 + A\phi_0\sin\tau\sin\theta_0\right) \tag{1.9}$$

This form implies that θ_0 and ϕ_0 are changing slowly on the fast timescale τ, since their derivatives are only $O(\varepsilon)$. Then, we can average each of the equations over a period of fast time, while treating θ_0 and ϕ_0 and their derivatives as constants:

$$\frac{d\theta_0}{d\tau} = \varepsilon\phi_0 \quad , \quad \frac{d\phi_0}{d\tau} = \varepsilon\left(-\sin\theta_0 + \frac{1}{2}A^2\sin\theta_0\cos\theta_0\right)$$

Assembling the system back into a second order equation governing θ_0, we get:

$$\frac{d^2\theta_0}{d\tau^2} + \varepsilon^2\left(\sin\theta_0 - A^2\frac{1}{2}\sin\theta_0\cos\theta_0\right) = 0$$

When we transform back to slow time, we see that this is identical to the slow dynamics equation in Eq.(1.6) that we obtained by using DPM:

$$\frac{d^2\theta_0}{dt^2} + \sin\theta_0 - \frac{1}{2}A^2\sin\theta_0\cos\theta_0 = 0$$

The theory of the method of averaging [26] guarantees that the dynamics of the original problem are captured by this averaged equation, up to $O(\varepsilon)$.

In general, problems for which DPM is applicable can also be studied using

the averaging method, however, DPM tends to be easier to use since there is no need to transform the system to the standard form required by the averaging method. Other perturbation methods, such as the the method of two timescales, can also be used for the study of such problems, but DPM is particularly tailored so as to minimize the amount of required mathematical manipulations.

1.2 Two coupled oscillators with vastly different frequencies

We have shown how DPM can be used to analyze the dynamics of a slow oscillator subject to a known external fast excitation. We will now consider an alternate situation where a slow oscillator is influenced by fast excitation through coupling to a much faster oscillator. As a simple example, consider the following two degree of freedom system:

$$\begin{aligned} &\frac{d^2y}{dt^2} + y + \alpha_1 x^2 y = 0 \\ &\frac{d^2x}{d\tau^2} + x + \varepsilon\alpha_2 y^2 x = 0 \\ &\text{where } \tau = \frac{1}{\varepsilon}t \ , \ \varepsilon << 1 \end{aligned} \tag{1.10}$$

The particular form of coupling is inspired from the system presented in [20] as a "paradigm for the interaction of high- and low-frequency modes". The coupling term in the slow oscillator equation is $O(1)$, while that in the fast oscillator equation is $O(\varepsilon)$; this suggests that the slow oscillator does not affect the leading order dynamics of the fast oscillator, so one would expect the problem to reduce to that of a slow oscillator subject to an external fast excitation. We numerically integrate the system of equations for typical parameter values: $\varepsilon = 0.05$, $\alpha_1 = -2$ and $\alpha_2 = 3$. Fig.1.3(a) and 1.3(b) display the solution for initial

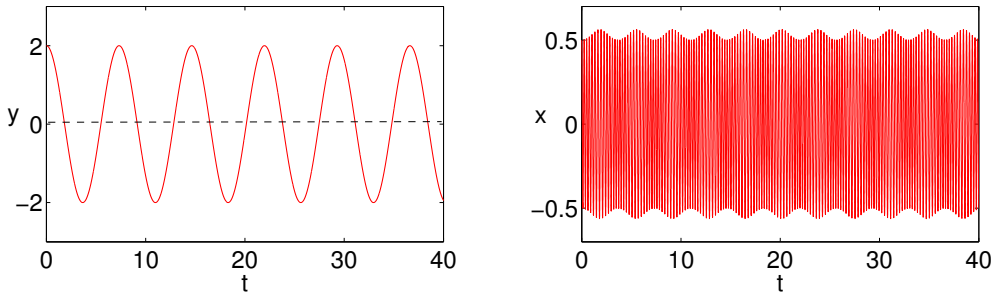

(a) y vs. time (b) x vs. time

Figure 1.3: Numerical integration of the two coupled oscillators with vastly different frequencies for $x(0) = 0.5$, $y(0) = 2$

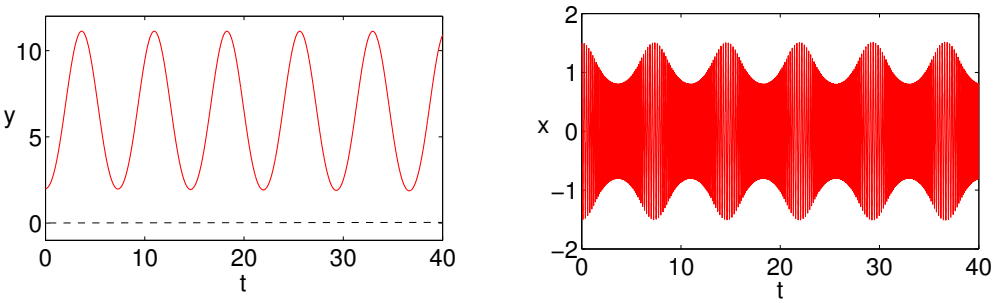

(a) y vs. time (b) x vs. time

Figure 1.4: Numerical integration of the two coupled oscillators with vastly different frequencies for $x(0) = 1.5$, $y(0) = 2$

amplitudes $x(0) = 0.5$, $y(0) = 2$ with zero initial velocities; y undergoes a slow oscillation about the origin while x is a fast oscillation with a slowly modulated amplitude and frequency. For a larger initial amplitude, $x(0) = 1.5$, the slow oscillation in Fig.1.4(a) is now about a non-zero value of y, and the modulation of the fast oscillation is now much more pronounced. To try to understand how these latter solutions arise, we start by applying the method of first order averaging. First we rewrite the y equation in terms of fast time, the system of equations becomes:

$$\frac{d^2y}{d\tau^2} + \varepsilon^2 y + \varepsilon^2 \alpha_1 x^2 y = 0$$

$$\frac{d^2x}{d\tau^2} + x + \varepsilon\alpha_2 y^2 x = 0 \tag{1.11}$$

The y equation can be readily written in standard form as:

$$\frac{dy}{d\tau} = \varepsilon\phi \quad , \quad \frac{d\phi}{d\tau} = -\varepsilon\left(y + \alpha_1 x^2 y\right) \tag{1.12}$$

For the x equation, we make use of the Van der Pol transformation:

$$x = a(\tau)\cos(\tau + \beta(\tau)) \quad , \quad x' = -a\sin(\tau + \beta)$$

where prime denotes differentiation with respect to τ. Equating the full expression for the derivative of x with the assumed form, we get:

$$a'\cos(\tau+\beta) - a(1+\beta')\sin(\tau+\beta) = -a\sin(\tau+\beta)$$

$$\Rightarrow \beta' = \frac{a'\cos(\tau+\beta)}{a\sin(\tau+\beta)} \tag{1.13}$$

We then substitute the assumed form of solution into the x equation of motion:

$$-a'\sin(\tau+\beta) - a\beta'\cos(\tau+\beta) + \varepsilon\alpha_2 y^2 a\cos(\tau+\beta) = 0$$

Using Eq.(1.13) to eliminate β' , we get:

$$a' = \varepsilon\alpha_2 y^2 a\sin(\tau+\beta)\cos(\tau+\beta)$$

Hence, Eqs.(1.11) are transformed into:

$$y' = \varepsilon\phi \quad , \quad \phi' = -\varepsilon\left(y + \alpha_1 y a^2\cos^2(\tau+\beta)\right)$$

$$a' = \varepsilon\alpha_2 y^2 a\sin(\tau+\beta)\cos(\tau+\beta) \quad , \quad \beta' = \varepsilon\alpha_2 y^2\cos^2(\tau+\beta)$$

This implies that all variables, y, ϕ, a and β, are slowly varying on the τ timescale. Thus, we can average the equations over τ, while treating these four variables and their derivatives as constants. The resulting averaged system reduces to:

$$y' = \varepsilon\phi \quad , \quad \phi' = -\varepsilon\left(y + \frac{1}{2}\alpha_1 a^2 y\right)$$

$$a' = 0 \quad , \quad \beta' = \frac{1}{2}\varepsilon\alpha_2 y^2$$

And the resulting approximate y equation becomes:

$$\frac{d^2y}{d\tau^2} + \varepsilon^2\left(1 + \frac{1}{2}\alpha_1 a^2\right)y = 0 \tag{1.14}$$

while x is given by:

$$x \approx a\cos(\tau + \beta) \quad , \quad a = \text{constant} \ , \ \beta' = \frac{1}{2}\varepsilon\alpha_2 y^2 \tag{1.15}$$

Since a is predicted to be a constant, this result can not account for solutions of the type displayed in Fig.1.4(a) and 1.4(b), in which y oscillates about a non zero mean and x has a strongly modulated amplitude. In order to capture the effect of y on the amplitude of x, we can possibly attempt going to higher orders in the method of averaging, which could provide an $O(\varepsilon)$ correction to the rate of change of the amplitude a. Instead, we suggest an alternative technique that is particularly suited for such problems and allows us to obtain an approximate closed form expression for the amplitude of the fast oscillator in terms of the slow oscillator.

1.2.1 DPM with a WKB rescaling of fast time

We rewrite the original x equation in terms of slow time, whereupon the system in Eqs.(1.10) becomes:

$$\begin{aligned} \frac{d^2y}{dt^2} + y + \alpha_1 x^2 y &= 0 \\ \frac{d^2x}{dt^2} + \frac{1}{\varepsilon^2}\left(1 + \varepsilon\alpha_2 y^2\right)x &= 0 \end{aligned} \tag{1.16}$$

Observing that y is an oscillator influenced by a much faster oscillator, we will employ DPM to study its dynamics; first we assume:

$$y = y_0(\eta) + \varepsilon^2 y_1(\eta, T) \tag{1.17}$$

where $\eta = t$ and T is a fast time to be defined later in terms of τ. The fast component of motion is assumed to be $O\left(\varepsilon^2\right)$ since the fast term appearing in the y equation is of $O(1)$, unlike in the example of section 1.1.1 in which the fast term was of $O(1/\varepsilon)$; for a rigorous justification of this, see [4]. Now with this assumption, y is to leading order a function of slow time. Thus the x equation appears, to leading order, as representing a fast oscillator with a slowly varying frequency:

$$\frac{d^2x}{d\eta^2} + \frac{1}{\varepsilon^2}\omega^2(\eta)\,x = 0 \quad \text{or} \quad \frac{d^2x}{d\tau^2} + \omega^2(\varepsilon\tau)\,x = 0$$

$$\text{where} \quad \omega(\eta) = \omega(\varepsilon\tau) = \sqrt{1 + \varepsilon\alpha_2 y_0^2} \tag{1.18}$$

For such an oscillator, the WKB method suggests a rescaling of fast time that transforms the equation into one that yields itself easily to regular perturbations [34]. This rescaling is expressed as:

$$\frac{dT}{d\tau} = \omega(\eta) \tag{1.19}$$

Then the second derivative of x with respect to time becomes:

$$\frac{d^2x}{d\eta^2} = \frac{d^2x}{dT^2}\frac{\omega^2}{\varepsilon^2} + \frac{1}{\varepsilon}\frac{d\omega}{d\eta}\frac{dx}{dT}$$

So the x equation is transformed into:

$$\frac{d^2x}{dT^2} + x + \varepsilon\frac{1}{\omega^2}\frac{d\omega}{d\eta}\frac{dx}{dT} = 0 \tag{1.20}$$

Next, we expand x into an asymptotic series:

$$x = x_0(\eta, T) + \varepsilon x_1(\eta, T) + \ldots$$

Substituting this into Eq.(1.20), and collecting terms of the same order, we obtain:

$$O(1): \quad \frac{\partial^2 x_0}{\partial T^2} + x_0 = 0$$

$$O(\varepsilon): \quad \frac{\partial^2 x_1}{\partial T^2} + x_1 = -2\frac{1}{\omega}\frac{\partial^2 x_0}{\partial T \partial T} - \frac{1}{\omega^2}\frac{d\omega}{d\eta}\frac{\partial x_0}{\partial T}$$

From the $O(1)$ equation, we get:

$$x_0 = a(\eta)\cos T$$

Substituting this into the $O(\varepsilon)$ equation and eliminating secular terms on the right hand side, we arrive at an equation governing the evolution of the amplitude a:

$$2\frac{1}{\omega}\frac{da}{d\eta} + a\frac{1}{\omega^2}\frac{d\omega}{d\eta} = 0$$

The above equation can be solved using the method of separation of variables to obtain the following expression for the amplitude of x:

$$a = \frac{C}{\sqrt{\omega}} = C\left(1 + \varepsilon\alpha_2 y_0^2\right)^{-\frac{1}{4}}$$

where C is an arbitrary constant that depends on initial conditions. Then x is approximately given by:

$$x \approx \frac{C}{\sqrt{\omega}}\cos T \quad \text{with} \quad \frac{dT}{d\eta} = \frac{1}{\varepsilon}\omega(\eta) = \frac{1}{\varepsilon}\sqrt{1 + \varepsilon\alpha_2 y_0^2} \tag{1.21}$$

For initial conditions with zero initial velocities and given initial amplitudes:

$$\begin{cases} x(0) = A \\ y(0) = B \end{cases} \Rightarrow A \approx C\left(1 + \varepsilon\alpha_2 B^2\right)^{-\frac{1}{4}} \Rightarrow C \approx A\left(1 + \varepsilon\alpha_2 B^2\right)^{\frac{1}{4}}$$

Now that we have an expression for x, we are ready to continue applying DPM to the equation of the slow oscillator. We substitute the assumed form of solution given by Eq.(1.17), along with the above expression for x, into the y equation of the system presented in Eqs.(1.16):

$$\frac{d^2 y_0}{d\eta^2} + y_0 + \alpha_1\left(\frac{C^2}{\omega}\cos^2 T\right)y_0 + \omega^2\frac{\partial^2 y_1}{\partial T^2} + O(\varepsilon) = 0$$

Ignoring $O(\varepsilon)$ terms and expanding the $\cos^2 T$, the equation becomes:

$$\frac{d^2y_0}{d\eta^2} + y_0 + \frac{\alpha_1 C^2}{2\omega} y_0 + \frac{\alpha_1 C^2}{2\omega} y_0 \cos 2T + \omega^2 \frac{\partial^2 y_1}{\partial T^2} = 0 \tag{1.22}$$

The equation is now ready to perform the second step of DPM which involves averaging over a period of fast timescale, T, while treating the purely slow functions as constants. The averaged equation reduces to:

$$\frac{d^2y_0}{d\eta^2} + y_0 + \frac{\alpha_1 C^2}{2\omega} y_0 = 0$$

Substituting in the expression for ω given by Eq.(1.18), we obtain the following equation governing the leading order slow dynamics of y:

$$\frac{d^2y_0}{d\eta^2} + y_0 + \frac{\alpha_1 C^2}{2\sqrt{1 + \varepsilon\alpha_2 y_0^2}} y_0 = 0 \tag{1.23}$$

The next step in DPM is to subtract the averaged equation from the full equation in Eq.(1.22). This leads to an approximate equation governing the fast component of y:

$$\omega^2 \frac{\partial^2 y_1}{\partial T^2} + \frac{\alpha_1 C^2}{2\omega} y_0 \cos 2T = 0$$

Since y_0 and ω are functions of slow time only, the above equation can be integrated twice with respect to fast time, τ, to obtain an expression for y_1:

$$y_1 = \frac{\alpha_1 C^2}{8\omega^3} y_0 \cos 2T + c_1 T + c_2$$

To satisfy the DPM assumption that fast motions are periodic on the fast timescale with a zero average, we set the arbitrary constants to zero. Then the fast component of y takes the form:

$$y_1 = \frac{\alpha_1 C^2}{8\omega^3} y_0 \cos 2T$$

In summary, by partitioning the slow motion according to DPM, as in Eq.(1.17), we are able to view the fast oscillator as one with a slowly varying frequency

and thus employ the rescaling of fast time in Eq.(1.19), as in the WKB method. This allows us to obtain the approximate expression in Eq.(1.21) for the fast oscillation, x, in terms of the leading order slow motion, y_0. Then continuing the DPM procedure results in Eq.(1.23) governing the leading order slow dynamics, y_0.

In Fig.1.5(a) and 1.5(b), we show the phase portrait for Eq.(1.23), for the values of C corresponding to the solutions displayed in Fig.1.3(a),(b) and 1.4(a),(b), respectively. For given values of ε and coupling strength, with $\alpha_1 < 0$, large enough initial amplitudes will lead to values of C for which the nonlinear slow dynamics equation possesses two new centers while the origin is unstable. This demystifies the occurrence of the non-local oscillations of y and brings us to the basic idea behind this method, which is that analysis of the bifurcations that might arise in the nonlinear slow dynamics equation can serve to shed light on bifurcations of the full system. This will be illustrated in more detail in chapters 3 and 4. Finally, we note that the slow dynamics equation obtained here is

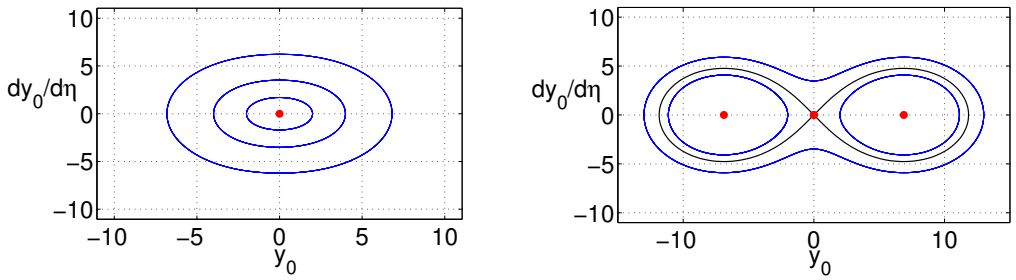

(a) C=0.562 (b) C=1.687

Figure 1.5: Phase portrait for the slow dynamics equation for different initial conditions

similar to the one obtained from the averaging method (Eq.(1.14)), in the sense

that the apparent effect of the fast oscillator on the slow oscillator is represented by the term $\alpha_1 a^2 y/2$. However, by capturing the dependence of a, the amplitude of the fast oscillator, on the slow oscillator y, this term becomes nonlinear and serves as a kind of feedback; the leading order slow oscillation is modulating the amplitude of the fast oscillation which in return is affecting the slow oscillation. The method that we presented here allows the characterization of this kind of interaction.

CHAPTER 2

DYNAMICS OF THREE COUPLED LIMIT CYCLE OSCILLATORS WITH VASTLY DIFFERENT FREQUENCIES [27]

In this chapter, the standard DPM assumptions are used to study an autonomous system of three coupled nonlinear oscillators with widely separated frequencies. When uncoupled, each of the oscillators possesses a limit cycle solution with a frequency $\omega_1 = O(1)$, $\omega_2 = O(1/\varepsilon)$ and $\omega_3 = O(1/\varepsilon^2)$ respectively, where $\varepsilon << 1$. We find that the coupling between such oscillators causes a change in the amplitude and frequency of the limit cycles of oscillators 1 and 2, and if the coupling between the oscillators is strong enough then the stable limit cycle of one of these two oscillators disappears. The limit cycle of the fastest oscillator, to leading order, is unchanged by the coupling.

Such a system in which several vastly different time scales interact, is ubiquitous in the nervous system, where rhythmically active subnetworks interact while oscillating at widely different frequencies [19]. It has been shown that a fast oscillatory neuron may regulate the frequency of a much slower oscillatory network [19].

Models which involve widely separated time scales also occur in astronomical applications. E.g. a study of the vibratory motion of a planet included oscillations with periods of (a) the orbital motions of the planets (tens and hundreds of years), (b) the secular orbital motions of the Solar System (tens and hundreds of thousands of years), and (c) galactic perturbations (tens and hundreds of millions of years) [1].

The system of equations, representing the coupled oscillators studied here, is presented in section 2.1. Section 2.2 describes the key assumptions of the method of direct partition of motion and presents the equations which the original system is transformed into at the end of the DPM procedure. The details of the DPM implementation are given in appendix A.1. Section 2.3 presents the approximate solution to the equations resulting from the DPM procedure, and the details of how the solution is obtained is given in appendix A.2. Section 2.4 discusses how varying the coupling strengths affects the dynamics of the system. Finally, section 2.5 presents a comparison between the approximate solution obtained from DPM and that from numerical integration.

2.1 The three coupled limit cycle oscillators

We will consider three Van der Pol type limit cycle oscillators x, y and z, which when uncoupled, are governed by the following equations:

$$\begin{aligned} \frac{d^2x}{dt_1^2} + x + \left(a_1 + b_1x^2\right)\frac{dx}{dt_1} &= 0 \\ \frac{d^2y}{dt_2^2} + y + \left(a_2 + b_2y^2\right)\frac{dy}{dt_2} &= 0 \\ \frac{d^2z}{dt_3^2} + z + \left(a_3 + b_3z^2\right)\frac{dz}{dt_3} &= 0 \end{aligned} \tag{2.1}$$

$$\text{where} \quad t_1 = \omega_1 t \quad , \quad t_2 = \frac{\omega_2}{\varepsilon}t \quad , \quad t_3 = \frac{\omega_3}{\varepsilon^2}t \quad , \quad \varepsilon << 1$$

Here, ω_1, ω_2 and ω_3 are O(1) quantities. We are interested in values of a_i and b_i (i=1,2,3) for which each of the equations above for x, y and z possesses a stable limit cycle solution that is an O(ε) perturbation off of a simple harmonic motion. The equations posed as such indicate that oscillation along these latter limit

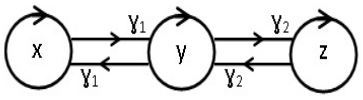

Figure 2.1: Symbolic diagram for the three coupled oscillator system

cycles of x, y and z occurs on the time scales t_1, t_2 and t_3 respectively, so z is a much faster oscillator than y, which is in turn a much faster oscillator than x. We will investigate the case of nearest neighbor nonlinear coupling, as shown in Fig.2.1. Then, the coupled system takes the following form:

$$\begin{aligned}
\frac{d^2x}{dt_1^2} + x + \left(a_1 + b_1x^2\right)\frac{dx}{dt_1} &= \gamma_1\left(1 + g_1x^2\right)\frac{dy}{dt_1} \\
\frac{d^2y}{dt_2^2} + y + \left(a_2 + b_2y^2\right)\frac{dy}{dt_2} &= \left(1 + g_2y^2\right)\left[\gamma_1\frac{dx}{dt_2} + \gamma_2\frac{dz}{dt_2}\right] \\
\frac{d^2z}{dt_3^2} + z + \left(a_3 + b_3z^2\right)\frac{dz}{dt_3} &= \gamma_2\left(1 + g_3z^2\right)\frac{dy}{dt_3}
\end{aligned} \tag{2.2}$$

This particular form of coupling is inspired by the work of Bourkha and Belhaq [5] in which the point of suspension of a self-excited pendulum is subjected to a horizontal parametric forcing. Various derivatives of x,y and z, with respect to the different time scales, appear in Eq.(2.2); these are related to the corresponding derivatives with respect to time t as follows:

$$\begin{aligned}
&\frac{dx}{dt_1} = \frac{1}{\omega_1}\frac{dx}{dt}\ ,\ \frac{d^2x}{dt_1^2} = \frac{1}{\omega_1^2}\frac{d^2x}{dt^2}\ ,\ \frac{dx}{dt_2} = \frac{\varepsilon}{\omega_2}\frac{dx}{dt} \\
&\frac{dy}{dt_1} = \frac{1}{\omega_1}\frac{dy}{dt}\ ,\ \frac{dy}{dt_2} = \frac{\varepsilon}{\omega_2}\frac{dy}{dt}\ ,\ \frac{dy}{dt_3} = \frac{\varepsilon^2}{\omega_3}\frac{dy}{dt}\ ,\ \frac{d^2y}{dt_2^2} = \frac{\varepsilon^2}{\omega_2^2}\frac{d^2y}{dt^2} \\
&\frac{dz}{dt_2} = \frac{\varepsilon}{\omega_2}\frac{dz}{dt}\ ,\ \frac{dz}{dt_3} = \frac{\varepsilon^2}{\omega_3}\frac{dz}{dt}\ ,\ \frac{d^2z}{dt_3^2} = \frac{\varepsilon^4}{\omega_3^2}\frac{d^2z}{dt^2}
\end{aligned} \tag{2.3}$$

Without loss of generality, from now on, we will assume $\omega_1 = 1$. Now, making use of these relations, with the dot denoting differentiation with respect to time t, the coupled system becomes:

$$\ddot{x} + x + \left(a_1 + b_1x^2\right)\dot{x} = \gamma_1\left(1 + g_1x^2\right)\dot{y}$$

$$\ddot{y} + \frac{\omega_2^2}{\varepsilon^2} y + \frac{\omega_2}{\varepsilon}\left(a_2 + b_2 y^2\right)\dot{y} = \frac{\omega_2}{\varepsilon}\left(1 + g_2 y^2\right)\left[\gamma_1 \dot{x} + \gamma_2 \dot{z}\right] \tag{2.4}$$

$$\ddot{z} + \frac{\omega_3^2}{\varepsilon^4} z + \frac{\omega_3}{\varepsilon^2}\left(a_3 + b_3 z^2\right)\dot{z} = \frac{\omega_3}{\varepsilon^2}\gamma_2\left(1 + g_3 z^2\right)\dot{y}$$

2.2 Direct partition of motion (DPM)

The main idea of DPM is that the solution is partitioned into a slow motion and a fast motion. In other words, one assumes that the solution can be written as a sum of two functions: a function changing on the slow time scale only, and another function changing on the fast time scale as well as the slow time scale. Here the slow time scale refers to the time scale of the free response of an oscillator, while the fast time scale refers to that of the fast excitation that the oscillator is subjected to. In problems of fast excitation, one is mainly interested in the slow dynamics, that is, the slow component of the solution, and the fast component is interesting only in how it affects the dynamics of the slow component. For the system described by Eqs.(2.4), the x oscillator can be considered to be subject to fast excitation by the y oscillator, and similarly, the y oscillator can be seen to be subject to fast excitation by the z oscillator. Accordingly, we will look for a solution partitioned in the following manner:

$$\begin{aligned} x &= X(t_1) + \varepsilon\xi(t_1, t_2, t_3) \\ y &= Y(t_2) + \varepsilon\eta(t_1, t_2, t_3) \\ z &= Z(t_3) + \varepsilon\zeta(t_1, t_2, t_3) \end{aligned} \tag{2.5}$$

The aim is to investigate the dynamics of the leading order motions X, Y and Z. We start by substituting Eqs.(2.5) into Eqs.(2.4). Terms of like powers of ε are

collected and then the key assumptions of DPM are utilized [4, 15, 30]. These key assumptions can be stated as follows:

1. ξ is periodic and has a zero average over the t_2 and t_3 time scales.
2. η is periodic and has a zero average over the t_3 timescale.

These assumptions lead to the following conditions on ξ and η:

$$\langle\xi\rangle_2 = \left\langle\frac{\partial\xi}{\partial t_2}\right\rangle_2 = \left\langle\frac{\partial^2\xi}{\partial t_2^2}\right\rangle_2 = \langle\xi\rangle_3 = \left\langle\frac{\partial\xi}{\partial t_3}\right\rangle_3 = \left\langle\frac{\partial^2\xi}{\partial t_3^2}\right\rangle_3 = \langle\eta\rangle_3 = \left\langle\frac{\partial\eta}{\partial t_3}\right\rangle_3 = \left\langle\frac{\partial^2\eta}{\partial t_3^2}\right\rangle_3 = 0 \tag{2.6}$$

Where the two operators $\langle\bullet\rangle_2$ and $\langle\bullet\rangle_3$ are defined to be the average over one period of oscillations on the t_2 and t_3 time scales, respectively. Denoting those periods by T_2 and T_3:

$$\langle\bullet\rangle_2 = \frac{1}{T_2}\int_0^{T_2}\bullet\, dt_2 \quad , \quad \langle\bullet\rangle_3 = \frac{1}{T_3}\int_0^{T_3}\bullet\, dt_3$$

The calculations performed are algebraically complicated and typical of DPM calculations [4, 15, 30]. We present the details in appendix A.1, with the result that the coupled system in Eqs.(2.4) is transformed to the following equations governing X,Y,Z and ξ,η,ζ:

$$\frac{d^2X}{dt_1^2} + X + \left(a_1 + b_1X^2\right)\frac{dX}{dt_1} - 2\gamma_1 g_1\omega_2 X\left\langle\xi\frac{dY}{dt_2}\right\rangle_2 = 0 \tag{2.7}$$

$$\frac{d^2Y}{dt_2^2} + Y + \left(a_2 + b_2Y^2\right)\frac{dY}{dt_2} - 2\gamma_2 g_2\frac{\omega_3}{\omega_2}Y\left\langle\eta\frac{dZ}{dt_3}\right\rangle_3 = 0 \tag{2.8}$$

$$\frac{d^2Z}{dt_3^2} + Z + \left(a_3 + b_3Z^2\right)\frac{dZ}{dt_3} = 0 \tag{2.9}$$

$$\frac{\partial^2\xi}{\partial t_2^2} - \frac{\gamma_1}{\omega_2}\left(1 + g_1X^2\right)\frac{dY}{dt_2} = 0 \tag{2.10}$$

$$\frac{\partial^2\eta}{\partial t_3^2} - \gamma_2\frac{\omega_2}{\omega_3}\left(1 + g_2Y^2\right)\frac{dZ}{dt_3} = 0 \tag{2.11}$$

$$\frac{d^2\zeta}{dt_3^2} + \zeta + \left(a_3 + b_3 Z^2\right)\frac{d\zeta}{dt_3} + 2b_3\zeta\frac{dZ}{dt_3}Z \quad - \gamma_2\left[\left(\frac{\omega_2}{\omega_3}\frac{dY}{dt_2} + \frac{d\eta}{dt_3}\right)\left(1 + g_3 Z^2\right)\right] = 0 \quad (2.12)$$

Recall that our goal is to understand the motion of X,Y and Z. Note that Eq.(2.9) governing Z, is independent of ζ, unlike Eq.(2.7) on X and Eq.(2.8) on Y which depend on ξ and η, respectively. Thus we will not need to solve Eq.(2.12) on ζ, which we nevertheless list here for completeness.

2.3 Solving for X, Y and Z

The equations listed at the end of the previous section can be tackled successively. First we will seek an approximate solution for the Z equation, since it is uncoupled from X and Y. This allows us to solve Eq.(2.11) for an expression of η in terms of Y and t_3. Plugging the expression for η and Z into Eq.(2.8) allows us to evaluate the definite integral and solve for an approximate expression for Y. Again, plugging the obtained expression for Y in Eq.(2.10) provides an expression for ξ in terms of X and t_2. Then, plugging the expression for ξ and Y into Eq.(2.7) allows us to evaluate the corresponding definite integral and solve for an approximate solution for X. For the convenience of the reader we present the final results here, and give the details of the described process in appendix A.2.

- The limit cycle solution for the Z equation is approximated as:

$$Z(t_3) \approx C_3 \cos(t_3) \quad , \quad C_3 = 2\sqrt{-\frac{a_3}{b_3}} \quad (2.13)$$

- The equation governing Y takes the following form:

$$\frac{d^2Y}{dt_2^2} + \alpha_2 Y + \beta_2 Y^3 + \left(a_2 + b_2 Y^2\right)\frac{dY}{dt_2} = 0 \quad (2.14)$$

$$\text{where} \quad \alpha_2 = 1 + \gamma_2^2 C_3^2 g_2 = 1 - 4\gamma_2^2\frac{a_3}{b_3}g_2 \quad , \quad \beta_2 = \gamma_2^2 C_3^2 g_2^2 = -4\gamma_2^2\frac{a_3}{b_3}g_2^2$$

The latter equation admits an approximate steady state solution that can be written as a Jacobi elliptic function:

$$Y(t_2) \approx C_2 \mathrm{cn}(A_2 t_2, k_2) \tag{2.15}$$

where $A_2^2 = \alpha_2 + \beta_2 C_2^2$, $k_2^2 = \dfrac{\beta_2 C_2^2}{2A_2^2}$, $\alpha_2 = 1 - 4\gamma_2^2 \dfrac{a_3}{b_3} g_2$, $\beta_2 = -4\gamma_2^2 \dfrac{a_3}{b_3} g_2^2$

Here, C_2 is the amplitude of the solution, the coefficient A_2 affects the frequency of the solution, and the modulus k_2 affects both the amplitude and frequency of the solution. The above expressions for A_2 and k_2 in terms of C_2 represent the frequency-amplitude relation for the solution.

The amplitude C_2 is a root of a Melnikov integral [24] and takes the value of the solution to the following equation:

$$H_2 = a_2 \mathrm{I}_1(k_2) + b_2 C_2^2 \mathrm{I}_2(k_2) = 0 \tag{2.16}$$

where $\mathrm{I}_1(k_2) = \dfrac{1}{3k_2^2}\left[\left(2k_2^2 - 1\right)\mathrm{E}(k_2) + \left(1 - k_2^2\right)\mathrm{K}(k_2)\right]$

$$\mathrm{I}_2(k_2) = \frac{1}{15k_2^4}\left[2\left(k_2^4 - k_2^2 + 1\right)\mathrm{E}(k_2) - \left(k_2^4 - 3k_2^2 + 2\right)\mathrm{K}(k_2)\right]$$

k_2 denotes the value of the modulus corresponding to C_2, $\mathrm{K}(k)$ is the complete elliptic integral of the first kind and $\mathrm{E}(k)$ is the complete elliptic integral of the second kind.

Such a limit cycle solution has a period T_2 expressed as:

$$T_2 = \frac{4\mathrm{K}(k_2)}{A_2}$$

From Eqs.(2.15) and (2.16), we can see that the steady state behavior of Y depends only on a_2, b_2, a_3, b_3, g_2 and γ_2.

It is worth noting that while the uncoupled y oscillator in Eqs.(2.1) has only one equilibrium point at the origin, Eq.(2.14) shows that Y can posses two additional equilibrium points given by :

$$Y = Y^* = \pm\sqrt{\frac{-\alpha_2}{\beta_2}} \quad , \quad \frac{dY}{dt_2} = 0 \tag{2.17}$$

Such a change of the number of equilibrium points of a system is a well known non-trivial effect of fast excitation [31]. We can see that these equilibrium points exist only if α_2 and β_2 have opposite signs.

- The equation governing X takes the following form:

$$\frac{d^2X}{dt_1^2} + \alpha_1 X + \beta_1 X^3 + \left(a_1 + b_1 X^2\right)\frac{dX}{dt_1} = 0 \tag{2.18}$$

$$\text{where} \quad \alpha_1 = 1 - 2\gamma_1^2 g_1 F \quad , \quad \beta_1 = -2\gamma_1^2 g_1^2 F$$

$$F = \frac{4C_2^2}{A_2^2 k_2^2 T_2}\left[\left(1 - k_2^2\right)\mathrm{K}(k_2) - \mathrm{E}(k_2)\right]$$

Note that the equation governing X is analogous in form to the Y equation and is treated similarly. Then, an approximate steady state solution for X can be written as:

$$X(t_1) \approx C_1 \mathrm{cn}(A_1 t_1, k_1) \tag{2.19}$$

$$\text{where} \quad A_1^2 = \alpha_1 + \beta_1 C_1^2 \quad , \quad k_1^2 = \frac{\beta_1 C_1^2}{2A_1^2} \quad , \quad \alpha_1 = 1 - 2\gamma_1^2 g_1 F \quad , \quad \beta_1 = -2\gamma_1^2 g_1^2 F$$

where, C_1 is a solution to the following equation:

$$H_1 = a_1 \mathrm{I}_1(k_1) + b_1 C_1^2 \mathrm{I}_2(k_1) = 0 \tag{2.20}$$

$$\text{with} \quad \mathrm{I}_1(k_1) = \frac{1}{3k_1^2}\left[\left(2k_1^2 - 1\right)\mathrm{E}(k_1) + \left(1 - k_1^2\right)\mathrm{K}(k_1)\right]$$

$$\mathrm{I}_2(k_1) = \frac{1}{15k_1^4}\left[2\left(k_1^4 - k_1^2 + 1\right)\mathrm{E}(k_1) - \left(k_1^4 - 3k_1^2 + 2\right)\mathrm{K}(k_1)\right]$$

The corresponding period of X in t_1 is:

$$T_1 = \frac{4\mathrm{K}(k_1)}{A_1}$$

Again, while the uncoupled x oscillator in Eqs.(2.1) has only one equilibrium point at the origin, Eq.(17) shows that X can posses two additional equilibrium points given by :

$$X = X^* = \pm\sqrt{\frac{-\alpha_1}{\beta_1}} \quad , \quad \frac{dX}{dt_1} = 0 \tag{2.21}$$

These equilibrium points exist only if α_1 and β_1 have opposite signs. From Eqs.(2.19) and (2.20), we can see that the steady state behavior of X depends on the following parameters: a_i and b_i for i=1,2,3, as well as g_i and γ_i for i=1,2.

2.4 Bifurcation of limit cycles

Notice that there are many parameters in the obtained results. In this section we discuss the effect of varying the coupling strengths γ_1 and γ_2 while holding the other parameters fixed. From Eq.(2.14), we can see that the behavior of Y does not depend on γ_1. However, as γ_2 is varied while the other parameters are fixed, α_2 and β_2 vary. Detailed analysis of the codimension two bifurcation that occurs in a system of the form of Eq.(2.14) can be found in the literature [14]. In particular, for certain parameter values there exists an unstable limit cycle solution, in addition to the stable one [14]. This unstable limit cycle is born through a Hopf bifurcation followed by a homoclinic bifurcation [14]. When that unstable limit cycle is first born, it encloses the origin and has a smaller amplitude than the stable limit cycle. As parameters are furthur varied, the two limit cycles

approach each other until they suddenly coalesce and disappear [14]. Once the cycles disappear, the only stable attractors for the system are the two equilibrium points given in Eq.(2.17).

It is found that as γ_2 is increased, the period of oscillation of the y oscillator increases, and for γ_2 equal to a critical value $\gamma_{2_{cr}}$, the limit cycle suddenly disappears. That is, for $\gamma_2 \geq \gamma_{2_{cr}}$, Eq.(2.16) has no real solution. Similarly, holding all other parameters fixed, as γ_1 is increased, α_1 and β_1 in Eq.(2.18) vary. Then the equation governing X undergoes the same bifurcations as the Y equation. It is found that as γ_1 is increased the period of the x oscillations increases and then the limit cycle of x suddenly disappears for γ_1 equal to a critical value $\gamma_{1_{cr}}$. That is, for $\gamma_1 \geq \gamma_{1_{cr}}$, Eq.(2.20) has no real solution.

While the Y equation is independent of γ_1, the X equation depends on both γ_2 and γ_1. This is because the X equation depends implicitly on the amplitude and period of Y through the factor F, as expressed in Eq.(2.18). Consequently, the value of $\gamma_{1_{cr}}$ varies as γ_2 is varied. The diagram in Fig.2.2 summarizes the dependence of the existence of stable limit cycle solutions for X and Y on the value of γ_1 and γ_2. The rest of the parameters were fixed to the following typical values:

$$a_1 = a_2 = a_3 = -0.1 \ , \ \ b_1 = b_2 = b_3 = 0.5$$

$$g_1 = g_2 = g_3 = -0.5 \ , \ \ \omega_1 = \omega_2 = \omega_3 = 1$$

$$\varepsilon = 0.04$$

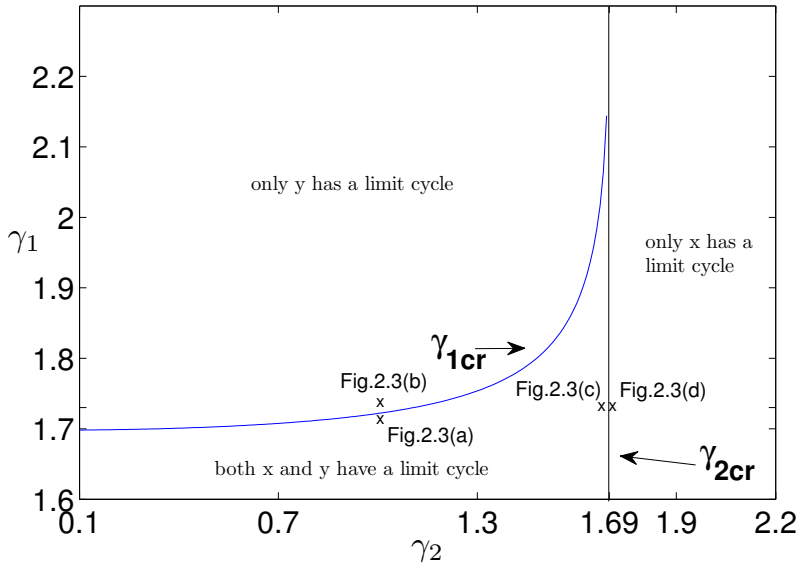

Figure 2.2: Regions are displayed in the γ_1 ,γ_2 plane for which different steady state solutions exist. The $\gamma_{1_{cr}}$ and $\gamma_{2_{cr}}$ curves are the boundaries on which bifurcations occur. ($\varepsilon = 0.04$.)

2.5 Numerical validation

In order to check the approximate formal solution that we obtained, we compare it to that from the numerical integration of Eqs.(2.4). Throughout this section, the other parameters are fixed to the set of values given in the previous section. Figures 2.3(a), (b), (c) and (d) show the approximate formal solution compared to that obtained from numerical integration. In all these plots, dotted lines correspond to the approximate formal solution of the X,Y and Z equations, and solid lines correspond to numerical solutions of the full system in Eqs.(2.4).

For a fixed $\gamma_2 = 1$, as γ_1 is increased, we can see that the limit cycle of x disappears for $\gamma_1 = 1.73$ (Fig.2.3(b)). Now, if instead, we fix $\gamma_1 = 1.73$ but increase γ_2, x regains its limit cycle solution as shown in Fig.2.3(c). As γ_2 is increased further,

as in Fig.2.3(d), the limit cycle of the y oscillator disappears. Thus, the appear-

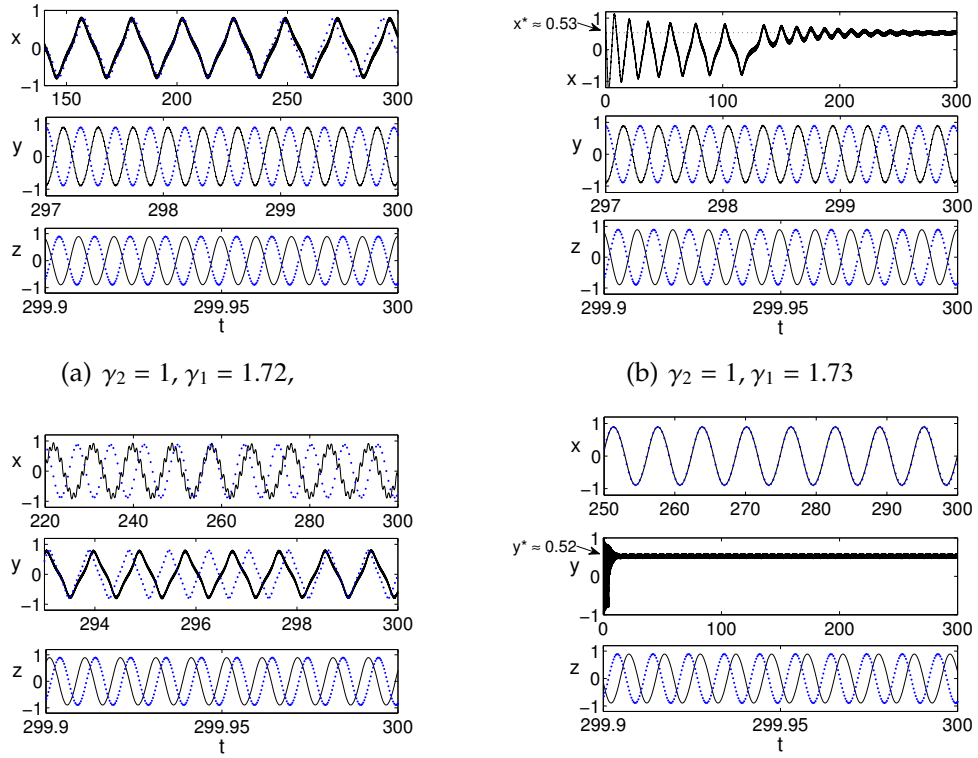

(a) $\gamma_2 = 1, \gamma_1 = 1.72$,

(b) $\gamma_2 = 1, \gamma_1 = 1.73$

(c) $\gamma_2 = 1.69, \gamma_1 = 1.73$

(d) $\gamma_2 = 1.7, \gamma_1 = 1.73$

Figure 2.3: Approximate formal solution (dotted lines) compared to that obtained from numerical integration of Eqs.(2.4) (solid lines); $\varepsilon = 0.04$

ance of limit cycles in the numerical solution agrees well with the bifurcation predictions obtained from the approximate formal solution. The observed difference in oscillation period between numerical and perturbation solutions (see e.g. x in Fig.2.3(a) and y in Fig.2.3(c)) is due to the approximate nature of the perturbation method, which involves a formal expansion of frequency in a power series in ϵ, and which produces inaccuracies due to the assumption that $\epsilon << 1$. Note that since the system is autonomous, the phase of the steady state periodic solution is arbitrary, which accounts for the difference in phase between numerical and perturbation solutions when the oscillation periods agree, e.g. y and z

in Fig.2.3(a).

2.6 Conclusion

The assumptions of DPM were employed to study the dynamics of three coupled nonlinear oscillators. The oscillators, when uncoupled, have a steady state limit cycle solution due to a Van der Pol type nonlinearity. The frequencies of these limit cycle solutions are widely separated such that $\omega_1 = O(1)$, $\omega_2 = O(1/\varepsilon)$ and $\omega_3 = O(1/\varepsilon^2)$, where $\varepsilon << 1$. To leading order, the approximate motion of each of the oscillators is found to be only affected by the coupling to a faster oscillator. So the fastest oscillator with frequency ω_3 is unaffected by the coupling to the slower oscillator, while the amplitude and the frequency of the limit cycles of the other two oscillators with frequencies ω_1 and ω_2 are found to vary as the strength of the nearest neighbor coupling is varied. We note that in a system of two such coupled oscillators, the faster oscillator acts like a forcing function and the system behaves like a forced single degree of freedom system comparable to that studied by Bourkha and Belhaq [5].

The steady state limit cycle motions of oscillators 1 and 2 take the form of a Jacobi elliptic function. It was shown that for coupling strength greater than certain critical values, such a stable limit cycle solution of one of the oscillators disappears. It is worth noting that since the fastest oscillator is unaffected by the form of coupling used, replacing the fastest oscillator by an external harmonic forcer of the same amplitude and frequency would lead to a non-autonomous system of two coupled oscillators with a similar behavior to the system considered here.

Finally, we note that the particular bifurcations that occur in such a system are highly dependent on the form of the coupling used. The coupling used here had the form of $(1 + gx^2)$ that is reminiscent of the linearization of the cosine function that often appears multiplying a fast forcer function in problems of mechanics and leads to the birth of new equilibrium points [31]. When the equation of a slow oscillator is averaged over a faster timescale, any fast variable present in that equation will average out to zero or a constant unless it multiplies another fast function, e.g. the fast component of motion. This is because according to the DPM assumptions, any fast component is to have zero average over that fast timescale. This leads to the need for a mixed nonlinear coupling term in order for nontrivial effects to occur. We expect different bifurcations to occur if different forms of nonlinear coupling are used.

CHAPTER 3

DYNAMICS OF A MASS-SPRING-PENDULUM SYSTEM WITH VASTLY DIFFERENT FREQUENCIES [28]

We investigate the dynamics of a simple pendulum coupled to a horizontal mass-spring system. The spring is assumed to have a very large stiffness value such that the natural frequency of the mass-spring oscillator, when uncoupled from the pendulum, is an order of magnitude larger than that of the oscillations of the pendulum. A well known variation of the mass-spring-pendulum system at hand is that in which the spring is constrained to move vertically instead of horizontally. It is known in the literature as a typical example in which auto parametric resonance can occur [32], that is, the system exhibits interesting dynamics if the ratio of the frequencies of the two degrees of freedom is 2:1 or 1:1; in such studies, the case in which the frequencies are widely separated is not given any attention. Another system similar to the one we study here is a mathematical model of two coupled Huygens's clocks; the system represents two pendula hanging from a rigid beam support that is connected on one side to a wall through a linear spring [3]. Again in the latter system, the frequency of the linear support system is considered to be of the same order of magnitude as that of the pendula.

Examples of a nonlinear oscillator coupled to a much faster oscillator are present in the literature [21, 27, 33]. However, in these previous studies, the leading order dynamics of the fast oscillator is unaffected by the slow oscillator, so the standard method of averaging was used to analyze the dynamics. This is not the case for the system we study here, as the amplitude and frequency of the fast oscillation, to leading order, are found to be a function of the amplitude of

the slow oscillation. We apply DPM to study the dynamics of the slow oscillator. Then the equation of the fast degree of freedom appears to be describing a fast oscillator with a slowly varying frequency, for which the WKB method is particularly suited. This motivates the use of a transformation of fast time, analogous to that proposed by the WKB method [34], that leads to an expression for the fast oscillator in terms of the slow one. We particularly study the motions in which the amplitude of the motion of the harmonic oscillator is an order of magnitude smaller than that of the pendulum. In this regime, a pitchfork bifurcation of periodic orbits is found to occur for energy values larger that a critical value. The bifurcation gives rise to non-local periodic and quasi-periodic orbits in which the pendulum oscillates about an angle between zero and $\pi/2$ from the downwards position. The bifurcating periodic orbits are nonlinear normal modes of the coupled system and correspond to fixed points of a Poincare map. An approximate expression for the value of the new fixed points of the map is obtained. These formal analytic results are confirmed by comparison with numerical integration.

In section 3.1, we present the system of equations representing the mass-spring-pendulum that we consider, and the scaled equations that correspond to the relevant regime of small motions of the mass-spring oscillator; we also illustrate the non-trivial solutions that the system exhibits. Appendix B.1 explains the motivation for the proposed form of solution while section 3.2 presents the end result of the DPM procedure in the form of an autonomous equation governing the leading order slow oscillation; we also present the approximate expression of the leading order fast oscillation. The details of obtaining the latter are presented in appendix B.3, while the DPM implementation is detailed in appendix

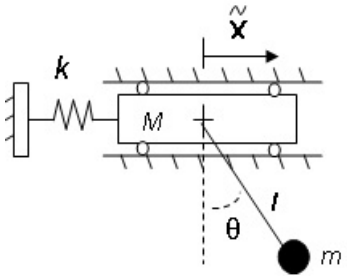

Figure 3.1: Schematic for the mass-spring-pendulum system

B.2. In section 3.3, we discuss the bifurcation that occurs in the slow dynamics and it's relation to the bifurcation in a Poincare map of the full system (Eqs.(3.1)). The details of the analysis of the slow dynamics and the predictions based on it are presented in Appendices B.4 and B.5. Section 3.4 briefly summarizes the main results. Then, in section 3.5, we compare the approximate solution to that from numerical integration of the full system (Eqs.(3.1)) and try to check the validity of the predictions we make based on the approximate solution.

3.1 The mass-spring-pendulum system

We consider a simple pendulum whose point of suspension is connected to a mass on a spring that is restricted to move horizontally, as shown in Fig.3.1. Ignoring dissipation, the system is governed by the following equations of motion:

$$ml^2\theta'' + ml\tilde{x}'' \cos\theta + mgl \sin\theta = 0$$

$$(M+m)\,\tilde{x}'' + ml\theta'' \cos\theta - ml\theta'^2 \sin\theta + k\tilde{x} = 0$$

where primes denotes differentiation with respect to time τ. We introduce the following change of variables:

$$x = \frac{\tilde{x}}{l} \quad , \quad t = \sqrt{\frac{g}{l}}\tau$$

The nondimensionalized equations, which we refer to as the full system, become:

$$\ddot{\theta} + \sin\theta = -\ddot{x}\cos\theta$$

$$\ddot{x} + \tilde{\Omega}^2 x = -\mu\left(\ddot{\theta}\cos\theta - \dot{\theta}^2\sin\theta\right) \tag{3.1}$$

$$\text{where} \quad \mu = \frac{m}{M+m} \quad , \quad \tilde{\Omega}^2 = \frac{kl}{g\,(M+m)}$$

where dots represent differentiation with respect to time t.

3.1.1 Assumptions

We are interested in the case where the linear oscillator has a natural frequency that is an order of magnitude larger than the linearized frequency of the pendulum, and its motion has an amplitude that is an order of magnitude smaller than that of the pendulum. This is implemented through the following rescaling:

$$x = \varepsilon\chi \quad , \quad \tilde{\Omega}^2 = \frac{\Omega^2}{\varepsilon^2}$$

Here, Ω and χ are $O(1)$ quantities while $\varepsilon << 1$. Without loss of generality, we take $\Omega = 1$. The rescaled equations become:

$$\ddot{\theta} + \sin\theta = -\varepsilon\ddot{\chi}\cos\theta$$

$$\ddot{\chi} + \frac{1}{\varepsilon^2}\chi = -\frac{\mu}{\varepsilon}\left(\ddot{\theta}\cos\theta - \dot{\theta}^2\sin\theta\right) \tag{3.2}$$

This system has a conserved quantity that can be expressed as:

$$h = \frac{1}{2}\varepsilon^2\dot{\chi}^2 + \frac{1}{2}\mu\dot{\theta}^2 + \mu\varepsilon\dot{\chi}\dot{\theta}\cos\theta + \frac{1}{2}\chi^2 + \mu\,(1-\cos\theta)$$

3.1.2 Typical solutions

We numerically integrate the full system in Eqs.(3.1), for typical parameter values and initial conditions (IC's), in order to illustrate the type of nontrivial solutions that it exhibits. As an example, we take $\mu = 0.4$ and $\tilde{\Omega} = 50$ ($\varepsilon = 0.02$). Since the system is conservative, we will look at how the dynamics change as the energy is increased.

For $h = 0.5$, we choose the following set of initial conditions:

$$\begin{cases} \dot{\theta}(0) = 0 \\ \theta(0) = \pi/9 \approx 0.349 \end{cases}, \begin{cases} \dot{x}(0) = 0 \\ x(0) = \varepsilon(0.9756) \approx 0.0195 \end{cases} \tag{3.3}$$

For the IC's in Eqs.(3.3), the pendulum oscillates about the downwards posi-

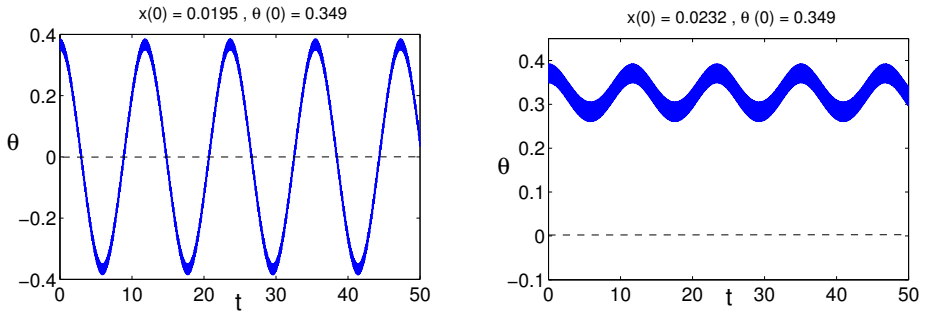

(a) IC's in Eqs.(3.3) (b) IC's in Eqs.(3.4)

Figure 3.2: Plot of θ vs. time for different initial conditions

tion $\theta = 0$, it's motion consists of a slow oscillation overlaid with a small fast oscillation, as shown in Fig.3.2(a); Fig.3.3(a) shows how the amplitude of the fast mass-spring oscillation is slowly modulated.

Fig.3.4(a) shows the Poincare map for the energy level $h = 0.5$, and the arrow points at the orbit corresponding to the IC's in Eqs.(3.3). The shown fixed point

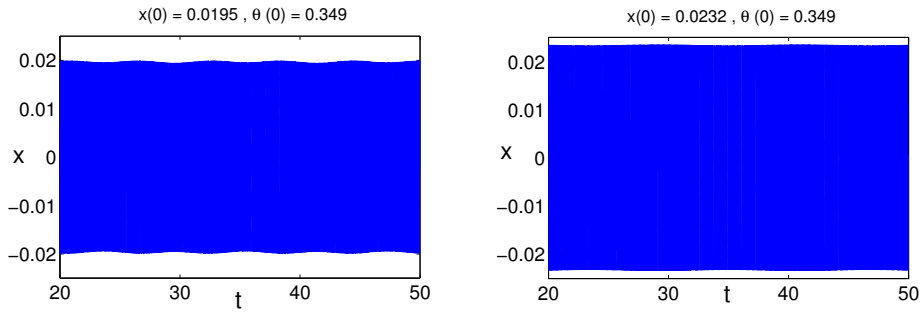

(a) IC's in Eqs.(3.3) (b) IC's in Eqs.(3.4)

Figure 3.3: Plot of x vs. time for different initial conditions

(center) of the map corresponds to a periodic orbit in which $\theta \approx -x$. This periodic orbit is a nonlinear normal mode of the coupled system that appears as a nearly straight line through the origin if viewed in the configuration plane θ vs. x. Now we look at the dynamics for $h = 0.7$, and choose the following set of

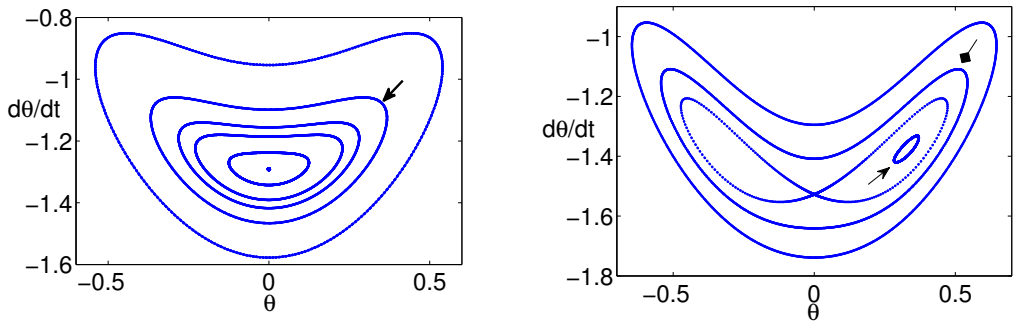

(a) $h = 0.5$ (b) $h = 0.7$

Figure 3.4: Poincare map ($x = 0$, $\dot{x} > 0$) for different energy values

initial conditions:

$$\begin{cases} \dot{\theta}(0) = 0 \\ \theta(0) = \pi/9 \approx 0.349 \end{cases}, \begin{cases} \dot{x}(0) = 0 \\ x(0) = \varepsilon(1.1626) \approx 0.0233 \end{cases} \tag{3.4}$$

Fig.3.2(b) shows how the slow oscillation, overlaid by a small fast oscillation, is now no longer about the origin. Instead, the pendulum oscillates about an angle ≈ 0.33. The amplitude of the fast mass-spring oscillation is still slowly

modulated but to a barely perceptible extent, as shown in Fig.3.3(b). It will later be clear that this is because the corresponding variation in the amplitude of θ is rather small, as shown in Fig.3.2(b).

Keeping the energy fixed at $h = 0.7$, we choose a different set of IC's:

$$\begin{cases} \dot{\theta}(0) = 0 \\ \theta(0) = \pi/6 \approx 0.5236 \end{cases}, \begin{cases} \dot{x}(0) = 0 \\ x(0) = \varepsilon(1.1370) \approx 0.0227 \end{cases} \tag{3.5}$$

As shown in Fig.3.5(a), the pendulum is back to oscillating about the downwards position and the modulation of the amplitude of x shown in Fig.3.5(b) is again visible. Fig.3.4(b) shows the Poincare map for $h = 0.7$. The arrows point

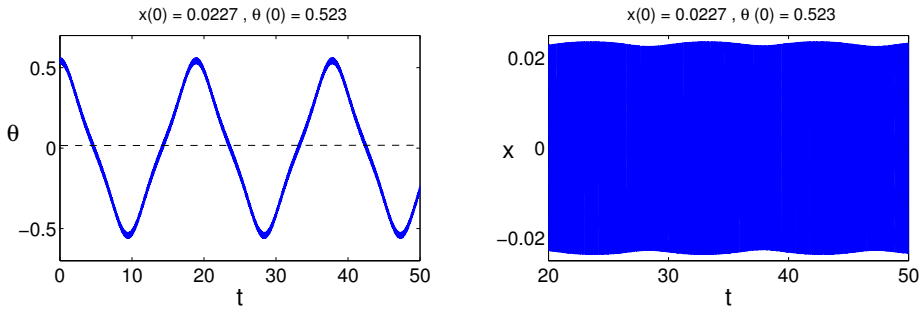

(a) θ vs. time (b) x vs. time

Figure 3.5: Numerical solution for the initial conditions in Eqs.(3.5)

to the orbits corresponding to the solutions in Fig.3.2(b) (pointed arrow) and Fig.3.5(a) (square head arrow). We can see from the Poincare map that the fixed point corresponding to the nonlinear normal mode with $\theta \approx -x$ has lost stability and is now a saddle point of the map. Consequently, we can predict that two new fixed points (centers) were born in the process, and that the oscillations of the pendulum about a non-zero angle correspond to closed orbits of the map about the new centers.

The aim of this paper is to shed light on these latter non-trivial solutions, in which the pendulum oscillates about a non-zero angle, and describe their dependence on initial conditions and the parameter μ.

3.2 The approximate solution

We look for a solution in which the slow oscillation is partitioned according to the method of direct partition of motion[4]:

$$\begin{cases} \chi = \chi(\xi, T) \\ \theta(\xi, T) = \theta_0(\xi) + \varepsilon\theta_1(\xi, T) \end{cases} \tag{3.6}$$

$$\text{where } \xi = t \ , \ \frac{dT}{dt} = \frac{\omega(\xi)}{\varepsilon} \quad \text{or } T = \int_0^{\xi} \frac{\omega(t')}{\varepsilon} dt' \tag{3.7}$$

$$\& \ \omega(\xi) = \frac{1}{\sqrt{1 - \mu\cos^2\theta_0}} \tag{3.8}$$

Here, we have introduced a new fast timescale, T, in a way similar to the WKB method[34]; the choice of $\omega(t)$ is justified in appendix B.3.

After applying the standard DPM procedure[4], we find that, to leading order, θ_0 is governed by the following equation (see appendix B.2 for the details):

$$\frac{d^2\theta_0}{d\xi^2} + \sin\theta_0 - \frac{1}{2}C^2 \frac{\cos\theta_0 \sin\theta_0}{(1 - \mu\cos^2\theta_0)\sqrt{1 - \mu\cos^2\theta_0}} = 0 \tag{3.9}$$

θ_1 is found to depend on θ_0 and χ as follows:

$$\theta_1 = -\chi\cos\theta_0 \tag{3.10}$$

Also, to leading order, χ is given by (see appendix B.3 for the details):

$$\chi \approx C\sqrt{\omega(\xi)}\cos T \tag{3.11}$$

where C is an arbitrary constant that depends on initial conditions. Consequently, the motion of the pendulum, in the rescaled system described by Eqs.(3.2), can be expressed as:

$$\theta \approx \theta_0 - \varepsilon\chi \cos\theta_0$$

where θ_0 is governed by Eq.(3.9) and χ is given by Eq.(3.11).

Recall that Eqs.(3.2) are a rescaled version of the original system of interest given by Eqs.(3.1), where χ is related to the motion of the mass-spring oscillator as follows:

$$x = \varepsilon\chi$$

Hence, the solution to Eqs.(3.1), for the assumed regime of motion, can be expressed in terms of the variables of Eqs.(3.1) as follows:

$$\theta \approx \theta_0 - x \cos\theta_0 \tag{3.12}$$

$$x \approx \varepsilon C \sqrt{\omega(\xi)} \cos T \tag{3.13}$$

3.3 The slow dynamics

At the end of the procedure that is described in Appendices B.2 and B.3, the solution to the two degree of freedom mass-spring-pendulum system is expressed in Eqs.(3.12) & (3.13) in terms of θ_0, the leading order slow motion of the pendulum, which is governed by the following equation:

$$\frac{d^2\theta_0}{d\xi^2} + \sin\theta_0 - \frac{1}{2}C^2 \frac{\cos\theta_0 \sin\theta_0}{(1-\mu\cos^2\theta_0)\sqrt{1-\mu\cos^2\theta_0}} = 0$$

The arbitrary constant C that appears in the equation can be expressed in terms of the initial conditions. For initial zero velocities, the initial conditions take the form:

$$\begin{cases} \dot{\theta}(0) = 0 \\ \theta(0) = A \end{cases}, \quad \begin{cases} \dot{x}(0) = 0 \\ x(0) = \varepsilon B \end{cases}$$

$$\Rightarrow \begin{cases} \dot{\theta}_0(0) = 0 \quad , \quad \theta_0(0) \approx A \\ x(0) = \varepsilon B \approx \varepsilon C \sqrt{\omega(0)} \end{cases} \quad \text{with} \quad \omega(0) = \frac{1}{\sqrt{1 - \mu \cos^2 A}}$$

$$\Rightarrow C = B\left(1 - \mu \cos^2 A\right)^{\frac{1}{4}} \tag{3.14}$$

Now, we rewrite the equation governing θ_0 as a system of two first order equations:

$$\dot{\theta}_0 = \phi$$

$$\dot{\phi} = -\sin\theta_0 + \frac{1}{2}C^2 \frac{\sin\theta_0 \cos\theta_0}{(1 - \mu\cos^2\theta_0)\sqrt{1 - \mu\cos^2\theta_0}} \tag{3.15}$$

For small enough values of C, the above system has a neutrally stable equilibrium point (center) at the origin ($\phi = 0, \theta_0 = 0$) and two saddle points at ($\phi = 0, \theta_0 = \pi, -\pi$), so that the phase portrait resembles that of the simple pendulum. As C increases in value, a pitchfork bifurcation takes place, in which the origin becomes a saddle point and two new centers are born. The critical value of C is related to the parameter μ as follows (see appendix B.4 for the details):

$$C_{cr}^2 = 2(1 - \mu)^{\frac{3}{2}} \tag{3.16}$$

In appendix B.4, it is explained how this condition on C translates into the following condition on the energy value h:

$$h_{cr} = 1 - \mu$$

For the value of μ used in section 3.1.2, the critical values of C and h are as follows:

$$\mu = 0.4 \Rightarrow \begin{cases} C_{cr}^2 = 2\,(1-\mu)^{\frac{3}{2}} = 0.9295 \Rightarrow C_{cr} = 0.9641 \\ h_{cr} = 1 - \mu = 0.6 \end{cases}$$

So a qualitative change in the solution is expected as h increases past $h = 0.6$, which explains the difference in solution between $h = 0.5$ and $h = 0.7$, cf. Fig.3.4(a),3.4(b). To illustrate the relation of the solution of the full system (Eqs.(3.1)) to the θ_0 dynamics, we find the value of C for the IC's presented in section 3.1.2. For the IC's in Eqs.(3.3) corresponding to Fig.3.2(a), we have:

$$\begin{cases} A = 0.349 \\ B = 0.9756 \end{cases} \Rightarrow C = B\left(1 - \mu\cos^2 A\right)^{\frac{1}{4}} = 0.8749$$

Fig.3.6(a) shows the corresponding phase portrait for the system in Eqs.(3.15) with this value of C. The slow oscillation of the pendulum in Fig.3.2(a) corresponds to the closed orbit surrounding the origin in this phase portrait. For the

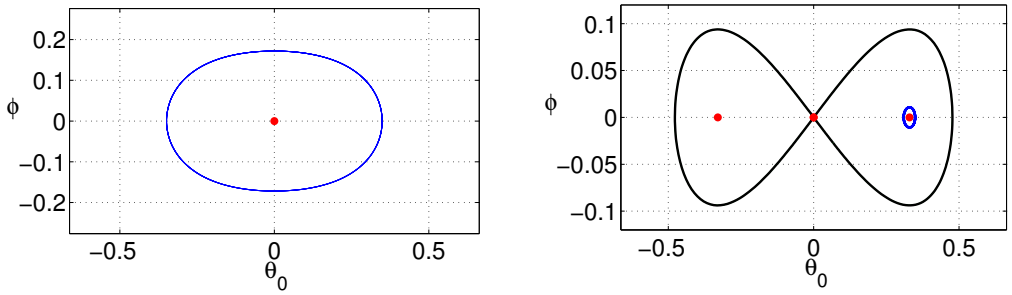

(a) IC's in Eqs.(3.3); $C = 0.8749$ (b) IC's in Eqs.(3.4); $C = 1.0427$

Figure 3.6: Phase portrait for the θ_0 equation for different IC's

IC's in Eqs.(3.4) corresponding to Fig.3.2(b), we have:

$$\begin{cases} A = 0.349 \\ B = 1.1626 \end{cases} \Rightarrow C = B\left(1 - \mu\cos^2 A\right)^{\frac{1}{4}} = 1.0427$$

For this value of C, Fig.3.6(b) shows that the origin is a saddle point and the system in Eqs.(3.15) has two non-trivial neutrally stable equilibrium points (centers). The slow oscillation of the pendulum in Fig.3.2(b) corresponds to the small closed orbit surrounding one of the non-trivial equilibrium points in this phase portrait.

For the same energy levels, different IC's result in different values of C and different orbits in the resulting phase plane. For the IC's in Eqs.(3.5), we get:

$$\begin{cases} A = 0.5236 \\ B = 1.1370 \end{cases} \Rightarrow C = B\left(1 - \mu \cos^2 A\right)^{\frac{1}{4}} = 1.0400$$

The resulting slow oscillation in Fig.3.5(a) corresponds to the closed orbit enclosing the homoclinic orbit in the phase portrait shown in Fig.3.7. This illustrates how, despite the presence of the two non-trivial equilibrium points, oscillations about the origin are still possible and correspond to large amplitude orbits that are outside the homoclinic orbit.

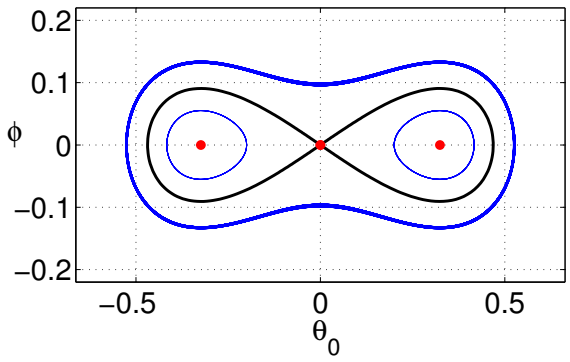

Figure 3.7: Phase portrait for the θ_0 equation for IC's in Eqs.(3.5), corresponding to $C = 1.04$

3.3.1 The predicted nonlinear normal modes

Note that each value of C leads to a phase portrait for Eq.(3.15) that is filled with closed orbits, however, out of those orbits, the only one which corresponds to a solution of the full system (Eqs.(3.1)) is that associated with the specific IC's that led to that value of C.

An interesting case occurs when the choice of IC's results in a phase portrait that has a non-trivial equilibrium point which coincides in value with the initial θ_0 amplitude, A. That is, we start with IC's of the form:

$$\begin{cases} \dot{\theta}(0) = 0 \\ \theta(0) = \theta_0(0) = A \end{cases}, \quad \begin{cases} \dot{x}(0) = 0 \\ x(0) = \varepsilon B \end{cases}$$

and the corresponding value of $C = B\left(1 - \mu\cos^2 A\right)^{\frac{1}{4}}$ results in non-trivial equilibrium points (centers) for the θ_0 equation at:

$$\theta_0 = \pm E \ , \ \phi = 0$$

Then, if $E = A$, θ_0 will remain equal to E for all time. It would mean that we are starting at a neutrally stable equilibrium point of the θ_0 equation, so the solution will remain at that point for all time.

Appendix B.4 shows that these special values of initial θ amplitude can be expressed in terms of h and μ as:

$$\theta(0) = \pm A^* = \pm\cos^{-1}\left(\frac{\mu - h \pm \sqrt{(h-\mu)^2 + 8\mu}}{4\mu}\right) \tag{3.17}$$

The corresponding value of x is expressed as:

$$x(0) = \varepsilon B^* = \varepsilon\sqrt{2\left(h - \mu\left(1 - \cos A^*\right)\right)} \tag{3.18}$$

Hence, we predict that these special initial amplitudes, with zero initial velocities, will lead to a solution in which:

$$\theta \approx A^* - x\cos A^* \tag{3.19}$$

Such a solution would be a nonlinear normal mode of the coupled mass-spring-pendulum system.

3.3.2 Relation of θ_0 to the Poincare map

For a given energy level, the phase portrait of the θ_0 equation is filled with closed orbits and the picture is topologically similar to that of the Poincare map. That is, for a given initial condition, the resulting orbit in the θ_0 phase plane corresponds to a closed orbit in the Poincare map, however, the orbits are not identical. This is due to the fact that, while $\theta \approx \theta_0$, $\dot{\theta}$ differs from $\dot{\theta}_0$ by an $O(1)$ quantity; as shown in appendix B.5, for the points of the Poincare map, $\dot{\theta}$ can be expressed in terms of $\dot{\theta}_0$ as follows:

$$\dot{\theta}_{Pm} \approx \dot{\theta}_0 - C\left(1 - \mu\cos^2\theta_0\right)^{-\frac{3}{4}}\cos\theta_0 \tag{3.20}$$

So for a given set of IC's, we can obtain the corresponding orbit in the Poincare map, by first numerically integrating the θ_0 equation to obtain θ_0 and $\dot{\theta}_0$ and then generating the orbit in the Poincare map by plotting the corresponding values of $\dot{\theta}_{Pm}$ vs. θ_0. This means that we can generate an approximate picture of the Poincare map of the full system (Eqs.(3.1)) by numerically integrating the slow dynamics equation governing θ_0 instead of integrating the full system (Eqs.(3.1)) which contains the fast dynamics and thus requires a much smaller step size of integration.

Also, by comparing this procedure with the results of numerical integration, we can obtain a check on the accuracy of the various approximations made in this work.

3.4 Summary of results

We restate here the original equations governing the considered mass-spring-pendulum system:

$$\ddot{\theta} + \sin\theta = -\ddot{x}\cos\theta$$

$$\ddot{x} + \frac{1}{\varepsilon^2}x = -\mu\left(\ddot{\theta}\cos\theta - \dot{\theta}^2\sin\theta\right)$$

We have shown that $\theta \approx \theta_0 + O(\varepsilon)$ where θ_0 is governed by the following equation:

$$\frac{d^2\theta_0}{dt^2} + \sin\theta_0 - \frac{1}{2}C^2\frac{\cos\theta_0\sin\theta_0}{(1-\mu\cos^2\theta_0)\sqrt{1-\mu\cos^2\theta_0}} = 0$$

where C is a constant that depends on the IC's. x is assumed to be $O(\varepsilon)$ and is found to be expressed as:

$$x \approx \varepsilon C\sqrt{\omega(t)}\cos T$$

$$\text{with}\quad \omega(t) = \frac{1}{\sqrt{1-\mu\cos^2\theta_0}}\quad\text{and}\quad T = \int_0^t \frac{\omega(t')}{\varepsilon}dt'$$

Our analysis gives that a pitchfork bifurcation occurs in a Poincare map ($x = 0$, $\dot{x} > 0$) as energy increases past the following critical value:

$$h_{cr} = 1 - \mu$$

This bifurcation corresponds to a bifurcation in periodic orbits of the full system (Eqs.(3.1)) in which the nonlinear normal mode corresponding to $\theta \approx -x$ loses

stability and two new stable nonlinear normal modes are born in which $\theta \approx A^* - x\cos A^*$, where A^* is expressed in terms of h and μ as:

$$A^* = \pm\cos^{-1}\left(\frac{\mu - h \pm \sqrt{(h-\mu)^2 + 8\mu}}{4\mu}\right)$$

These new nonlinear normal modes correspond to the non-trivial fixed points of the Poincare map.

3.5 Comparison to numerics

We compare the solution resulting from the numerical integration of the original equations with that from the integration of the θ_0 equation. Figs.3.8(a) to 3.10(b) display comparison plots for several initial conditions. Unless otherwise mentioned, we have set $\mu = 0.4$ and $\tilde{\Omega} = 50$ ($\varepsilon = 0.02$). In the plots of θ vs.

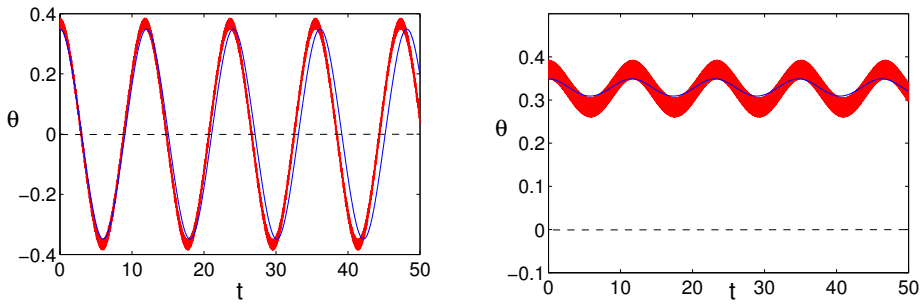

(a) IC's in Eqs.(3.3) (b) IC's in Eqs.(3.4)

Figure 3.8: Comparison plots of θ vs. time for different IC's

time, the thick line corresponds to the solution of the numerical integration of the full system (Eqs.(3.1)), and the apparent thickness is due to the fast component present in the oscillation of the pendulum; the thin line corresponds to the approximate solution, that is from the numerical integration of the θ_0 equation,

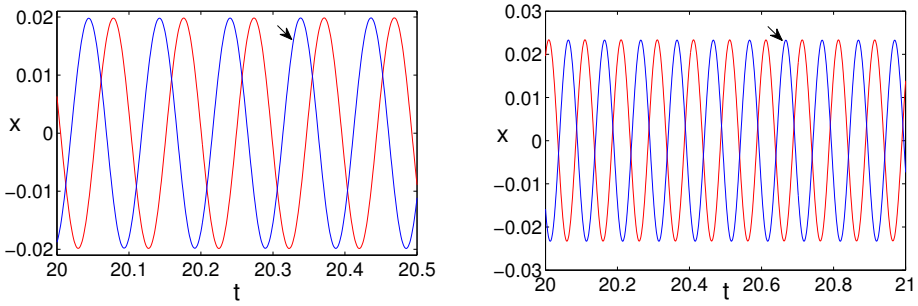

(a) IC's in Eqs.(3.3) (b) IC's in Eqs.(3.4)

Figure 3.9: Comparison plots of x vs. time for different IC's

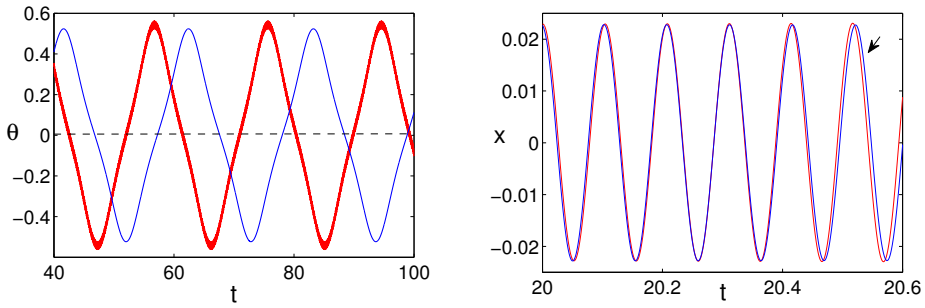

(a) θ vs. time (b) x vs. time

Figure 3.10: Comparison plots for IC's in Eqs.(3.5)

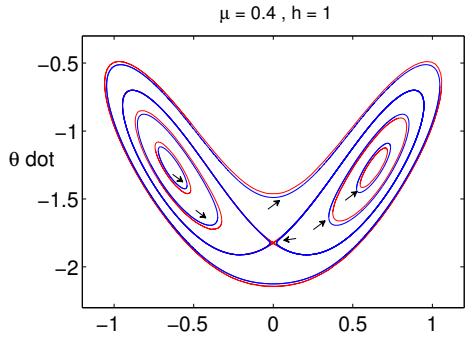

Figure 3.11: Comparison of the predicted Poincare map orbits (arrows) with those from the integration of the full system (Eqs.(3.1))

and captures only the leading order slow component of the pendulum oscillation. In the plots of x vs. time, the arrow points at the approximate solution. Fig.3.11 displays the Poincare map orbits for $h = 1$. Near each of the orbits, a

small arrow points to the orbit which is predicted from the θ_0 equation for corresponding initial conditions. We can see that the approximate solution compares well with that from numerical integration of the full system (Eqs.(3.1)).

3.6 Conclusion

We have used the method of direct partition of motion to study the dynamics of a mass-spring-pendulum system, in which the harmonic oscillator is restricted to move horizontally. We have considered the case where the stiffness of the spring is very large, so that the frequency of the oscillation of the uncoupled harmonic oscillator is an order of magnitude larger than that of the uncoupled pendulum. We have also limited our attention to the regime of motion where the amplitude of motion of the harmonic oscillator is an order of magnitude smaller than that of the pendulum. Under these assumptions, an approximate expression for the solution of the two degree of freedom system is found in terms of θ_0, the leading order slow oscillation of the pendulum. An equation governing θ_0 is presented and found to undergo a pitchfork bifurcation for a critical value of C which is a parameter related to the initial amplitudes of θ and x. It is shown that the pitchfork bifurcation in the slow dynamics equation corresponds to a pitchfork bifurcation of periodic orbits of the full system (Eqs.(3.1)) that occurs as the energy is increased past a critical value which is expressed in terms of the parameter μ. This bifurcation can be seen to occur in a Poincare map of the full system (Eqs.(3.1)), where the fixed point corresponding to the nonlinear normal mode ($\theta \approx -x$) loses stability and two new centers are born in the map. The new centers correspond to new periodic motions, which are nonlinear normal modes with $\theta \approx A^* - x\cos A^*$, where the expression for A^* is found

in terms of μ and h. For these modes, the motion of the pendulum is predicted to be a small fast oscillation about the non-zero value $\theta = A^*$. Along with these special motions, quasi-periodic motions exist in which the pendulum undergoes slow oscillation about a non-zero angle, with overlaid fast oscillation. These latter orbits correspond to closed orbits about the new centers in the Poincare map. A relation between $\dot{\theta}$ and $\dot{\theta}_0$ is given for points of the Poincare map, such that the orbits of the map can be generated approximately by numerically integrating the slow dynamics equation. Finally, the approximate solution, as well as the predications made based on it, are checked against numerical integration of the full system (Eqs.(3.1)) and found to agree well.

CHAPTER 4

ON THE DYNAMICS OF A THIN ELASTICA [29]

We revisit the problem of the thin elastica studied by Cusumano and Moon [11] who presented a two degree of freedom model, representing the first bending and first torsional modes of the elastica. The model was shown to capture much of the behavior observed in the experiments such as loss of planar stability and the existence of non-local modes [11]. A variety of perturbation methods were used to study the elastica model [22], however, that analysis required that the coupling parameter be of $O(\varepsilon)$. This does not apply to the experimental system [11] in which the coupling parameter was ≈ 1.74 which is rather of $O(1)$. The experimental system also had a ratio of frequencies ≈ 44 which can be considered to be of $O(1/\varepsilon)$ where $\varepsilon << 1$. This latter observation implies that the system is best viewed as one with vastly different frequencies and that DPM can be useful for understanding its dynamics. Also, the fact that the coupling is $O(1)$ allows the slow variable to influence the leading order dynamics of the fast variable, which appears as a fast oscillator with a slowly varying frequency. As illustrated in chapter 3, the use of a rescaling of fast time, in a manner that is inspired by the WKB method, allows us to capture such a strong slow modulation of a fast oscillator by a much slower one. This procedure leads us to the new understanding that two basic factors behind the appearance of the non-local modes exhibited by the model are the strong nonlinear inertial coupling and the large difference in frequency between the two degrees of freedom.

In section 4.1, we present the two degree of freedom model of the thin elastica and illustrate the non-local modes that it exhibits. In section 4.2, we present the form of the assumed solution and the end results of the DPM procedure

which consist of an equation governing the leading order dynamics of the slow variable (the bending mode), as well as an expression of the fast variable (the torsional mode) in terms of the slow variable. We also discuss the special solutions corresponding to the non-local modes and present an expression for the critical energy value above which these solutions exist. Finally, in section 4.3, we validate the approximate solution by comparing it to that from numerical integration. The procedure for obtaining the approximate solution is detailed in appendices C.1 and C.2, while appendix C.3 explains how we obtain the expression for the non-local modes and the critical energy value in terms of the parameters.

4.1 The two degree of freedom elastica model

Ignoring dissipation and external forcing, the equations governing the two degree of freedom elastica model presented by Cusumano and Moon [11] are:

$$\ddot{y} + y - \gamma \dot{x}^2 y = 0$$

$$\left(\mu + \gamma y^2\right)\ddot{x} + \mu\Omega^2 x + 2\gamma y\dot{y}\dot{x} = 0 \tag{4.1}$$

where y and x represent the first bending and torsional mode, respectively. μ is a dimensionless parameter related to moment of inertia, γ is a coupling parameter and Ω is the ratio of the dimensionless natural frequencies of the two modes. The conserved energy of the system can be expressed as:

$$h = \frac{1}{2}\left(\mu + \gamma y^2\right)\dot{x}^2 + \frac{1}{2}\dot{y}^2 + \frac{1}{2}\left(\mu\Omega^2 x^2 + y^2\right) \tag{4.2}$$

To illustrate the bifurcation that occurs as energy is increased, giving rise to the non-local modes, we will numerically integrate the system in Eqs.(4.1) with

parameter values that match those reported in the experimental setup [11]:

$$\gamma = 1.74 \quad , \quad \mu = 0.0113 \quad , \quad \Omega = 44$$

We will choose a value of the energy h and take initial conditions of the form:

$$\begin{cases} y(0) = b \quad , \quad x(0) = \sqrt{\frac{(2h-b^2)}{\mu\Omega^2}} \\ \dot{y}(0) = 0 \quad , \quad \dot{x}(0) = 0 \end{cases}$$

Figs.4.1(a) and (b) displays the torsional mode variable, x, which is typically

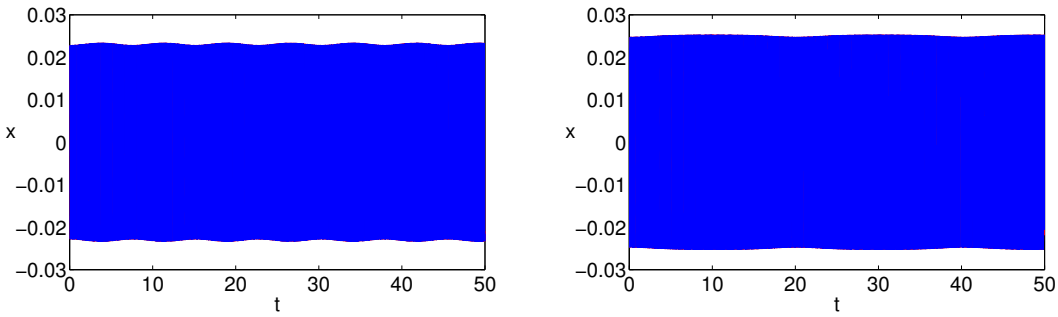

(a) $h = 0.006,\ b = 0.025$ (b) $h = 0.007,\ b = 0.025$

Figure 4.1: Plot of x vs. time for different initial conditions

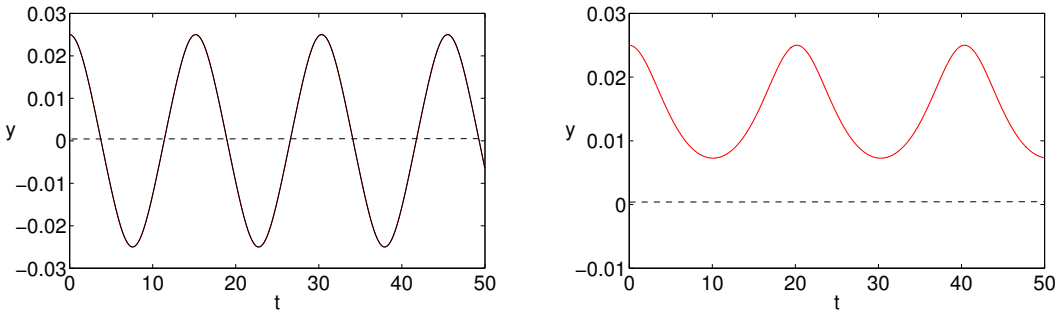

(a) $h = 0.006,\ b = 0.025$ (b) $h = 0.007,\ b = 0.025$

Figure 4.2: Plot of y vs. time for different initial conditions

a fast oscillation with a slowly modulated amplitude. Fig.4.2(a) shows the oscillation of the bending mode variable, y, typical of low enough energies. As

the energy is slightly increased, we can see y undergoing a non-local oscillation having a non-zero mean value, as in Fig.4.2(b). With a careful choice of initial amplitudes, y appears to be almost fixed about a non-zero value as shown in Fig.4.3(a). The latter oscillation corresponds to a non-local mode that arises as the energy increases past a critical value. Still, for a large enough initial amplitude, oscillations about the origin are possible, as illustrated in Fig.4.4. The

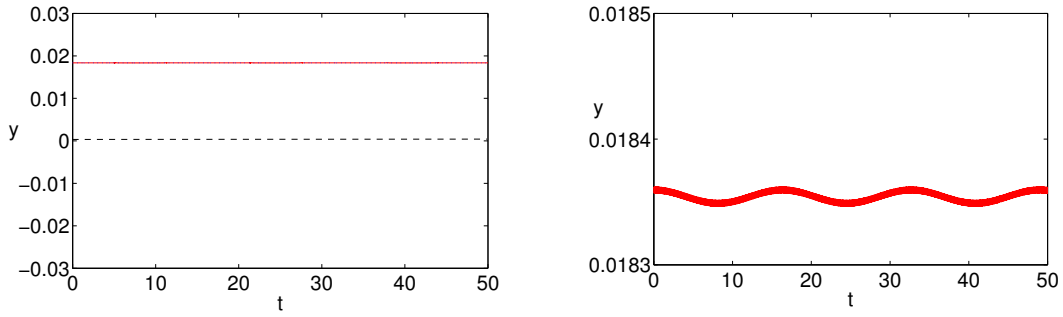

(a) (b) zoom in on the solution

Figure 4.3: Plot of y vs. time for the initial conditions with $h = 0.007$, $b = 0.0184$

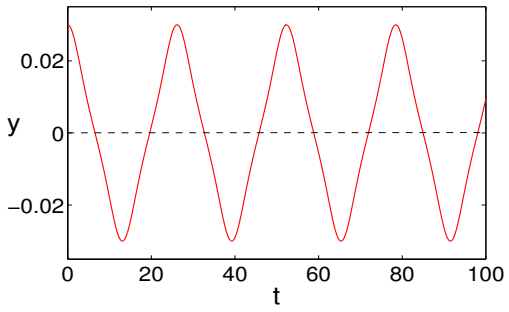

Figure 4.4: Plot of y vs. time for the initial conditions with $h = 0.007$, $b = 0.03$

bifurcation that gives rise to the non-local modes corresponds to a pitchfork bifurcation in a Poincare map of the system, as illustrated in Figs.4.5(a) and (b). As energy increases past a critical value, the fixed point of the map, corresponding

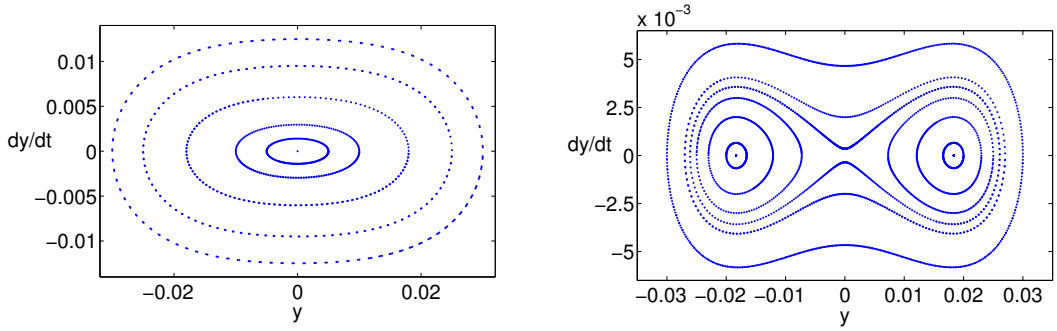

(a) $h = 0.006$ (b) $h = 0.007$

Figure 4.5: Plot of a Poincare map ($x = 0$, $\dot{x} > 0$) for different energy levels

to the torsional mode with $y = 0$, loses stability and two new centers are born corresponding to two non-local modes. Closed orbits about each of these centers correspond to solutions of the type illustrated in Fig.4.2(b), while the large orbits engulfing both centers correspond to oscillations about the origin as in Fig.4.4.

The aim of the paper is to explain the dependence of the solution on initial conditions and the parameters of the system. We will also obtain an expression for the critical energy value at which the bifurcation occurs and an approximate expression for the non-local modes it gives rise to.

4.2 The approximate solution

For the system studied experimentally in [11], $\Omega \approx 44$, so we will assume:

$$\Omega = \frac{1}{\varepsilon} \quad , \quad \varepsilon << 1$$

Also, we rescale x so that:

$$x = \chi \sqrt{\frac{\varepsilon}{\gamma}} \quad \text{where} \quad \chi = O(1)$$

Then the system in Eqs.(4.1) becomes:

$$\ddot{y} + y - \varepsilon \dot{\chi}^2 y = 0$$

$$\left(1 + \kappa y^2\right)\ddot{\chi} + \frac{1}{\varepsilon^2}\chi + 2\kappa y \dot{y}\dot{\chi} = 0 \tag{4.3}$$

where we have divided the x equation by μ and defined a new parameter $\kappa = \frac{\gamma}{\mu}$. The corresponding energy expression is:

$$h = \frac{1}{2}\left(\frac{1}{\kappa} + y^2\right)\varepsilon \dot{\chi}^2 + \frac{1}{2}\dot{y}^2 + \frac{1}{2}\left(\frac{1}{\varepsilon\kappa}\chi^2 + y^2\right) \tag{4.4}$$

Applying the strategy first illustrated in chapter 3, we will look for a solution of the form suggested by DPM and WKB:

$$\chi = \chi(\xi, T) \quad , \quad y = y_0(\xi) + \varepsilon y_1(\xi, T) \tag{4.5}$$

$$\text{where } \xi = t \text{ and } \frac{dT}{dt} = \frac{\omega(\xi)}{\varepsilon} \ , \ \omega(\xi) = \omega_0(\xi) + \varepsilon\omega_1(\xi) + ...$$

At the end of the DPM procedure detailed in appendix C.2, we obtain the following equation governing the leading order slow dynamics:

$$\frac{d^2 y_0}{d\xi^2} + y_0 - y_0 \frac{C^2}{2\varepsilon}\left(1 + \kappa y_0^2\right)^{-\frac{3}{2}} = 0 \tag{4.6}$$

We assume initial conditions (IC's) of the form:

$$\begin{cases} y(0) = b \\ x(0) = \chi(0)\sqrt{\frac{\varepsilon}{\gamma}} = a\sqrt{\frac{\varepsilon}{\gamma}} \end{cases} \quad \rightarrow \quad \begin{cases} y_0(0) \approx b \\ \chi(0) = a \end{cases}$$

then the constant appearing in Eq.(4.6) can be related to the initial amplitudes by the following relation:

$$C^2 = \gamma a^2 \sqrt{1 + \kappa b^2}$$

In appendix C.1, we show that the fast variable χ can be expressed in terms of the slow variable y_0 as:

$$\chi \approx C\sqrt{\omega_0(\xi)}\cos T \tag{4.7}$$

$$\text{with} \quad \omega_0 = \left(1 + \kappa y_0^2\right)^{-\frac{1}{2}}$$

Also, the fast component of y is found to be:

$$y_1 \approx y_0\omega_0\frac{C^2}{8}\cos 2T$$

Knowing the initial amplitudes a and b, we solve for the corresponding value of C, then we plot the phase portrait and pick out the orbit corresponding to $y_0(0) = b,\ \dot{y}_0(0) = 0$. This latter orbit will correspond approximately to the leading order slow oscillation of the bending variable y, so this allows us to tell what type of solution the full system will have. The arrows in Fig.4.6(a), (b) and (c) point to the orbits corresponding to the solutions in Fig.4.2(a), Fig.4.2(b) and Fig.4.4, respectively. Fig.4.6(d) shows the phase plane for the y_0 equation with the value of C corresponding to the initial conditions that led to the non-local mode displayed in Fig.4.3(a). We can see that one of the centers is at ($y_0 = 0.0184$, $\dot{y}_0 = 0$), then the orbit corresponding to ($y_0(0) = b = 0.0184$, $\dot{y}_0(0) = 0$) is the fixed point itself. In appendix C.3, we show that for each energy value satisfying the following condition:

$$h > h_{cr} = \frac{1}{\kappa} \tag{4.8}$$

there exists an initial amplitude b^* that will lead to a value of C such that the y_0 equation has a fixed point with $y_0 = b^*$; Such initial conditions will lead to the non-local modes. As explained in appendix C.3, b^* is found to be:

$$b^* = \sqrt{\frac{2}{3}\left(h - \frac{1}{\kappa}\right)} \tag{4.9}$$

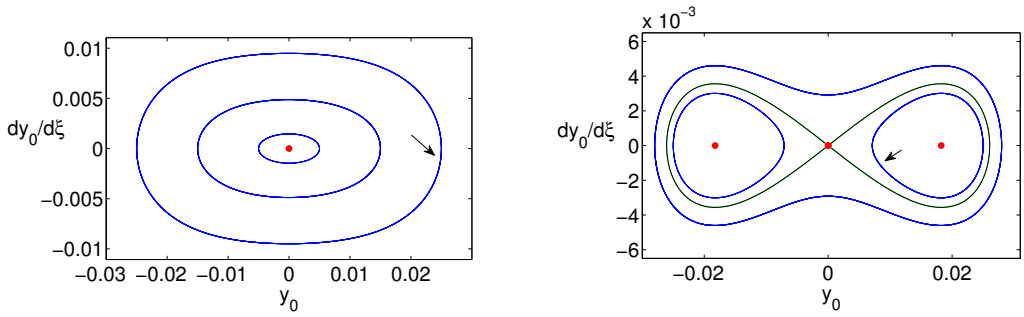

(a) $h = 0.006, b = 0.025; C = 0.2042$ (b) $h = 0.007, b = 0.025; C = 0.2213$

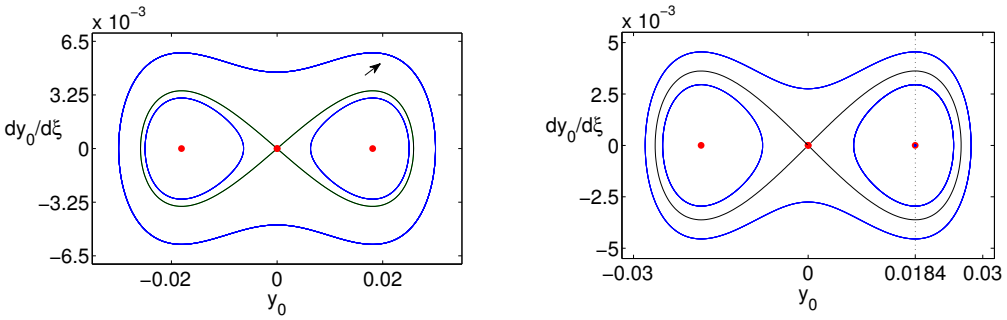

(c) $h = 0.007, b = 0.03; C = 0.2203$ (d) $h = 0.007, b = 0.0184; C = 0.2215$

Figure 4.6: Phase plane for the y_0 equation corresponding to different IC's

In other words, for a fixed energy level, the following initial conditions:

$$\begin{cases} y(0) = b^* = \sqrt{\frac{2}{3}\left(h - \frac{1}{\kappa}\right)} \quad , \quad x(0) = a^* = \sqrt{\varepsilon\kappa\left(2h - b^{*2}\right)} \\ \dot{y}(0) = 0 \qquad\qquad\qquad\qquad , \quad \dot{x}(0) = 0 \end{cases} \tag{4.10}$$

will lead to non-local modes in which:

$$y_0 \approx b^* \quad , \quad \chi \approx a^* \cos\left(\frac{\omega^*}{\varepsilon}t\right)$$

$$\text{So that} \quad y \approx b^* + \varepsilon\frac{a^{*2}b^*}{8}\cos\left(2\frac{\omega^*}{\varepsilon}t\right) \quad \& \quad x \approx \sqrt{\frac{\varepsilon}{\gamma}}a^*\cos\left(\frac{\omega^*}{\varepsilon}t\right) \tag{4.11}$$

$$\text{where} \quad \omega^* = \left(1 + \kappa b^{*2}\right)^{-\frac{1}{2}} \tag{4.12}$$

The expression for the non-local mode solution shows that the bending variable will have a frequency that is twice that of the torsional one, which is consistent with what was observed in [11].

4.3 Validation

Taking the same parameter values as in section 2, we choose a value of $h = 0.05$ and compare the approximate solution obtained from numerical integration of the y_0 equation to that of the full system. Fig.4.7(a),(b),(c) and Fig.4.8(a),(b),(c) display plots of y vs time and x vs time, respectively, for three different initial conditions. The approximate solution is represented by a dashed line while the numerical solution of the full system is represented by a solid line. It is hard to distinguish the two solutions as they almost completely overlap, this illustrates that the two solutions agree well. In appendix C.4, we present more compari-

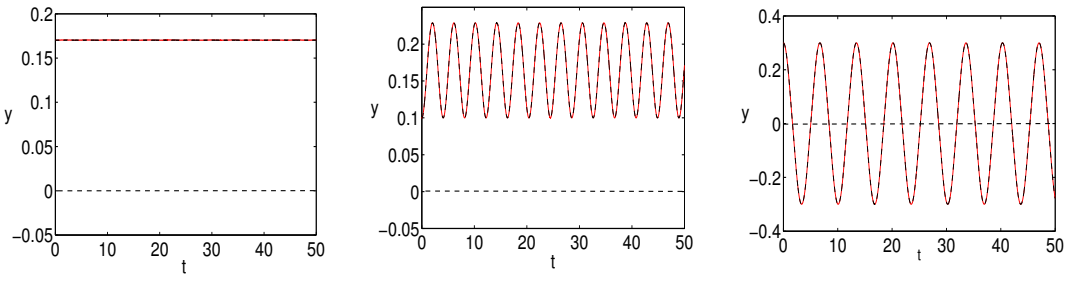

(a) $h = 0.05, b = 0.1703$ (b) $h = 0.05, b = 0.1$ (c) $h = 0.05, b = 0.3$

Figure 4.7: y vs time for different IC's

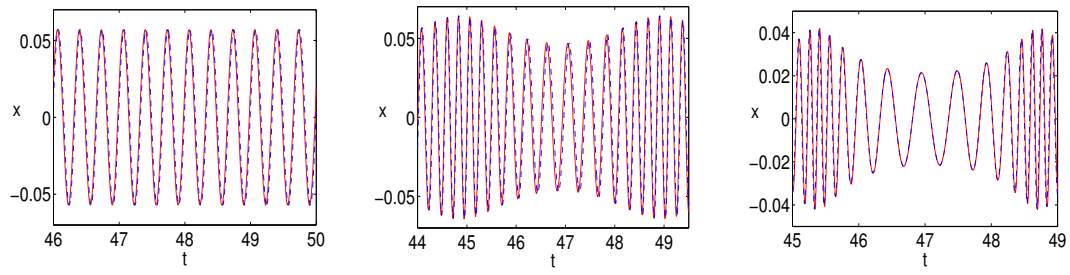

(a) $h = 0.05, b = 0.1703$ (b) $h = 0.05, b = 0.1$ (c) $h = 0.05, b = 0.3$

Figure 4.8: x vs time for different IC's

son plots of solutions for different energy values as well as for a larger γ value.

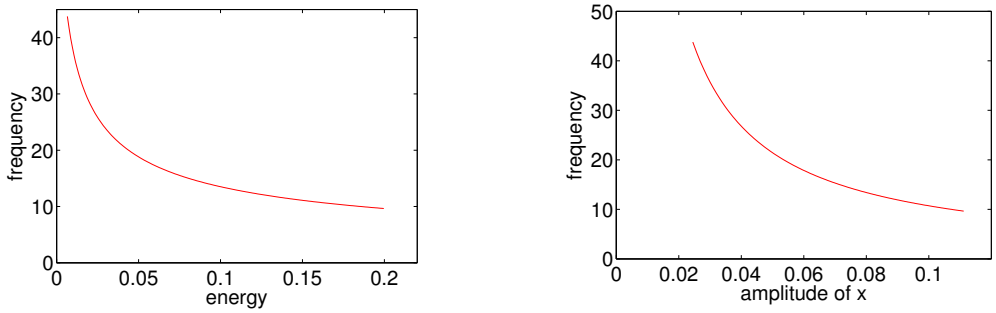

(a) (b)

Figure 4.9: Frequency-amplitude characteristics for the non-local mode solution (a) frequency vs. energy value (b) frequency vs. amplitude of the torsional variable x

The error in the approximate solution becomes more visible for larger values of energy far from the bifurcation value. In [11], the frequency amplitude characteristics of the non-linear modes were obtained numerically and presented as a plot of frequency vs. amplitude of the torsional variable, as well as frequency vs. energy. Here, we have obtained in Eqs.(4.10),(4.11) and (4.12) approximate analytic expressions for the frequency and amplitude of y for the non-local mode solutions, as a function of the energy value and the parameters. Fig.4.3 shows the frequency amplitude characteristic curves that we obtain using these latter equations. The two plots match very well those presented in [11].

4.4 Conclusion

The method of direct partition of motion was used to study the dynamics of the thin elastica model presented in [11]. This was based on the observation that the frequency ratio for the experimental setup was of $O(1/\varepsilon)$ and so the system is best viewed as one with vastly different frequencies. It was also observed

that the coupling parameter value corresponding to the experimental setup was $O(1)$ such that the slow variable affects the leading order dynamics of the fast variable. This required the treatment of the fast variable as an oscillator with a slowly varying frequency and thus using a rescaling of fast time inspired by the WKB method. The procedure leads to an approximate expression for the non-local modes, as well as the critical energy value at which they arise, in terms of the parameters of the system. The results are checked by comparison to numerical integration and found to agree well. This treatment provides new insight on the dynamics of the elastica. Particularly, it allows us to see that the occurrence of these non-local modes is primarily due to the strong modulation of the amplitude of the fast torsional oscillation by the slow bending oscillation, as well as highlight the role of strong inertial coupling in making this possible.

CHAPTER 5

CONCLUSION

The method of direct partition of motion (DPM) [4] was devised for facilitating the study of systems subject to external high frequency excitation that often takes the form of a fast harmonic oscillation with a given amplitude and frequency. In this thesis, we illustrated through three model systems that its basic assumptions can also serve to study autonomous systems with vastly different frequencies, in which an oscillator is coupled to a much faster one. The first problem concerned three Van der Pol type oscillators with frequencies: $\omega_1 = O(1)$, $\omega_2 = O(1/\varepsilon)$ and $\omega_3 = O(1/\varepsilon^2)$, respectively, where $\varepsilon << 1$. Employing the DPM assumptions, we found that the fastest oscillator is unaffected by the type of coupling used, and its apparent effect on the second oscillator is a modulation of its linear term as well as an added cubic term. So the leading order motion of the second oscillator appears to be governed by a Duffing-Van der Pol equation which admits limit cycle solutions that can be expressed in terms of a Jacobi elliptic function. The amplitude and frequency of the latter solution are functions of system parameters and the limit cycle is found to disappear as the strength of coupling to the fastest oscillator exceeds a critical value. When the limit cycle of the second oscillator does exist, the slowest oscillator appears to be parametrically excited by an oscillation that is a Jacobi elliptic function whose amplitude and frequency depend on the parameters. This is in contrast to problems previously presented in the literature where the forcer is often a harmonic function with a prescribed amplitude and frequency. We showed that the DPM assumptions can be applied for such a problem and allows us to express the limit cycle of the slowest oscillator as a Jacobi elliptic function, similarly to the second oscillator. The critical strength of coupling between oscillator 1 and 2, at

which the slowest limit cycle disappears, depends on the strength of coupling between oscillator 2 and 3 which determines the amplitude and frequency of oscillator 2 that acts as the forcer of oscillator 1.

Then we investigated the dynamics of a mass-spring-pendulum system and a model of a thin elastica, which both represent an oscillator coupled to a much faster one. What these two problems share with the first one is the presence of a slow oscillator influenced by a much faster one. However, unlike the first problem, the coupling allows the slow oscillator to modulate the frequency and amplitude of the fast oscillator that is exciting it. This leads to a kind of feedback that causes an apparent added nonlinearity in the dynamics of the slow oscillator, which would not have been present if the fast oscillation had a constant amplitude and frequency that are independent of the slow oscillator. To the best of our knowledge, this phenonmenon has not been previously studied in the literature. For both of these problems, assuming that the motion of the slow oscillator is partitioned according to DPM, allows us to identify the fast oscillator as one with a slowly varying frequency and motivates the use of a rescaling of fast time analogous to that suggested by the WKB method. The WKB method is often used to find the solution to an equation of a fast oscillator with a frequency that is explicitly a function of slow time. Here, we extended its use to the situation where the frequency of the fast oscillator is implicitly a function of slow time through the dependence on the amplitude of the slow oscillator that it is coupled to. The wide separation between the frequencies along with the slow oscillator's ability to modulate the fast oscillator's amplitude and frequency, gives rise to non-local modes that are born through a pitchfork bifurcation of periodic orbits. For the mass-spring-pendulum system, these modes

correspond to solutions in which the pendulum undergoes a a small amplitude fast oscillation about an angle between 0 and $\pi/2$ from the vertically downwards position. Whereas for the thin elastica model, the non-local modes correspond to solutions in which the bending mode motion consists of a static non-zero deflection overlaid by a small fast oscillation of a frequency that is twice that of the corresponding torsional oscillation. These latter solutions of the elastica model qualitatively resemble experimental observations [10]. The use of DPM, in conjunction with the WKB rescaling of fast time, allows us to derive an approximate expression for the non-local modes, as well as the critical value of energy at which the bifurcation occurs, in terms of the parameters in each system. This analysis provides new insight into the old problem of the thin elastica. Particularly, it allows us to identify two factors that cause the non-local modes of the type observed experimentally: the presence of vastly different frequencies and strong inertial coupling between the bending and torsional modes of the system.

We believe that the kind of interaction illustrated here might be of relevance to systems arising in different areas of science in which nonlinear interactions are present between oscillators of vastly different frequencies. In particular, it is known that oscillations of vastly different frequencies are present in neuronal systems [6]. Interestingly, "Recent findings from the human neocortex show that the power of fast gamma oscillations (30-150 Hz) is modulated by the phase of slower theta oscillations (5-8 Hz)." [16]. Also, "More recently, evidence has emerged that suggests nonlinear coupling among different frequencies may play an equally important role in interareal communication" [8]. This suggests that the mechanism we explained here might be present in neuronal systems,

and that the method we developed might aid in the efforts of modeling nonlinear interactions between neuronal oscillations of different frequencies, specifically, the slow modulation of a fast neuronal oscillation by a much slower one.

APPENDIX A

A.1 Details of the direct partition of motion

The method of direct partition of motion (DPM) is used to study the dynamics of the following system:

$$\begin{aligned} \ddot{x} + x + \left(a_1 + b_1 x^2\right)\dot{x} &= \gamma_1\left(1 + g_1 x^2\right)\dot{y} \\ \ddot{y} + \frac{\omega_2^2}{\varepsilon^2}y + \frac{\omega_2}{\varepsilon}\left(a_2 + b_2 y^2\right)\dot{y} &= \frac{\omega_2}{\varepsilon}\left(1 + g_2 y^2\right)\left[\gamma_1\dot{x} + \gamma_2\dot{z}\right] \\ \ddot{z} + \frac{\omega_3^2}{\varepsilon^4}z + \frac{\omega_3}{\varepsilon^2}\left(a_3 + b_3 z^2\right)\dot{z} &= \frac{\omega_3}{\varepsilon^2}\gamma_2\left(1 + g_3 z^2\right)\dot{y} \end{aligned} \tag{A.1}$$

where we seek an approximate solution partitioned as follows:

$$\begin{aligned} x &= X(t_1) + \varepsilon\xi(t_1, t_2, t_3) \\ y &= Y(t_2) + \varepsilon\eta(t_1, t_2, t_3) \\ z &= Z(t_3) + \varepsilon\zeta(t_1, t_2, t_3) \end{aligned} \tag{A.2}$$

The key assumption of DPM is that a fast component of motion is periodic and has a zero average over that fast time scale [4]. Such a condition on ξ and η and their derivatives can be written as:

$$\langle\xi\rangle_2 = \left\langle\frac{\partial\xi}{\partial t_2}\right\rangle_2 = \left\langle\frac{\partial^2\xi}{\partial t_2^2}\right\rangle_2 = \langle\xi\rangle_3 = \left\langle\frac{\partial\xi}{\partial t_3}\right\rangle_3 = \left\langle\frac{\partial^2\xi}{\partial t_3^2}\right\rangle_3 = \langle\eta\rangle_3 = \left\langle\frac{\partial\eta}{\partial t_3}\right\rangle_3 = \left\langle\frac{\partial^2\eta}{\partial t_3^2}\right\rangle_3 = 0 \tag{A.3}$$

In addition, a slow function, that is, a function of one time scale only, is assumed not to change significantly over a period of a faster time scale, such that:

$$\langle X(t_1)\rangle_2 = X(t_1)\ ,\ \langle X(t_1)\rangle_3 = X(t_1)\ ,\ \langle Y(t_2)\rangle_3 = Y(t_2) \tag{A.4}$$

$$\left\langle\frac{dX}{dt_1}\right\rangle_2 = \frac{dX}{dt_1}\ ,\ \left\langle\frac{d^2X}{dt_1^2}\right\rangle_2 = \frac{d^2X}{dt_1^2}\ ,\ \left\langle\frac{dX}{dt_1}\right\rangle_3 = \frac{dX}{dt_1}\ ,\ \left\langle\frac{d^2X}{dt_1^2}\right\rangle_3 = \frac{d^2X}{dt_1^2}$$

$$\left\langle \frac{dY}{dt_2} \right\rangle_3 = \frac{dY}{dt_2} \quad , \quad \left\langle \frac{d^2Y}{dt_2^2} \right\rangle_3 = \frac{d^2Y}{dt_2^2}$$

The strategy is to make use of the assumptions in Eqs.(A.3) and (A.4), in order to derive equations that govern X,Y and Z. To that end, we perform the following steps:

- substitute Eqs.(A.2) into the system in Eqs.(A.1); the derivatives are given by the following expressions:

$$\dot{x} = \frac{dX}{dt_1} + \varepsilon\frac{\partial\xi}{\partial t_1} + \omega_2\frac{\partial\xi}{\partial t_2} + \frac{\omega_3}{\varepsilon}\frac{\partial\xi}{\partial t_3}$$

$$\ddot{x} = \frac{d^2X}{dt_1^2} + \varepsilon\frac{\partial^2\xi}{\partial t_1^2} + \frac{\omega_2^2}{\varepsilon}\frac{\partial^2\xi}{\partial t_2^2} + \frac{\omega_3^2}{\varepsilon^3}\frac{\partial^2\xi}{\partial t_3^2} + 2\omega_2\frac{\partial^2\xi}{\partial t_1\partial t_2} + 2\frac{\omega_3}{\varepsilon}\frac{\partial^2\xi}{\partial t_1\partial t_3} + 2\frac{\omega_2\omega_3}{\varepsilon^2}\frac{\partial^2\xi}{\partial t_2\partial t_3}$$

$$\dot{y} = \frac{\omega_2}{\varepsilon}\frac{dY}{dt_2} + \varepsilon\frac{\partial\eta}{\partial t_1} + \omega_2\frac{\partial\eta}{\partial t_2} + \frac{\omega_3}{\varepsilon}\frac{\partial\eta}{\partial t_3}$$

$$\ddot{y} = \frac{\omega_2^2}{\varepsilon^2}\frac{d^2Y}{dt_2^2} + \varepsilon\frac{\partial^2\eta}{\partial t_1^2} + \frac{\omega_2^2}{\varepsilon}\frac{\partial^2\eta}{\partial t_2^2} + \frac{\omega_3^2}{\varepsilon^3}\frac{\partial^2\eta}{\partial t_3^2} + 2\omega_2\frac{\partial^2\eta}{\partial t_1\partial t_2} + 2\frac{\omega_3}{\varepsilon}\frac{\partial^2\eta}{\partial t_1\partial t_3} + 2\frac{\omega_2\omega_3}{\varepsilon^2}\frac{\partial^2\eta}{\partial t_2\partial t_3}$$

$$\dot{z} = \frac{\omega_3}{\varepsilon^2}\frac{dZ}{dt_3} + \varepsilon\frac{\partial\zeta}{\partial t_1} + \omega_2\frac{\partial\zeta}{\partial t_2} + \frac{\omega_3}{\varepsilon}\frac{\partial\zeta}{\partial t_3}$$

$$\ddot{z} = \frac{\omega_3^2}{\varepsilon^4}\frac{d^2Z}{dt_3^2} + \varepsilon\frac{\partial^2\zeta}{\partial t_1^2} + \frac{\omega_2^2}{\varepsilon}\frac{\partial^2\zeta}{\partial t_2^2} + \frac{\omega_3^2}{\varepsilon^3}\frac{\partial^2\zeta}{\partial t_3^2} + 2\omega_2\frac{\partial^2\zeta}{\partial t_1\partial t_2} + 2\frac{\omega_3}{\varepsilon}\frac{\partial^2\zeta}{\partial t_1\partial t_3} + 2\frac{\omega_2\omega_3}{\varepsilon^2}\frac{\partial^2\zeta}{\partial t_2\partial t_3}$$

- collect terms of $O(1/\varepsilon^4)$ in the z equation, this results in an equation governing $Z(t_3)$:

$$\frac{d^2Z}{dt_3^2} + Z + \left(a_3 + b_3Z^2\right)\frac{dZ}{dt_3} = 0 \tag{A.5}$$

- collect terms of $O(1/\varepsilon^3)$ in the y equation, this provides an expression for η in terms of Y and Z:

$$\frac{\partial^2\eta}{\partial t_3^2} - \gamma_2\frac{\omega_2}{\omega_3}\left(1 + g_2Y^2\right)\frac{dZ}{dt_3} = 0 \tag{A.6}$$

- collect terms of $O(1/\varepsilon^2)$ in the y equation:

$$\frac{d^2Y}{dt_2^2} + Y + \left(a_2 + b_2Y^2\right)\frac{dY}{dt_2} - 2\gamma_2g_2\frac{\omega_3}{\omega_2}Y\left(\eta\frac{dZ}{dt_3}\right) \tag{A.7}$$

$$+\frac{\omega_3}{\omega_2}Y^2\left[b_2\frac{\partial\eta}{\partial t_3}-\gamma_2 g_2\frac{\partial\zeta}{\partial t_3}+\gamma_1 g_2\frac{\partial\xi}{\partial t_3}\right]+\frac{\omega_3}{\omega_2}\left[a_2\frac{\partial\eta}{\partial t_3}-\gamma_2\frac{\partial\zeta}{\partial t_3}-\gamma_1\frac{\partial\xi}{\partial t_3}+2\frac{\partial^2\eta}{\partial t_2\partial t_3}\right]=0$$

- Average Eq.(A.7) over the fastest time scale t_3, making use of Eqs.(A.3) and (A.4), the result is an equation governing $Y(t_2)$:

$$\frac{d^2Y}{dt_2^2}+Y+\left(a_2+b_2Y^2\right)\frac{dY}{dt_2}-2\gamma_2 g_2\frac{\omega_3}{\omega_2}Y\left\langle\eta\frac{dZ}{dt_3}\right\rangle_3=0 \tag{A.8}$$

- collect terms of $O(1/\varepsilon^3)$ from the x equation:

$$\frac{\partial^2\xi}{\partial t_3^2}=0 \quad\Rightarrow\quad \xi=\tilde{\xi}(t_1,t_2)+t_3\hat{\xi}(t_1,t_2)$$

$$\Rightarrow\ \xi=\tilde{\xi}(t_1,t_2)=\xi(t_1,t_2) \tag{A.9}$$

  We have set $\hat{\xi}$ to zero, to abide by the assumption that a fast component of motion is to be periodic on the fast time scale. Note, however, that we have not enforced the condition given in Eq.(A.3) which requires that ξ is to have a zero average over a period in t_3, and that's because the periodicity restriction we've just enforced has established that ξ is not a function of t_3, so ξ instead would be unchanged under the operation of averaging over a period of t_3.

- looking at $O(1/\varepsilon^2)$ terms in the x equation

$$\frac{\partial^2\xi}{\partial t_2\partial t_3}=0$$

  we see that this condition is readily satisfied by the result in Eq.(A.9).

- collect terms of $O(1/\varepsilon)$ in the x equation:

$$\frac{\partial^2\xi}{\partial t_2^2}-\frac{\gamma_1}{\omega_2}\left(1+g_1X^2\right)\frac{dY}{dt_2}+2\frac{\omega_3}{\omega_2^2}X^2\left[b_1\frac{\partial\xi}{\partial t_3}-\gamma_1 g_1\frac{\partial\eta}{\partial t_3}\right]+\frac{\omega_3}{\omega_2^2}\left[2\frac{\partial^2\xi}{\partial t_1\partial t_3}+a_1\frac{\partial\xi}{\partial t_3}-\gamma_1\frac{\partial\eta}{\partial t_3}\right]=0 \tag{A.10}$$

- substitute the expression for ξ from Eq.(A.9) in Eq.(A.10), then average Eq.(A.10) over the fastest time scale t_3, always using Eqs.(A.3) and (A.4). We obtain an equation governing ξ in terms of X and Y:

$$\frac{\partial^2 \xi}{\partial t_2^2} - \frac{\gamma_1}{\omega_2}\left(1 + g_1 X^2\right)\frac{dY}{dt_2} = 0 \tag{A.11}$$

- collect terms of O(1) in the x equation:

$$\begin{aligned}\frac{d^2X}{dt_1^2} + X + \left(a_1 + b_1 X^2\right)\frac{dX}{dt_1} + X\left[2b_1\omega_3\xi\frac{\partial\xi}{\partial t_3} - 2\gamma_1 g_1\omega_2\xi\frac{dY}{dt_2} - 2\gamma_1 g_1\omega_3\xi\frac{\partial\eta}{\partial t_3}\right] \\ +\omega_2 X^2\left[b_1\frac{\partial\xi}{\partial t_2} - \gamma_1 g_1\frac{\partial\eta}{\partial t_2}\right] + \left[a_1\omega_2\frac{\partial\xi}{\partial t_2} - \gamma_1\omega_2\frac{\partial\eta}{\partial t_2} + 2\omega_2\frac{\partial^2\xi}{\partial t_1\partial t_2}\right] = 0\end{aligned} \tag{A.12}$$

- substitute Eq.(A.11) into Eq.(A.12) and then average Eq.(A.12) over the fastest time scale t_3, finally average the resulting equation over the t_2 time scale. The result is an equation governing X:

$$\frac{d^2X}{dt_1^2} + X + \left(a_1 + b_1 X^2\right)\frac{dX}{dt_1} - 2\gamma_1 g_1\omega_2 X\left\langle\xi\frac{dY}{dt_2}\right\rangle_2 = 0 \tag{A.13}$$

A.2 Details of solving for X, Y and Z

We start by finding an approximate solution for Z. We rescale a_3 and b_3 so that Eq.(A.5) looks as follows:

$$\frac{d^2Z}{dt_3^2} + Z + \varepsilon\left(a_3 + b_3 Z^2\right)\frac{dZ}{dt_3} = 0 \tag{A.14}$$

We expand Z in an asymptotic series:

$$Z(t_3) = Z_0(t_3) + \varepsilon Z_1(t_3) + ...$$

First, we collect the leading order terms to get an equation for Z_0:

$$\frac{d^2Z_0}{dt_3^2} + Z_0 = 0 \quad \Rightarrow \quad Z_0 = C_3\cos(t_3)$$

Then we substitute this expression for Z_0 into the equation we obtain from collecting the O(ε) terms in Eq.(A.14). The result is an equation governing Z_1:

$$\frac{d^2Z_1}{dt_3^2} + Z_1 - \left(a_3 + b_3 Z_0^2\right)\frac{dZ_0}{dt_3} = 0$$

$$\Rightarrow \quad \frac{d^2Z_1}{dt_3^2} + Z_1 = a_3 C_3 \sin(t_3) + b_3 C_3^3 \cos^2(t_3)\sin(t_3)$$

$$= a_3 C_3 \sin(t_3) + \frac{b_3 C_3^3}{4}\left[\sin(3t_3) + \sin(t_3)\right]$$

Removing secular terms provides the following values for C_3, the amplitude of Z_0:

$$C_3 = 0 \;\text{ or }\; C_3 = 2\sqrt{-\frac{a_3}{b_3}}$$

Hence, the limit cycle solution for the Z equation is expressed as:

$$Z(t_3) \approx C_3 \cos(t_3) \quad , \quad C_3 = 2\sqrt{-\frac{a_3}{b_3}} \tag{A.15}$$

Substituting this in the equation governing η, we get:

$$\frac{\partial^2\eta}{\partial^2 t_3} + \gamma_2\frac{\omega_2}{\omega_3}\left(1 + g_2Y^2\right)C_3\sin(t_3) = 0$$

We solve for η by integrating twice over t_3:

$$\eta = \gamma_2 C_3\frac{\omega_2}{\omega_3}\left(1 + g_2Y^2\right)\sin(t_3) + c_1(t_1,t_2)\,t_3 + c_2(t_1,t_2)$$

Now, to satisfy the assumption that η is periodic and has a zero average over t_3, the functions c_1 and c_2 need to be identically zero. So the expression for η reduces to:

$$\eta = \eta(t_2,t_3) = \gamma_2 C_3\frac{\omega_2}{\omega_3}\left(1 + g_2Y^2\right)\sin(t_3) \tag{A.16}$$

The two expressions for Z and η in Eqs.(A.15) and (A.16) are substituted in the equation for Y which we restate here:

$$\frac{d^2Y}{dt_2^2} + Y + \left(a_2 + b_2Y^2\right)\frac{dY}{dt_2} - 2\gamma_2 g_2\frac{\omega_3}{\omega_2}Y\left\langle\eta\frac{dZ}{dt_3}\right\rangle_3 = 0$$

The definite integral that Z and η appear in can now be evaluated as follows:

$$\left\langle \eta \frac{dZ}{dt_3} \right\rangle_3 = \frac{1}{2\pi} \int_0^{2\pi} \gamma_2 C_3 \frac{\omega_2}{\omega_3} \left(1 + g_2 Y^2\right) \sin(t_3) \left(-C_3 \sin(t_3)\right) dt_3$$

$$= -\frac{1}{2\pi} \gamma_2 C_3^2 \frac{\omega_2}{\omega_3} \left(1 + g_2 Y^2\right) \int_0^{2\pi} \sin^2(t_3) dt_3$$

$$= -\frac{\gamma_2 C_3^2}{2} \frac{\omega_2}{\omega_3} \left(1 + g_2 Y^2\right)$$

Then, the equation governing Y becomes:

$$\frac{d^2Y}{dt_2^2} + Y + \left(a_2 + b_2 Y^2\right) \frac{dY}{dt_2} + \gamma_2^2 C_3^2 g_2 Y \left(1 + g_2 Y^2\right) = 0 \tag{A.17}$$

This equation can be rewritten as:

$$\frac{d^2Y}{dt_2^2} + \alpha_2 Y + \beta_2 Y^3 + \left(a_2 + b_2 Y^2\right) \frac{dY}{dt_2} = 0 \tag{A.18}$$

$$\text{where} \quad \alpha_2 = 1 + \gamma_2^2 C_3^2 g_2 = 1 - 4\gamma_2^2 \frac{a_3}{b_3} g_2 \quad , \quad \beta_2 = \gamma_2^2 C_3^2 g_2^2 = -4\gamma_2^2 \frac{a_3}{b_3} g_2^2$$

We rescale a_2 and b_2 such that the equation becomes:

$$\frac{d^2Y}{dt_2^2} + \alpha_2 Y + \beta_2 Y^3 + \varepsilon \left(a_2 + b_2 Y^2\right) \frac{dY}{dt_2} = 0$$

The global bifurcations that occur in such a system as α_2 and β_2 are varied, are presented in the literature [14]. It is known that for a range of parameter values, the system has a stable limit cycle, but as the parameters are varied, this stable limit cycle could disappear after colliding with an unstable limit cycle. After that, the system will have two stable equilibrium points, other than the origin which is a saddle for such parameter values. Here, we will seek an expression for that stable limit cycle solution, which we assume to be an O(ε) perturbation off of a closed orbit of the conservative system corresponding to $\varepsilon = 0$. These

closed orbits are known to take the form of Jacobi elliptic functions [9]. First, we rewrite the second order equation as a system of two first order equations:

$$\frac{dY}{dt_2} = W \quad , \quad \frac{dW}{dt_2} = -\alpha_2 Y - \beta_2 Y^3 - \varepsilon\left(a_2 + b_2 Y^2\right) W$$

As we mentioned, the solutions of the $\varepsilon = 0$ system can be written as:

$$Y = C\,\mathrm{cn}\,(At_2, k) \quad \text{where} \quad A^2 = \alpha_2 + \beta_2 C^2 \quad , \quad k^2 = \frac{\beta_2 C^2}{2A^2}$$

Here, cn is one of the periodic Jacobi elliptic functions which has a period in time t_2 given by:

$$T_2 = \frac{4\mathrm{K}\,(k)}{A}$$

where K(k) is the complete elliptic integral of the first kind. We can see that the period depends on the coefficient A and the modulus k, which in turn depend on the amplitude C and the parameters α_2 and β_2 of the system. This relation captures the frequency-amplitude dependence brought about by the cubic non-linearity that was introduced into the equation on Y due to the coupling with Z. When ε is non zero, depending on the parameters of the system, some of these closed orbits might persist and turn into limit cycles. The amplitude of such a limit cycle, when it exists, takes the values that make the Melnikov integral around that orbit equal to zero [24]. The Melnikov integral around these orbits can be written as:

$$M = \int_0^{T_2} -\left(a_2 + b_2 Y^2\right) W^2 dt_2$$

$$\text{with} \quad Y = C\,\mathrm{cn}\,(At_2, k) \quad , \quad W = \frac{dY}{dt_2} = -CA\,\mathrm{sn}\,(At_2, k)\;\mathrm{dn}\,(At_2, k)$$

$$\Rightarrow M = -\int_0^{T_2} a_2 C^2 A^2\,\mathrm{sn}^2\,(At_2, k)\;\mathrm{dn}^2\,(At_2, k) dt_2$$

$$-\int_0^{T_2} b_2 C^4 A^2\,\mathrm{cn}^2\,(At_2, k)\;\mathrm{sn}^2\,(At_2, k)\;\mathrm{dn}^2\,(At_2, k) dt_2$$

where sn and dn are periodic Jacobi elliptic functions. For a fixed set of parameter values: a_3, b_3, a_2, b_2, γ_2 and g_2, we substitute the expressions for A and k in terms of C into the above expression, and look for values of C for which M=0. These values give the amplitude of the limit cycle of the non-zero ε system, when such a limit cycle exists. We denote this special amplitude by C_2. The M=0 condition, which determines C_2, can be written concisely as:

$$H_2 = a_2 \mathrm{I}_1(k_2) + b_2 C_2^2 \mathrm{I}_2(k_2) = 0 \tag{A.19}$$

$$\text{where} \quad \mathrm{I}_1(k_2) = \frac{1}{3k_2^2}\left[\left(2k_2^2 - 1\right)\mathrm{E}(k_2) + \left(1 - k_2^2\right)\mathrm{K}(k_2)\right]$$

$$\mathrm{I}_2(k_2) = \frac{1}{15k_2^4}\left[2\left(k_2^4 - k_2^2 + 1\right)\mathrm{E}(k_2) - \left(k_2^4 - 3k_2^2 + 2\right)\mathrm{K}(k_2)\right]$$

where k_2 denotes the value of the modulus corresponding to C_2 and $\mathrm{E}(k)$ is the complete elliptic integral of the second kind. The expressions for I_1 and I_2 were obtained by evaluating the definite integrals appearing in the expression for M [7].

Hence, for each set of parameter values, Eq.(A.19) can be solved numerically to give the value of C_2 and then the approximate expression for Y is given by:

$$Y(t_2) \approx C_2 \mathrm{cn}(A_2 t_2, k_2) \tag{A.20}$$

$$\text{where} \quad A_2^2 = \alpha_2 + \beta_2 C_2^2 \quad , \quad k_2^2 = \frac{\beta_2 C_2^2}{2A_2^2} \quad , \quad \alpha_2 = 1 - 4\gamma_2^2 \frac{a_3}{b_3} g_2 \quad , \quad \beta_2 = -4\gamma_2^2 \frac{a_3}{b_3} g_2^2$$

and this solution has a period T_2 expressed as:

$$T_2 = \frac{4\mathrm{K}(k_2)}{A_2}$$

Note that for certain parameter values, Eq.(A.19) could have more than one solution. Based on the knowledge of the sequence of bifurcations that occur for such a system [14], we know that the stable limit cycle always has a larger amplitude than any unstable limit cycle that might exist simultaneously. So C_2

is taken to be the solution to Eq.(A.19) with the largest value. Also, for certain parameter values, there could be no solutions to Eq.(A.19) and that would mean that no limit cycle solution exists for the Y equation.

Substituting Eq.(A.20) into the equation governing ξ, we obtain

$$\frac{\partial^2 \xi}{\partial t_2^2} - \frac{\gamma_1}{\omega_2}\left(1 + g_1 X^2\right)\frac{dY}{dt_2} = 0 \quad \Rightarrow \quad \frac{\partial \xi}{\partial t_2} = \frac{\gamma_1}{\omega_2}\left(1 + g_1 X^2\right) Y + c_3\left(t_1\right)$$

$$\Rightarrow \quad \frac{\partial \xi}{\partial t_2} = \frac{\gamma_1}{\omega_2}\left(1 + g_1 X^2\right) Y \tag{A.21}$$

We have set c_3 to be identically zero in order to satisfy the condition that ξ has a zero average over t_2. Now, we can use this result, along with Eq.(A.20), to evaluate the definite integral that appears in the X equation:

$$\left\langle \xi \frac{dY}{dt_2} \right\rangle_2 = \frac{1}{T_2}\int_0^{T_2} \xi \frac{dY}{dt_2} dt_2 = \frac{1}{T_2}\left[(\xi Y)\big|_0^{T_2} - \int_0^{T_2} \frac{d\xi}{dt_2} Y dt_2 \right] = -\frac{1}{T_2}\int_0^{T_2} \frac{\gamma_1}{\omega_2}\left(1 + g_1 X^2\right) Y^2 dt_2$$

$$= -\frac{\gamma_1}{\omega_2}\left(1 + g_1 X^2\right)\frac{1}{T_2}\int_0^{T_2} C_2^2 \mathrm{cn}^2(A_2 t_2, k_2) dt_2$$

$$\Rightarrow \quad \left\langle \xi \frac{dY}{dt_2} \right\rangle_2 = \frac{\gamma_1}{\omega_2}\left(1 + g_1 X^2\right) F \quad \text{where} \quad F = \frac{4C_2^2}{A_2^2 k_2^2 T_2}\left[\left(1 - k_2^2\right)\mathrm{K}\left(k_2\right) - \mathrm{E}\left(k_2\right)\right] \tag{A.22}$$

The expression for F was obtained by evaluating the definite integral of cn^2 [7]. Note that we have set the constant term generated by the integration by parts to zero. This is because Y is assumed periodic in t_2 with period T_2, then this would be also true for ξ as seen from Eq.(A.21).

After substituting Eq.(A.22), the X equation becomes:

$$\frac{d^2 X}{dt_1^2} + X + \left(a_1 + b_1 X^2\right)\frac{dX}{dt_1} - 2\gamma_1^2 g_1 X\left(1 + g_1 X^2\right) F = 0$$

We rewrite this as:

$$\frac{d^2 X}{dt_1^2} + \alpha_1 X + \beta_1 X^3 + \left(a_1 + b_1 X^2\right)\frac{dX}{dt_1} = 0 \tag{A.23}$$

$$\text{where} \quad \alpha_1 = 1 - 2\gamma_1^2 g_1 F \quad , \quad \beta_1 = -2\gamma_1^2 g_1^2 F$$

This equation has the same form as Eq.(A.18) and so it will admit a similar solution to that given in Eq.(A.20). An approximate solution for X can then be written as:

$$X(t_1) \approx C_1 \mathrm{cn}(A_1 t_1, k_1) \tag{A.24}$$

$$\text{where} \quad A_1^2 = \alpha_1 + \beta_1 C_1^2 \quad , \quad k_1^2 = \frac{\beta_1 C_1^2}{2A_1^2} \quad , \quad \alpha_1 = 1 - 2\gamma_1^2 g_1 F \quad , \quad \beta_1 = -2\gamma_1^2 g_1^2 F$$

$$F = \frac{4C_2^2}{A_2^2 k_2^2 T_2}\left[\left(1 - k_2^2\right)\mathrm{K}(k_2) - \mathrm{E}(k_2)\right]$$

C_1 is determined by numerically solving the following equation:

$$H_1 = a_1 \mathrm{I}_1(k_1) + b_1 C_1^2 \mathrm{I}_2(k_1) = 0 \tag{A.25}$$

$$\text{with} \quad \mathrm{I}_1(k_1) = \frac{1}{3k_1^2}\left[\left(2k_1^2 - 1\right)\mathrm{E}(k_1) + \left(1 - k_1^2\right)\mathrm{K}(k_1)\right]$$

$$\mathrm{I}_2(k_1) = \frac{1}{15k_1^4}\left[2\left(k_1^4 - k_1^2 + 1\right)\mathrm{E}(k_1) - \left(k_1^4 - 3k_1^2 + 2\right)\mathrm{K}(k_1)\right]$$

The corresponding period of X in t_1 is:

$$T_1 = \frac{4\mathrm{K}(k_1)}{A_1}$$

Again, we note here that the X equation will admit such a limit cycle for a certain set of values of the parameters, only if these values allow a solution to Eq.(A.25). Note that if parameters in the Y equation are such that the only stable steady state solution is an equilibrium point, then Y takes on a constant value. In this case, the term including $\frac{dY}{dt_2}$ in Eq.(A.13) vanishes, and Y has no influence on X, in which case the form of the equation governing X reduces to that of Eq.(A.5) on Z, so the X steady state solution becomes analogous to Eq.(A.15). That is, the limit cycle of X becomes very close to a harmonic oscillation $X \approx 2\sqrt{\frac{-a_1}{b_1}}\cos t_1$ which corresponds to the dotted X solution in Fig.2.3(d).

APPENDIX B

B.1 Motivation for the assumed form of solution

The considered mass-spring-pendulum system is governed by the following system of equations:

$$\ddot{\theta} + \sin\theta = -\varepsilon\ddot{\chi}\cos\theta$$

$$\ddot{\chi} + \frac{1}{\varepsilon^2}\chi = -\frac{\mu}{\varepsilon}\left(\ddot{\theta}\cos\theta - \dot{\theta}^2\sin\theta\right)$$

In its present form, each of the equations contains the second derivative of both χ and θ. We can rewrite the system of equations so that each second derivative appears in only one of the equations, as follows:

$$\ddot{\theta} + \frac{1}{1-\mu\cos^2\theta}\left(\sin\theta + \mu\dot{\theta}^2\cos\theta\sin\theta - \frac{1}{\varepsilon}\chi\cos\theta\right) = 0$$

$$\ddot{\chi} + \frac{1}{1-\mu\cos^2\theta}\left(\frac{1}{\varepsilon^2}\chi - \frac{\mu}{\varepsilon}\left(\dot{\theta}^2\sin\theta + \cos\theta\sin\theta\right)\right) = 0$$

In this latter form, the θ equation appears as that of a nonlinear oscillator parametrically forced by χ, which we expect to be a fast oscillation. Hence this suggests the partitioning of the θ motion into a slow component overlaid by a fast component, as in the DPM ansatz. Also, we can see that the χ equation appears as that of a fast oscillator with a frequency whose magnitude is modulated by θ which we expect to be a slow oscillation, that is, it appears as an equation of a fast oscillator with a slowly changing frequency, similar to that which the WKB method is well suited for. This suggests rescaling fast time in the following manner:

$$\frac{dT}{dt} = \frac{\omega(t)}{\varepsilon} \quad \text{or} \quad T = \int_0^t \frac{\omega(t')}{\varepsilon}dt'$$

Based on the aforementioned logic, we look for a solution of the form:

$$\begin{cases} \chi = \chi(\xi, T) \\ \theta(\xi, T) = \theta_0(\xi) + \varepsilon\theta_1(\xi, T) \end{cases} \tag{B.1}$$

$$\text{where } \xi = t \ , \ \frac{dT}{dt} = \frac{\omega(\xi)}{\varepsilon} \quad \text{or } T = \int_0^{\xi} \frac{\omega(t')}{\varepsilon} dt'$$

Here, $\omega(\xi)$ is to be chosen such that the fast oscillation is a perturbation of a harmonic oscillation on the new timescale T. That is, we will choose $\omega(t)$ so as the χ equation has the form:

$$\frac{\partial^2 \chi}{\partial T^2} + \chi + O(\varepsilon) = 0$$

then, an approximate expression for χ can be found using regular perturbations.

B.2 Details of the method of direct partition of motion

The method of direct partition of motion is based on the following three main assumptions:

- the motion of the slow oscillator, which is subject to fast parametric forcing, is partitioned as a sum of a leading order purely slow motion and an overlaid fast component.
- all functions of fast time are periodic with a zero average over a period of fast oscillation.
- purely slow motions are treated as constants when averaging over a period of fast oscillation.

We start by substituting the form of solution presented in Eq.(B.1) into the following equations of motion:

$$\ddot{\theta} + \sin\theta = -\varepsilon\ddot{\chi}\cos\theta$$

$$\ddot{\chi} + \frac{1}{\varepsilon^2}\chi = -\frac{\mu}{\varepsilon}\left(\ddot{\theta}\cos\theta - \dot{\theta}^2\sin\theta\right) \tag{B.2}$$

The θ equation becomes:

$$\frac{1}{\varepsilon}\left(\omega^2\frac{\partial^2\theta_1}{\partial T^2} + \omega^2\frac{\partial^2\chi}{\partial T^2}\cos\theta_0\right) + \frac{d^2\theta_0}{d\xi^2} + \sin\theta_0 \tag{B.3}$$

$$-\omega^2\frac{\partial^2\chi}{\partial T^2}\theta_1\sin\theta_0 + \frac{\partial\chi}{\partial T}\frac{d\omega}{d\xi}\cos\theta_0 + 2\omega\frac{\partial^2\chi}{\partial\xi\partial T}\cos\theta_0$$

$$+2\omega\frac{\partial^2\theta_1}{\partial\xi\partial T} + \frac{\partial\theta_1}{\partial T}\frac{d\omega}{d\xi} = 0$$

we proceed to apply the standard DPM procedure [4] to this equation:

1. we average Eq.(B.3) over a period of fast timescale, while making use of the second and third assumption of DPM. The resulting averaged equation is:

$$\frac{d^2\theta_0}{d\xi^2} + \sin\theta_0 - \omega^2\sin\theta_0\left\langle\frac{\partial^2\chi}{\partial T^2}\theta_1\right\rangle_T = 0 \tag{B.4}$$

   where $\langle\bullet\rangle_T$ denotes averaging over a period of fast oscillation:

$$\langle\bullet\rangle_T = \frac{1}{2\pi}\int_0^{2\pi}(\bullet)\,dT$$

2. we subtract Eq.(B.4) from Eq.(B.3), then retaining the leading order terms only, gives:

$$\frac{\partial^2\theta_1}{\partial T^2} + \frac{\partial^2\chi}{\partial T^2}\cos\theta_0 = 0 \tag{B.5}$$

3. we integrate the latter equation twice with respect to T:

$$\theta_1 = -\chi\cos\theta_0 + c_1T + c_2$$

4. in order to satisfy the second assumption of DPM, we set $c_1 = c_2 = 0$, and obtain the following expression for θ_1:

$$\theta_1 = -\chi \cos\theta_0 \tag{B.6}$$

Substituting the latter into Eq.(B.4), we get:

$$\frac{d^2\theta_0}{d\xi^2} + \sin\theta_0 + \omega^2 \left\langle \frac{\partial^2\chi}{\partial T^2}\chi \right\rangle_T \cos\theta_0 \sin\theta_0 = 0 \tag{B.7}$$

From appendix B.3, we have:

$$\chi \approx C\sqrt{\omega(\xi)}\cos T$$

$$\text{with} \quad \omega(\xi) = \frac{1}{\sqrt{1-\mu\cos^2\theta_0}}$$

So the averaged term in Eq.(B.7) becomes:

$$\left\langle \frac{\partial^2\chi}{\partial T^2}\chi \right\rangle_T = \frac{1}{2\pi}\int_0^{2\pi} \left(-C\sqrt{\omega(\xi)}\cos T\right)\left(C\sqrt{\omega(\xi)}\cos T\right) dT$$

$$= -\frac{1}{2}C^2\omega$$

We substitute this into Eq.(B.7) along with the expression for $\omega(\xi)$. Then the equation governing θ_0, to leading order, takes the following form:

$$\frac{d^2\theta_0}{d\xi^2} + \sin\theta_0 - \frac{1}{2}C^2 \frac{\cos\theta_0 \sin\theta_0}{(1-\mu\cos^2\theta_0)\sqrt{1-\mu\cos^2\theta_0}} = 0$$

B.3 Solving for χ

For convenience, we restate here the assumed form of solution:

$$\begin{cases} \chi = \chi(\xi, T) \\ \theta(\xi, T) = \theta_0(\xi) + \varepsilon\theta_1(\xi, T) \end{cases}$$

$$\text{where } \xi = t \ , \quad \frac{dT}{dt} = \frac{\omega(\xi)}{\varepsilon} \quad \text{or } T = \int_0^{\xi} \frac{\omega(t')}{\varepsilon} dt'$$

We substitute this into the following equations of motion:

$$\ddot{\theta} + \sin\theta = -\varepsilon\ddot{\chi}\cos\theta$$

$$\ddot{\chi} + \frac{1}{\varepsilon^2}\chi = -\frac{\mu}{\varepsilon}\left(\ddot{\theta}\cos\theta - \dot{\theta}^2\sin\theta\right)$$

The χ equation becomes:

$$\frac{1}{\varepsilon^2}\left(\omega^2\frac{\partial^2\chi}{\partial T^2} + \chi + \mu\omega^2\frac{\partial^2\theta_1}{\partial T^2}\cos\theta_0\right) + \frac{1}{\varepsilon}\left(\frac{d\omega}{d\xi}\frac{\partial\chi}{\partial T}\right. \tag{B.8}$$

$$+2\omega\frac{\partial^2\chi}{\partial\xi\partial T} + \mu\frac{d\omega}{d\xi}\frac{\partial\theta_1}{\partial T}\cos\theta_0 + 2\omega\mu\left[\cos\theta_0\frac{\partial^2\theta_1}{\partial\xi\partial T} - \sin\theta_0\frac{d\theta_0}{d\xi}\frac{\partial\theta_1}{\partial T}\right]$$

$$\left.-\omega^2\mu\sin\theta_0\left[\theta_1\frac{\partial^2\theta_1}{\partial T^2} + \frac{\partial\theta_1}{\partial T}^2\right] + \mu\cos\theta_0\frac{d^2\theta_0}{d\xi^2} - \mu\sin\theta_0\frac{d\theta_0}{d\xi}^2\right) = 0$$

In order to eliminate the second derivative of θ_0 from the above equation, we substitute the expression for θ_1 from Eq.(B.6) into Eq.(B.3) in Appendix B.2. Then, the θ equation becomes:

$$\frac{d^2\theta_0}{d\xi^2} + \sin\theta_0 + \omega^2\frac{\partial^2\chi}{\partial T^2}\chi\cos\theta_0\sin\theta_0 + 2\omega\frac{\partial\chi}{\partial T}\frac{d\theta_0}{d\xi}\sin\theta_0 = 0$$

$$\Rightarrow \frac{d^2\theta_0}{d\xi^2} = -\sin\theta_0 - \omega^2\frac{\partial^2\chi}{\partial T^2}\chi\cos\theta_0\sin\theta_0 - 2\omega\frac{\partial\chi}{\partial T}\frac{d\theta_0}{d\xi}\sin\theta_0 = 0$$

We substitute this expression into Eq.(B.8), along with the expression for θ_1 from Eq.(B.6). Then, multiplying by ε^2, the χ equation becomes:

$$\omega^2\left(1 - \mu\cos^2\theta_0\right)\frac{\partial^2\chi}{\partial T^2} + \chi + \varepsilon\left(\frac{d\omega}{d\xi}\frac{\partial\chi}{\partial T} + 2\omega\frac{\partial^2\chi}{\partial\xi\partial T}\right. \tag{B.9}$$

$$-\mu\frac{d\omega}{d\xi}\frac{\partial\chi}{\partial T}\cos^2\theta_0 + 2\omega\mu\left[-\frac{\partial^2\chi}{\partial\xi\partial T}\cos^2\theta_0 + \sin\theta_0\cos\theta_0\frac{d\theta_0}{d\xi}\frac{\partial\chi}{\partial T}\right]$$

$$\left.-\omega^2\mu\sin\theta_0\cos^2\theta_0\left[2\frac{\partial^2\chi}{\partial T^2}\chi + \frac{\partial\chi}{\partial T}^2\right] - \mu\sin\theta_0\left[\cos\theta_0 + \frac{d\theta_0}{d\xi}^2\right]\right) = 0$$

For the above equation to be of the form:

$$\frac{\partial^2 \chi}{\partial T^2} + \chi + O(\varepsilon) = 0$$

we choose:

$$\omega(\xi) = \frac{1}{\sqrt{1 - \mu \cos^2 \theta_0}} \tag{B.10}$$

The χ equation becomes:

$$\frac{\partial^2 \chi}{\partial T^2} + \chi + \varepsilon \left(\frac{1}{\omega^2} \frac{d\omega}{d\xi} \frac{\partial \chi}{\partial T} + \frac{2}{\omega} \frac{\partial^2 \chi}{\partial \xi \partial T} - \omega^2 \mu \sin\theta_0 \cos^2\theta_0 \left[2\chi \frac{\partial^2 \chi}{\partial T^2} + \frac{\partial \chi}{\partial T}^2 \right] \right. \tag{B.11}$$

$$\left. -\mu \sin\theta_0 \left[\cos\theta_0 + \frac{d\theta_0}{dt}^2 \right] + 2\omega\mu \sin\theta_0 \cos\theta_0 \frac{d\theta_0}{dt} \frac{\partial \chi}{\partial T} \right) = 0$$

Now, we are ready to expand χ in an asymptotic series:

$$\chi(\xi, T) = \chi_0(\xi, T) + \varepsilon \chi_1(\xi, T) + ...$$

Substituting this into Eq.(B.11), and collecting terms of the same order, we get:

$$O(1) : \frac{\partial^2 \chi_0}{\partial T^2} + \chi_0 = 0$$

$$O(\varepsilon) : \frac{\partial^2 \chi_1}{\partial T^2} + \chi_1 = -\frac{1}{\omega^2} \frac{d\omega}{d\xi} \frac{\partial \chi_0}{\partial T} - \frac{2}{\omega} \frac{\partial^2 \chi_0}{\partial \xi \partial T} - 2\omega\mu \sin\theta_0 \cos\theta_0 \frac{d\theta_0}{d\xi} \frac{\partial \chi_0}{\partial T}$$

$$+ \omega^2 \mu \sin\theta_0 \cos^2\theta_0 \left[2 \frac{\partial^2 \chi_0}{\partial T^2} \chi_0 + \frac{\partial \chi_0}{\partial T}^2 \right]$$

$$+ \mu \sin\theta_0 \left[\cos\theta_0 + \frac{d\theta_0}{d\xi}^2 \right]$$

The first equation gives:

$$\chi_0 = X(\xi) \cos T$$

Then, killing secular terms from the χ_1 equation results in the following equation relating the amplitude X and θ_0:

$$\frac{1}{\omega^2} \frac{d\omega}{d\xi} X + \frac{2}{\omega} \frac{dX}{d\xi} + 2\omega\mu \sin\theta_0 \cos\theta_0 \frac{d\theta_0}{d\xi} X = 0$$

we rearrange the equation into:

$$\frac{1}{\omega}\frac{d\omega}{d\xi} + \frac{2}{X}\frac{dX}{d\xi} + 2\omega^2\mu \sin\theta_0 \cos\theta_0 \frac{d\theta_0}{d\xi} = 0$$

integrating with respect to t, we get:

$$\int \frac{1}{\omega} d\omega + \int \frac{2}{X} dX + \int 2\omega^2\mu \sin\theta_0 \cos\theta_0 d\theta_0 = 0$$

$$\Rightarrow \ln\omega + 2\ln X + \int 2\omega^2\mu \sin\theta_0 \cos\theta_0 d\theta_0 = k \tag{B.12}$$

where k is an arbitrary constant.

$$but \quad \omega(\xi) = \frac{1}{\sqrt{1-\mu\cos^2\theta_0}} = \left(1-\mu\cos^2\theta_0\right)^{-\frac{1}{2}}$$

$$\Rightarrow d\omega = -\frac{1}{2}\left(1-\mu\cos^2\theta_0\right)^{-\frac{3}{2}} (2\mu \sin\theta_0 \cos\theta_0)\, d\theta_0$$

$$= -\omega^3\mu \sin\theta_0 \cos\theta_0 d\theta_0$$

$$\Rightarrow \int 2\omega^2\mu \sin\theta_0 \cos\theta_0 d\theta_0 = -\int \frac{2}{\omega} d\omega = -2\ln\omega$$

So Eq.(B.12) becomes:

$$\ln\omega + 2\ln X - 2\ln\omega = k$$

$$\Rightarrow \ln\left(\frac{X^2}{\omega}\right) = k$$

$$\Rightarrow X(\xi) = C\sqrt{\omega(\xi)} \tag{B.13}$$

As a result, to leading order, χ is given by:

$$\chi \approx C\sqrt{\omega(\xi)}\cos T \tag{B.14}$$

$$\text{with} \quad \omega(\xi) = \frac{1}{\sqrt{1-\mu\cos^2\theta_0}}$$

where C is an arbitrary constant that depends on initial conditions.

B.4 The bifurcation in the slow dynamics

θ_0 is governed by the following equation:

$$\frac{d^2\theta_0}{dt^2} + \sin\theta_0 - \frac{C^2}{2}\frac{\sin\theta_0\cos\theta_0}{(1-\mu\cos^2\theta_0)\sqrt{1-\mu\cos^2\theta_0}} = 0 \tag{B.15}$$

We rewrite this as a system of two first order equations:

$$\dot{\theta}_0 = \phi$$

$$\dot{\phi} = -\sin\theta_0 + \frac{C^2}{2}\frac{\sin\theta_0\cos\theta_0}{(1-\mu\cos^2\theta_0)\sqrt{1-\mu\cos^2\theta_0}} \tag{B.16}$$

Looking for the value of θ_0 that corresponds to equilibrium points of this equation (with $\phi = 0$):

$$\sin\theta_0 = 0 \quad \text{or} \quad 1 - \frac{C^2}{2}\frac{\cos\theta_0}{(1-\mu\cos^2\theta_0)\sqrt{1-\mu\cos^2\theta_0}} = 0$$

So the first condition gives $\theta_0 = 0, \pi, -\pi$ while the second condition allows two additional equilibrium points $\theta_0 = E$ such that:

$$1 - \frac{C^2}{2}\frac{\cos E}{(1-\mu\cos^2 E)\sqrt{1-\mu\cos^2 E}} = 0$$

$$\Rightarrow \left(1-\mu\cos^2 E\right)^3 = \frac{C^4}{4}\cos^2 E \tag{B.17}$$

To know when a root to this equation actually exists,

$$\text{let } \alpha = \cos^2 E \quad \text{so} \quad 0 \le \alpha \le 1$$

Consider the two functions f & g, illustrated in Fig.B.1:

$$f(\alpha) = (1-\mu\alpha)^3 \quad , \quad g(\alpha) = \frac{C^4}{4}\alpha$$

f is a decreasing function of α with :

$$f(0) = 1 \text{ and } f(1) = (1-\mu)^3$$

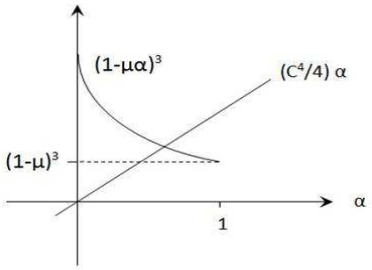

Figure B.1: Schematic of the two functions $f(\alpha)$ & $g(\alpha)$

The function g is the line through the origin, with a slope of $C^4/4$. So, the two functions will intersect for some $\alpha \in [0, 1]$ when the following condition is met:

$$\frac{C^4}{4} \geq (1-\mu)^3 \tag{B.18}$$

Hence, when C satisfies this above condition, two new equilibrium points will exist at ($\theta_0 = \pm E$, $\phi = 0$), such that $\cos E$ satisfies Eq.(B.17).

The Jacobian for the system in Eqs.(B.16) has a zero trace while the determinant is given by the following expression:

$$\Delta = \cos\theta_0 + \frac{C^2}{8}\frac{3\mu\sin^2(2\theta_0) - 4\cos(2\theta_0)\left(1-\mu\cos^2\theta_0\right)}{(1-\mu\cos^2\theta_0)^{\frac{5}{2}}}$$

looking at the value of this determinant for $\theta_0 = 0$:

$$\Delta_{\theta_0=0} = 1 - \frac{C^2}{2}\frac{1}{(1-\mu)^{\frac{3}{2}}}$$

$$\Delta_{\theta_0=0} > 0 \Rightarrow \frac{C^4}{4} \leq (1-\mu)^3$$

So the origin goes from being a center to a saddle as the two new equilibrium points are born, hence, a pitchfork bifurcation takes place. To check the determinant for $\theta_0 = \pm E$, we solve for C^2 from Eq.(B.17):

$$C^2 = \frac{2\left(1-\mu\cos^2 E\right)^{\frac{3}{2}}}{\cos E} \tag{B.19}$$

substituting this into the expression for the determinant, we get:

$$\Delta_{\theta_0=E} = \frac{\mu \sin^2(2E) + 2\sin^2(E)}{2\cos E\,(1-\mu\cos^2 E)} > 0$$

where we have used Eq.(B.19), with the fact that $\mu = m/(M+m) < 1$, to judge that $\cos E > 0$. This confirms that the two new equilibrium points are centers.

To summarize, when the following condition is met:

$$C^2 > 4\,(1-\mu)^{\frac{3}{2}} \tag{B.20}$$

the approximate equation governing θ_0 undergoes a pitchfork bifurcation where two new equilibrium points are born ($\theta_0 = \pm E$, $\phi = 0$), such that:

$$\left(1-\mu\cos^2 E\right)^3 = \frac{C^4}{4}\cos^2 E$$

The arbitrary constant C that appears in the equation can be expressed in terms of the initial conditions. As mentioned in section 4, for initial zero velocities, the initial conditions take the form:

$$\begin{cases} \dot{\theta}(0) = 0 \\ \theta(0) = A \end{cases}, \quad \begin{cases} \dot{x}(0) = 0 \\ x(0) = \varepsilon B \end{cases}$$

$$\Rightarrow \begin{cases} \dot{\theta}_0(0) = 0 \quad , \quad \theta_0(0) \approx A \\ x(0) = \varepsilon B \approx \varepsilon C\sqrt{\omega(0)} \end{cases}$$

$$\text{with} \quad \omega(0) = \frac{1}{\sqrt{1-\mu\cos^2 A}}$$

Then C can be expressed as follows:

$$\Rightarrow C = B\left(1-\mu\cos^2 A\right)^{\frac{1}{4}}$$

The bifurcation condition in Eq.(B.20) becomes:

$$B^4\left(1-\mu\cos^2 A\right) > 4\,(1-\mu)^3 \tag{B.21}$$

Also, for such initial conditions, the energy function h that corresponds to the full system (3.1), is:

$$h = \frac{1}{2}B^2 + \mu(1 - \cos A)$$

solving for B^2 in terms of h and substituting the resulting expression into Eq.(B.21), we can derive a minimum required value of h so that the bifurcation occurs:

$$[2h - 2\mu(1 - \cos A)]^2 \left(1 - \mu\cos^2 A\right) > 4(1 - \mu)^3$$

$$\Rightarrow h - \mu(1 - \cos A) \geq \sqrt{\frac{(1 - \mu)^3}{1 - \mu\cos^2 A}}$$

$$h \geq \mu(1 - \cos A) + \sqrt{\frac{(1 - \mu)^3}{1 - \mu\cos^2 A}}$$

The expression on the right hand side of the equality increases as A increases. For $A = 0$ it takes the value $1 - \mu$. This leads to the following minimum requirement for the pitchfork bifurcation to happen:

$$h > 1 - \mu$$

Now, going back to the full system (3.1), we recall from Eq.(3.12) that the approximate θ motion took the form:

$$\theta \approx \theta_0 - x\cos\theta_0$$

where θ_0 is governed by Eq.(B.15). So, when the condition for the existence of the two new equilibrium points is met, we expect certain solutions that obey approximately the following relation:

$$\theta \approx E - x\cos E$$

That is, if we start with an initial condition $\theta(0) = \theta_0(0) = E, \dot{\theta} = \phi = 0$, then the approximate equation for θ_0 predicts that θ_0 will remain equal to E for all time,

since $\theta_0 = E, \phi = 0$ is a neutrally stable fixed point (center) of Eqs.(B.16).

Now we look for the initial amplitude of θ that corresponds to such solutions. That is, for each constant value of h that allows the mentioned bifurcation to occur, we look for $\theta_0(0) = A$, such that $E = A$. From Eq.(B.19), we have:

$$C^2 = \frac{2\left(1 - \mu\cos^2 E\right)^{3/2}}{\cos E} \tag{B.22}$$

but the expression for C in terms of the initial conditions is:

$$C = B\left(1 - \mu\cos^2 A\right)^{\frac{1}{4}}$$

$$\Rightarrow B^2 = \frac{C^2}{\sqrt{1 - \mu\cos^2 A}} \tag{B.23}$$

We substitute Eq.(B.22) into Eq.(B.23), and require:

$$E = A = \theta_0(0) \tag{B.24}$$

We get:

$$B^2 = \frac{2\left(1 - \mu\cos^2 A\right)}{\cos A}$$

Now, we can substitute this relation into the expression for h, in order to solve for A:

$$h = \frac{1}{2}B^2 + \mu(1 - \cos A) = \frac{\left(1 - \mu\cos^2 A\right)}{\cos A} + \mu(1 - \cos A)$$

we rewrite this as:

$$2\mu\cos^2 A + (h - \mu)\cos A - 1 = 0$$

$$\Rightarrow \cos A = \frac{\mu - h \pm \sqrt{(h-\mu)^2 + 8\mu}}{4\mu}$$

$$\Rightarrow A = \cos^{-1}\left(\frac{\mu - h \pm \sqrt{(h-\mu)^2 + 8\mu}}{4\mu}\right) \tag{B.25}$$

For such a solution to exist, we need:

$$\frac{\mu - h \pm \sqrt{(h-\mu)^2 + 8\mu}}{4\mu} < 1$$

$$\Rightarrow -3\mu - h \pm \sqrt{(h-\mu)^2 + 8\mu} < 0 \Rightarrow (h-\mu)^2 + 8\mu < (3\mu + h)^2$$

$$\Rightarrow -8h\mu + 8\mu - 8\mu^2 < 0$$

$$\Rightarrow h > 1 - \mu$$

which coincides with the condition for the existence of the pitchfork bifurcation.

To summarize, for a fixed value of μ, we expect to see a fixed point in the map ($x = 0$ & $\dot{x} > 0$) if we choose a value for h that meets $h > 1 - \mu$, and integrate the system in Eqs.(3.1), with the following initial conditions:

$$\begin{cases} \theta(0) = \pm A^* = \pm \cos^{-1}\left(\frac{\mu - h \pm \sqrt{(h-\mu)^2+8\mu}}{4\mu}\right) & , \quad \dot{\theta}(0) = 0 \\ x(0) = \varepsilon B^* = \varepsilon\sqrt{2(h - \mu(1 - \cos A))} & , \quad \dot{x}(0) = 0 \end{cases}$$

Fig.B.3 shows the pendulum oscillation for the special IC's for which θ is predicted to be $\theta \approx A^* - x\cos A^*$, that is, θ is predicted to undergo no slow oscillation and instead the motion of the pendulum will consist of a fast oscillation about the $\theta = A^*$. Due to the error in the approximate solution and numerical integration, θ undergoes a small amplitude slow oscillation instead of no slow oscillation. Fig.B.2(a) shows that this slow oscillation gets smaller in amplitude as energy is increased farther from the bifurcation value. This can be explained by the fact that the value of A^* increases as energy increases and thus the relative error decreases. The solution also gets closer to the predicted one as ε is decreased, as illustrated in Fig.B.2(b).

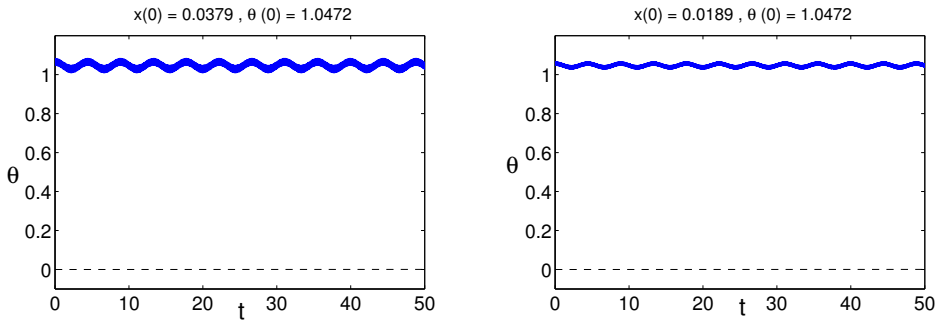

(a) $\varepsilon = 0.02$ (b) $\varepsilon = 0.01$

Figure B.2: θ vs. time for the initial condition corresponding to $\theta(0) = A^*$; $h = 2$ with different ε values

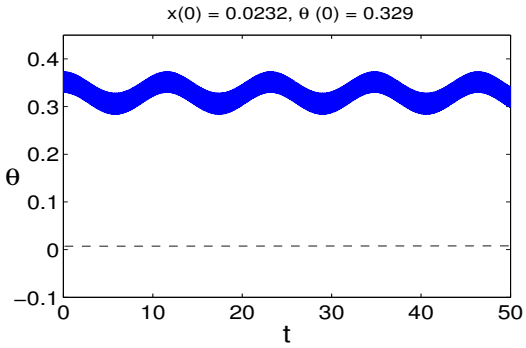

Figure B.3: θ vs. time for the initial condition corresponding to $\theta(0) = A^*$; $h = 0.7$ with $\varepsilon = 0.02$

B.5 Relating the curves of the Poincare map to θ_0

The Poincare map considered in the body of this paper corresponds to a plot of $\dot{\theta}$ vs. θ with $x = 0$ and $\dot{x} > 0$. If we could relate $\dot{\theta}$ to $\dot{\theta}_0$, and θ to θ_0, then we can approximately generate the Poincare map of the full system (3.1) from the solution to the θ_0 equation. θ was found to be expressed as:

$$\theta \approx \theta_0 - x \cos \theta_0$$

With x assumed to be $O(\varepsilon)$, we can say:

$$\theta \approx \theta_0 + O(\varepsilon)$$

To find an expression for $\dot{\theta}$ in terms of $\dot{\theta}_0$, we differentiate both sides of the expression for θ with respect to time:

$$\begin{aligned} \frac{d\theta}{dt} &= \frac{d\theta_0}{dt} - \frac{dx}{dt}\cos\theta_0 + x\frac{d\theta_0}{dt}\sin\theta_0 \\ \Rightarrow \frac{d\theta}{dt} &= \frac{d\theta_0}{dt} - \frac{dx}{dt}\cos\theta_0 + O(\varepsilon) \end{aligned} \tag{B.26}$$

Note that since x is $O(\varepsilon)$, we ignore the term multiplied by x, however, we retain the term containing the derivative of x since x oscillates with a frequency of $O(1/\varepsilon)$ and so $\dot{x}$ is of $O(1)$. In order to eliminate $\dot{x}$ from the expression for $\dot{\theta}$, we observe that:

$$\begin{aligned} x \approx \varepsilon C\sqrt{\omega(t)}\cos T \quad &\Rightarrow \frac{dx}{dt} \approx \varepsilon C\frac{d}{dt}\left(\sqrt{\omega}\right)\cos T - C\omega\sqrt{\omega}\sin T \\ &\Rightarrow \frac{dx}{dt} \approx -C\omega\sqrt{\omega}\sin T + O(\varepsilon) \end{aligned}$$

where we have used the fact that:

$$\frac{dT}{dt} = \frac{\omega(t)}{\varepsilon}$$

Now, for the Poincare map, we have:

$$\begin{cases} x = 0 \Rightarrow \cos T = 0 \\ \dot{x} > 0 \Rightarrow \sin T < 0 \end{cases} \Rightarrow \sin T = -1$$

$$\text{then } \frac{dx}{dt} \approx C\omega\sqrt{\omega} + O(\varepsilon)$$

Substituting this into Eq.(B.26), we get:

$$\frac{d\theta}{dt} = \frac{d\theta_0}{dt} - C\omega\sqrt{\omega}\cos\theta_0 + O(\varepsilon)$$

Substituting the following expression for $\omega(t)$:

$$\omega(t) = \frac{1}{\sqrt{1-\mu\cos^2\theta_0}} = \left(1-\mu\cos^2\theta_0\right)^{-\frac{1}{2}}$$

We obtain the following expression for the $\dot{\theta}$ values, corresponding to points in the Poincare map, in terms of $\dot{\theta}_0$ and θ_0:

$$\frac{d\theta}{dt} \approx \frac{d\theta_0}{dt} - C\left(1-\mu\cos^2\theta_0\right)^{-\frac{3}{4}}\cos\theta_0$$

APPENDIX C

C.1 The WKB solution for the fast degree of freedom

The assumed solution has the following form:

$$\chi = \chi(\xi, T) \quad , \quad y = y_0(\xi) + \varepsilon y_1(\xi, T) \tag{C.1}$$

$$\text{where } \xi = t \text{ and } \frac{dT}{dt} = \frac{\omega(\xi)}{\varepsilon} \ , \ \omega(\xi) = \omega_0(\xi) + \varepsilon\omega_1(\xi) + ...$$

Here, we are stretching the new fast timescale to accommodate for the cubic order term, $2\kappa y\dot{y}\dot{\chi}$, that is present in the equation of the fast oscillator. We plug the expression for the solution into Eqs.(4.3); multiplying the χ equation by ε^2, we get:

$$\omega_0^2\left(1+\kappa y_0^2\right)\frac{\partial^2\chi}{\partial T^2} + \chi + \varepsilon\left[2\kappa\omega_0^2\left(y_0\frac{\partial y_1}{\partial T}\frac{\partial\chi}{\partial T} + y_0 y_1\frac{\partial^2\chi}{\partial T^2}\right) + 2\kappa\omega_0 y_0\frac{dy_0}{d\xi}\frac{\partial\chi}{\partial T}\right.$$
$$\left. + \left(1+\kappa y_0^2\right)\left(2\omega_0\frac{\partial^2\chi}{\partial\xi\partial T} + \frac{d\omega_0}{d\xi}\frac{\partial\chi}{\partial T} + 2\omega_0\omega_1\frac{\partial^2\chi}{\partial T^2}\right)\right] = 0 \tag{C.2}$$

As in the WKB method [34], we ought to choose ω_0, so that the χ equation takes the form:

$$\frac{\partial^2\chi}{\partial T^2} + \chi + O(\varepsilon) = 0$$

This results in the following expression for ω_0:

$$\omega_0 = \left(1+\kappa y_0^2\right)^{-\frac{1}{2}} \tag{C.3}$$

The equation governing χ then becomes:

$$\frac{\partial^2\chi}{\partial T^2} + \chi + \varepsilon\left[2\kappa\omega_0^2\left(y_0\frac{\partial y_1}{\partial T}\frac{\partial\chi}{\partial T} + y_0 y_1\frac{\partial^2\chi}{\partial T^2}\right) + 2\kappa\omega_0 y_0\frac{dy_0}{d\xi}\frac{\partial\chi}{\partial T}\right.$$
$$\left. + \frac{2}{\omega_0}\frac{\partial^2\chi}{\partial\xi\partial T} + \frac{1}{\omega_0^2}\frac{d\omega_0}{d\xi}\frac{\partial\chi}{\partial T} + 2\frac{\omega_1}{\omega_0}\frac{\partial^2\chi}{\partial T^2}\right] = 0 \tag{C.4}$$

This χ equation can now be solved approximately using regular perturbations. We expand χ into an asymptotic series:

$$\chi = \chi_0(\xi, T) + \varepsilon\chi_1(\xi, T) + ...$$

Substituting this into Eq.(C.4), and collecting terms of the same order, we obtain:

$$O(1): \quad \frac{\partial^2\chi_0}{\partial T^2} + \chi_0 = 0 \tag{C.5}$$

$$O(\varepsilon): \quad \frac{\partial^2\chi_1}{\partial T^2} + \chi_1 = -2\kappa\omega_0^2\left(y_0\frac{\partial y_1}{\partial T}\frac{\partial\chi_0}{\partial T} + y_0y_1\frac{\partial^2\chi_0}{\partial T^2}\right) - 2\kappa\omega_0y_0\frac{dy_0}{d\xi}\frac{\partial\chi_0}{\partial T}$$
$$-\frac{2}{\omega_0}\frac{\partial^2\chi_0}{\partial\xi\partial T} - \frac{1}{\omega_0^2}\frac{d\omega_0}{d\xi}\frac{\partial\chi_0}{\partial T} - 2\frac{\omega_1}{\omega_0}\frac{\partial^2\chi_0}{\partial T^2} \tag{C.6}$$

Solving Eq.(C.5) for χ_0, we get:

$$\chi_0 = X(\xi)\cos T \tag{C.7}$$

From appendix C.2, we have the following expression for y_1:

$$y_1 = \frac{1}{8}y_0X^2\cos 2T$$

We substitute this, along with Eq.(C.7), into Eq.(C.6) which becomes:

$$\frac{\partial^2\chi_1}{\partial T^2} + \chi_1 = -2\kappa\omega_0^2\left(\frac{1}{4}y_0^2X^3\sin 2T\sin T - \frac{1}{8}y_0^2X^3\cos 2T\cos T\right)$$
$$+2\kappa\omega_0y_0\frac{dy_0}{d\xi}X\sin T + \frac{2}{\omega_0}\frac{dX}{d\xi}\sin T + \frac{1}{\omega_0^2}\frac{d\omega_0}{d\xi}X\sin T + 2\frac{\omega_1}{\omega_0}X\cos T$$

We make use of the following trigonometric identities:

$$\sin 2T\sin T = \frac{1}{2}\cos T - \frac{1}{2}\cos 3T \qquad , \qquad \cos 2T\cos T = \frac{1}{2}\cos T + \frac{1}{2}\cos 3T$$

Then, eliminating secular terms from the χ_1 equation results in an expression for ω_1 as well as an equation governing X:

$$\omega_1(\xi) = \frac{\kappa}{16}y_0^2X^2\omega_0^3 \tag{C.8}$$

$$\frac{2}{\omega_0}\frac{dX}{d\xi} + \frac{X}{\omega_0^2}\frac{d\omega_0}{d\xi} + 2\kappa\omega_0 y_0 \frac{dy_0}{d\xi} X = 0 \tag{C.9}$$

We rearrange Eq.(C.9) into:

$$\frac{2}{X}\frac{dX}{d\xi} + \frac{1}{\omega_0}\frac{d\omega_0}{d\xi} + 2\kappa\omega_0^2 y_0 \frac{dy_0}{d\xi} = 0 \tag{C.10}$$

Recall from Eq.(C.3), that ω_0 is chosen to be:

$$\omega_0 = \left(1 + \kappa y_0^2\right)^{-\frac{1}{2}}$$

Then, integrating Eq.(C.10) with respect to ξ, gives:

$$\begin{aligned} 2\ln X + \ln\omega_0 + \ln\left(1 + \kappa y_0^2\right) &= k \\ \Rightarrow 2\ln X + \ln\omega_0 + \ln\left(\omega_0^{-2}\right) &= k \\ \Rightarrow \ln\left(\frac{X^2}{\omega_0}\right) &= k \\ \Rightarrow X(\xi) &= C\sqrt{\omega_0(\xi)} \end{aligned} \tag{C.11}$$

where C is an arbitrary constant that depends on initial conditions. Hence, to leading order, χ takes the following form:

$$\chi \approx C\sqrt{\omega_0(\xi)}\cos T \tag{C.12}$$

C.2 The DPM solution for the slow degree of freedom

The assumed solution has the form:

$$\chi = \chi(\xi, T) \quad , \quad y = y_0(\xi) + \varepsilon y_1(\xi, T)$$

$$\text{where } \xi = t \text{ and } \frac{dT}{d\xi} = \frac{\omega(\xi)}{\varepsilon} \quad , \quad \omega(\xi) = \omega_0(\xi) + \varepsilon\omega_1(\xi) + ...$$

After substituting this into Eqs.(4.3), the equation governing the slow degree of freedom becomes:

$$\frac{1}{\varepsilon}\left[\omega_0^2\,\frac{\partial^2 y_1}{\partial T^2} - y_0\omega_0^2\left(\frac{\partial \chi}{\partial T}\right)^2\right] + \frac{d^2 y_0}{d\xi^2} + y_0 - 2y_0\omega_0\left[\frac{\partial \chi}{\partial \xi}\frac{\partial \chi}{\partial T} + \omega_1\left(\frac{\partial \chi}{\partial T}\right)^2\right]$$

$$-\omega_0^2 y_1\left(\frac{\partial \chi}{\partial T}\right)^2 + 2\omega_0\frac{\partial^2 y_1}{\partial \xi \partial T} + \frac{d\omega_0}{d\xi}\frac{\partial y_1}{\partial T} + 2\omega_0\omega_1\frac{\partial^2 y_1}{\partial T^2} = 0 \qquad \text{(C.13)}$$

From appendix C.1, we have that $\chi \approx \chi_0 = X(t)\cos T$. Substituting this into Eq.(C.13) and expanding the various trigonometric terms, we get:

$$\frac{1}{\varepsilon}\left[\omega_0^2\,\frac{\partial^2 y_1}{\partial T^2} - y_0\omega_0^2 X^2\left(\frac{1}{2} - \frac{1}{2}\cos 2T\right)\right] + \frac{d^2 y_0}{d\xi^2} + y_0 - 2y_0\omega_0\left[-\frac{dX}{d\xi}\frac{1}{2}\sin 2T + \omega_1 X^2\left(\frac{1}{2} - \frac{1}{2}\cos 2T\right)\right]$$

$$-\omega_0^2 y_1 X^2\left(\frac{1}{2} - \frac{1}{2}\cos 2T\right) - 2\omega_0\frac{dX}{d\xi}\sin T + \frac{d\omega_0}{d\xi}\frac{\partial y_1}{\partial T} + 2\omega_0\omega_1\frac{\partial^2 y_1}{\partial T^2} = 0 \qquad \text{(C.14)}$$

Now we are ready to carry out the standard steps of the method of direct partition of motion; First, we average Eq.(C.14) over the fast timescale T, with the assumption that the fast component of motion, y_1, and its derivatives are periodic on this fast timescale with a zero average. DPM also assumes that any purely slow function, that does not vary on the fast T timescale, is invariant under averaging over fast time. The resulting averaged equation is:

$$\frac{1}{\varepsilon}\left[-\frac{1}{2}y_0\omega_0^2 X^2\right] + \frac{d^2 y_0}{d\xi^2} + y_0 - y_0\omega_0\omega_1 X^2 + \frac{1}{2}\omega_0^2 X^2\left\langle y_1 \cos 2T\right\rangle_T = 0 \qquad \text{(C.15)}$$

$$\text{where} \quad \langle \bullet \rangle_T = \frac{1}{2\pi}\int_0^{2\pi} (\bullet)\, dT$$

The second standard step of DPM is to subtract Eq.(C.15) from Eq.(C.14), then the resulting equation takes the form:

$$\frac{1}{\varepsilon}\left[\omega_0^2\frac{\partial^2 y_1}{\partial T^2} + \frac{1}{2}y_0\omega_0^2 X^2\cos 2T\right] + O(1) = 0$$

Hence, to leading order, the equation governing y_1 becomes:

$$\frac{\partial^2 y_1}{\partial T^2} + \frac{1}{2}y_0 X^2\cos 2T = 0$$

Integrating twice with respect to T, we obtain the following expression for y_1:

$$y_1 \approx \frac{1}{8} y_0 X^2 \cos 2T \tag{C.16}$$

Note that we have set the constants of integration to zero in order to satisfy the DPM assumption that the fast component, y_1, is periodic on the T timescale with a zero average. Now, the integral appearing in Eq.(C.15) can be evaluated as:

$$\langle y_1 \cos 2T \rangle_T \approx \left\langle \frac{1}{8} y_0 X^2 \cos^2 2T \right\rangle_T = \frac{1}{16} y_0 X^2$$

Substituting this into Eq.(C.15), we obtain the following approximate equation governing y_0:

$$\frac{d^2 y_0}{d\xi^2} + y_0 - y_0 \left(\frac{1}{2\varepsilon} \omega_0^2 X^2 + \omega_0 \omega_1 X^2 - \frac{1}{32} \omega_0^2 X^4 \right) = 0 \tag{C.17}$$

From appendix C.1, we recall that:

$$\omega_1(\xi) = \frac{\kappa}{16} y_0^2 X^2 \omega_0^3 \quad \& \quad X(\xi) = C \sqrt{\omega_0(\xi)}$$

$$\text{where} \quad \omega_0 = \left(1 + \kappa y_0^2\right)^{-\frac{1}{2}}$$

Substituting these expressions into Eq.(C.17), the y_0 equation becomes:

$$\frac{d^2 y_0}{d\xi^2} + y_0 - y_0 \left(\frac{C^2}{2\varepsilon} \left(1 + \kappa y_0^2\right)^{-\frac{3}{2}} + \frac{\kappa C^4}{16} y_0^2 \left(1 + \kappa y_0^2\right)^{-3} - \frac{C^4}{32} \left(1 + \kappa y_0^2\right)^{-2} \right) = 0 \tag{C.18}$$

where C is an arbitrary constant that depends on the initial conditions. Comparing the magnitude of the denominators of the nonlinear terms in the above equation, we expect the first nonlinear term to be the dominant one. Hence, for simplification of the required algebraic manipulation, we will ignore the last two terms in the equation. Consequently, y_0 is, to leading order, governed by the following reduced equation:

$$\frac{d^2 y_0}{d\xi^2} + y_0 - y_0 \frac{C^2}{2\varepsilon} \left(1 + \kappa y_0^2\right)^{-\frac{3}{2}} = 0 \tag{C.19}$$

To find an expression for C, we consider initial conditions with zero velocities and initial amplitudes a and b as follows:

$$\begin{cases} y(0) = b \\ x(0) = \chi(0)\sqrt{\frac{\varepsilon}{\gamma}} = a\sqrt{\frac{\varepsilon}{\gamma}} \end{cases} \quad \rightarrow \quad \begin{cases} y_0(0) = b \\ \chi_0(0) = a \end{cases}$$

Recalling that:

$$\chi_0 = C\sqrt{\omega_0}\cos T \quad \text{where} \quad \omega_0 = \left(1 + \kappa y_0^2\right)^{-\frac{1}{2}}$$

then,

$$\chi_0(0) = C\left(1 + \kappa\left(y_0(0)\right)^2\right)^{-\frac{1}{4}} \quad \Rightarrow \quad a = C\left(1 + \kappa b^2\right)^{-\frac{1}{4}}$$
$$\Rightarrow C^2 = a^2\sqrt{1 + \kappa b^2} \tag{C.20}$$

C.3 The slow dynamics bifurcation

We restate here the equation governing the leading order dynamics of the slow degree of freedom:

$$\frac{d^2 y_0}{d\xi^2} + y_0 - y_0\frac{C^2}{2\varepsilon}\left(1 + \kappa y_0^2\right)^{-\frac{3}{2}} = 0$$

We rewrite this equation as a system of two first order differential equations:

$$\dot{y}_0 = \phi \quad , \quad \dot{\phi} = -y_0 + y_0\frac{C^2}{2\varepsilon}\left(1 + \kappa y_0^2\right)^{-\frac{3}{2}} \tag{C.21}$$

The system in Eq.(C.21) could possess non-trivial equilibrium points corresponding to $(\phi = 0, y_0 = E)$, such that E satisfies the following relation:

$$1 - \frac{C^2}{2\varepsilon}\left(1 + \kappa E^2\right)^{-\frac{3}{2}} = 0$$

$$\Rightarrow 2\varepsilon\left(1 + \kappa E^2\right)^{\frac{3}{2}} = C^2$$

Plugging in the expression for C from Eq.(C.20), we obtain the following relation between E, the value of y_0 for the nontrivial equilibrium point, and the initial amplitudes a and b:

$$\Rightarrow 2\varepsilon\left(1+\kappa E^2\right)^{\frac{3}{2}} = a^2\sqrt{1+\kappa b^2}$$

The initial condition that corresponds to the bifurcating non-local modes, i.e. fixed points in the Poincare map, will be $y_0(0) = b^*$ such that $E = b^*$, then b^* has to satisfy the following relation:

$$2\varepsilon\left(1+\kappa b^{*2}\right)^{\frac{3}{2}} = a^2\sqrt{1+\kappa b^{*2}}$$

$$\Rightarrow 2\varepsilon\left(1+\kappa b^{*2}\right) = a^2 \tag{C.22}$$

For such initial conditions with zero velocities, the energy, as given by Eq.(4.4), reduces to:

$$h = \frac{1}{2}\left(\frac{1}{\varepsilon\kappa}a^2 + b^{*2}\right)$$

$$\Rightarrow a^2 = \left(2h - b^{*2}\right)\varepsilon\kappa$$

Plugging this expression for a into Eq.(C.22), we get:

$$\Rightarrow 2\varepsilon\left(1+\kappa b^{*2}\right) = \left(2h - b^{*2}\right)\varepsilon\kappa$$

$$\Rightarrow b^* = \sqrt{\frac{2}{3}\left(h - \frac{1}{\kappa}\right)} \tag{C.23}$$

Such special initial condition will exist when the energy satisfies the following condition:

$$h > h_{cr} = \frac{1}{\kappa} \tag{C.24}$$

C.4 Validation plots for different parameter and energy values

We show more comparison plots for different initial conditions. The parameter values are the same as specified in section 2, except in Figures C.3 and C.4 in

which γ is set to 5 instead of 1.74.

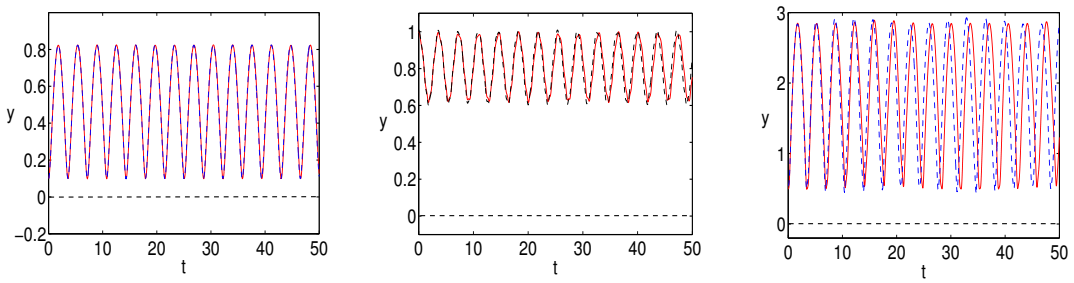

(a) $h = 0.4$, $b = 0.1$ (b) $h = 1$, $b = 1$ (c) $h = 5$, $b = 0.5$

Figure C.1: y vs time for different IC's

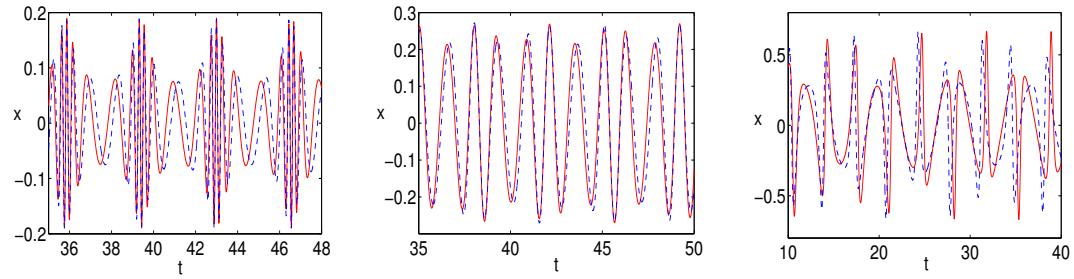

(a) $h = 0.4$, $b = 0.1$ (b) $h = 1$, $b = 1$ (c) $h = 5$, $b = 0.5$

Figure C.2: x vs time for different IC's

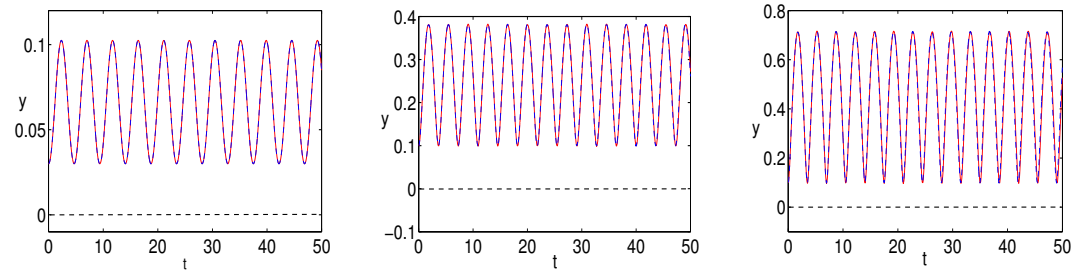

(a) $h = 0.01$, $b = 0.03$ (b) $h = 0.1$, $b = 0.1$ (c) $h = 0.3$, $b = 0.1$

Figure C.3: y vs time for different IC's; with $\gamma = 5$

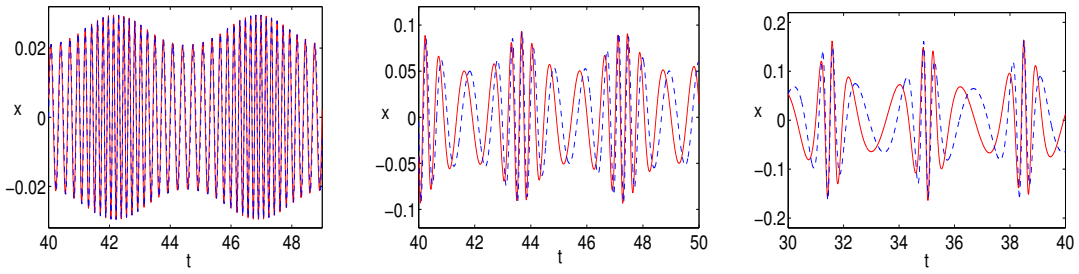

(a) $h = 0.01, b = 0.03$ (b) $h = 0.1, b = 0.1$ (c) $h = 0.3, b = 0.1$

Figure C.4: x vs time for different IC's; with $\gamma = 5$

BIBLIOGRAPHY

[1] Yu. Barkin, V. Vilke, *Celestial Mechanics of Planet Shells*, Astronomical and Astrophysical Trans., 23(6):533-553 (2004)

[2] M. Belhaq, S. Sah, *Horizontal fast excitation in delayed van der Pol oscillator*, Commun Nonlinear Sci Numer Simul, 13, 1706-1713 (2008)

[3] V.N. Belykh, E.V. Pankratova, *Chaotic dynamics of two Van der Pol-Duffing oscillators with Huygens coupling*, Regular and Chaotic Dynamics, Vol. 15, Nos. 23, pp. 274-284 (2010)

[4] I.I. Blekhman, *Vibrational mechanics-nonlinear dynamic effects, general approach, application*, Singapore: World Scientific (2000)

[5] R Bourkha, M Belhaq, *Effect of fast harmonic excitation on a self-excited motion in van der Pol oscillator*, Chaos, Solitons & Fractals, Vol. 34, 2, p. 621 (2007)

[6] G. Buzsaki *Rhythms of the brain*, Oxford, New York : Oxford University Press, (2006)

[7] P. Byrd, M. Friedman, *Handbook of Elliptic Integrals for Engineers and Scientists, 2nd ed.*, Berlin: Springer-Verlag (1971)

[8] C.C. Chen, et. al, *Nonlinear Coupling in the Human Motor System*, J. of Neuroscience, Vol. 30, No. 25: 8393-8399 (2010)

[9] V.T. Coppola, R.H. Rand, *Averaging using elliptic functions: approximation of limit cycles*, Acta Mechanica 81, 125-142 (1990).

[10] J.P. Cusumano, F.C. Moon *Chaotic non-planar vibrations of the thin elastica, part I: Experimental observation of planar instability*, J. Sound Vib. 179(2), 185-208 (1995)

[11] J.P. Cusumano, F.C. Moon *Chaotic non-planar vibrations of the thin elastica, part II: derivation and analysis of a low-dimensional model.*, J. Sound Vib. 179(2), 209-226 (1995)

[12] A. Fahsi, M. Belhaq, *Effect of fast harmonic excitation on frequency-locking in a van der Pol-Mathieu-Duffing oscillator*, Commun Nonlinear Sci Numer Simul, Vol. 14, Issue 1, p. 244-253 (2009)

[13] A. Fidlin, *Nonlinear Oscillations in Mechanical Engineering*, Berlin, New York: Springer (2006)

[14] J. Guckenheimer, P. Holmes, *Nonlinear Oscillations, Dynamical Systems, and Bifurcations of Vector Fields*, New York: Springer (1983)

[15] J.S. Jensen, *Non-Trivial Effects of Fast Harmonic Excitation*, PhD dissertation, DCAMM Report, S83, Dept. Solid Mechanics, Technical University of Denmark (1999)

[16] O. Jensen, L. L. Colgin, *Cross-frequency coupling between neuronal oscillations*, Trends in Cognitive Sciences, Vol. 11, Issue: 7, pp. 267-269 (2007)

[17] P.L. Kapitza, *Collected Papers by P.L. Kapitza, Vol. 2* Ter Haar D (ed), Pergamon Press, London, pp 714-726

[18] L.D. Landau, E.M. Lifshitz, *Course of Theoretical Physics, Vol. 1: Mechanics*. Pergamon Press, Oxford (1976)

[19] F. Nadim, Y. Manor, M.P. Nusbaum, E. Marder, *Frequency regulation of a slow rhythm by a fast periodic input*, J. Neurosci., 18(13):5053-5067 (1998)

[20] S.A. Nayfeh, A.H. Nayfeh, *Nonlinear interactions between two widely spaced modes - external excitation*, Int. J. Bifurcation Chaos, Vol 3, Issue 2, pp. 417-427 (1993)

[21] A.H. Nayfeh, C.M. Chin, *Nonlinear interactions in a parametrically excited system with widely spaced frequencies*, Nonlinear Dynamics 7: 195-216 (1995)

[22] C.H. Pak, R.H. Rand, F.C. Moon, *Free vibrations of a thin elastica by normal modes.*, Nonlinear Dynamics 3: 347-364 (1992)

[23] P. Popovic, A.H. Natfeh, K. Oh, S.A. Nayfeh, *An experimental investigation of energy transfer from a high-frequency mode to a low-frequency mode in a flexible structure* J. of Vibration and Control, Vol. 1, No. 1, 115-128 (1995)

[24] R.H. Rand, *Lecture Notes in Nonlinear Vibrations*, version 52 (2005), http://audiophile.tam.cornell.edu/randdocs

[25] S. Sah, M. Belhaq, *Effect of vertical high-frequency parametric excitation on self-excited motion in a delayed van der Pol oscillator*, Chaos, Solitons & Fractals, Vol 37, Issue 5, p. 1489-1496 (2008)

[26] J.A. Sanders, F. Verhulst, *Averaging methods in nonlinear dynamical systems*, New York: Springer-Verlag (1985)

[27] H. Sheheitli, R.H. Rand, *Dynamics of three coupled limit cycle oscillators with vastly different frequencies*, Nonlinear Dynamics, 64, 131-145 (2011)

[28] H. Sheheitli, R.H. Rand, *Dynamics of a mass-spring-pendulum system with vastly different frequencies*, submitted to Nonlinear Dynamics.

[29] H. Sheheitli, R.H. Rand, *On the dynamics of a thin elastica*, submitted to Int. J. Nonlinear Mechanics.

[30] J.J. Thomsen, *Vibrations and Stability, Advanced Theory, Analysis and Tools*, Germany: Springer-Verlag Berlin Heidelberg (2003)

[31] J.J. Thomsen, *Slow high-frequency effects in mechanics: problems, solutions, potentials*, Int. J. Bifurcation and Chaos, Vol. 15, Issue 9, pp. 2799-2818 (2005)

[32] A. Tondl et al., Autoparametric resonance in mechanical systems, Cambridge University Press, New York (2000)

[33] J.M. Tuwankotta, F. Verhulst, *Hamiltonian systems with widely separated frequencies*, Nonlinearity 16: 689-706 (2003)

[34] D.C. Wilcox *Perturbation methods in the computer age*, DCW Industries Inc., California (1995)